Chemical Osmosis
in Clayey Sediments

Field Experiments
and Numerical Modelling

Ana María Francisca Garavito Rojas

VRIJE UNIVERSITEIT

Chemical Osmosis
in Clayey Sediments

Field Experiments
and Numerical Modelling

ACADEMISCH PROEFSCHRIFT

ter verkrijging van de graad Doctor aan
de Vrije Universiteit Amsterdam,
op gezag van de rector magnificus
prof.dr. T. Sminia,
in het openbaar te verdedigen
ten overstaan van de promotiecommissie
van de faculteit der Aard- en Levenswetenschappen
op maandag 6 februari 2006 om 13.45 uur
in de aula van de universiteit,
De Boelelaan 1105

door

Ana María Francisca Garavito Rojas

geboren te Bogotá, Colombia

promotor: prof.dr. J.J. de Vries

copromotor: dr. H. Kooi

I want to dedicate this book to my Family.

"People tend to think too much and to feel too little". - Graffiti, Amsterdam Zuid

Contents

Acknowledgements

I wish to thank all the many people and institutions that with their support helped me during the course of my PhD. With no particular order I start mentioning TRIAS (Tripartatite Approach to Soil System Processes) and its three funding partners: NWO (Netherlands' Organization of Scientific Research), Delft Cluster and SKB (Foundation for the Development and Transfer of Knowledge of Soils) that provided the financial support essential for the developing of this research. My thanks go to Henk Kooi and Guus Loch for starting this activity and opening the track for me and others.

I would like to thank Henk Kooi for his supervision during my doctoral research. As my supervisor, he has constantly forced me to remain focused on achieving my goal. His observations and comments helped me to establish the overall direction of the research and to move forward with investigation in depth. I would like to thank him for his critical comments that over the years, made me realize the richness and complexity of the problem. Although he is probably one of the hardest-working researchers at the Hydro-group he is always remarkably available for any scientific discussion.

I am grateful to Professor Co de Vries who is my promoter and who has contributed greatly towards the shaping of this thesis.

Michel Groen from the Technical Department at the VU has been the person with whom I had to collaborate most closely. His notable expertise, technical skills and enthusiasm for field work have been the trigger that led to the development of the new instrumentation presented in this work. This would have not been possible without him and the help of his other colleagues: Niek van Harlingen , Harry Visch, Hans Bakker, Harry Visch and Frans Backer. For them and all the other guys of the Technical and Electronics Department : Thanks! From my department, I'm thankful to Richard de Jeu who was always willing to help with the good functioning of the loggers. Martin Konert and Maurice Hooyen from the Sedimentology Laboratory, thanks for your cooperation and patience with my bentonite and pots all over your lab. Beyond the VU, I have had the opportunity to interact with many other teams. In particular, the project partners at Utrecht and Delft Universities, the SCK in Mol Belgium, GeoDelft and the USGS in Washington. I could not possibly list all the people in those teams, and therefore I will restrict myself to the few I closely cooperated with.

The first person I can think of is Katja Heister at the University of Utrecht who has been a constant and immense support. I thank her for sharing information with me and for

her various good suggestions during all the phases of the thesis work. Special thanks to her supervisor Guus Loch for his stimulating discussions and collaborations. Equally, Sam Bader and Ruud Schotting from the University of Delft for sharing their time and knowledge in our cooperative work. I would like to express my sincere thanks to Geert Greeuw, Remco Schrijver and Kees Versluis from GeoDelft that greatly collaborated and supported me from the very beginning. My special thanks also go to Chris Neuzil from the USGS whose article is probably the most referred to in the field. His work was always a great source of motivation. I am very grateful to him for sharing his knowledge and expertise that influenced my research and resulted in a cooperative joint publication. He has also provided me with all the data sets needed for, and has made significant contributions to the publication. I greatly appreciate him and his colleague at the USGS Cliff Voss for their generous time and hospitality during the time I spent in Washington. I would like to express my appreciation to the people of SCK in Mol Belgium. The work in Belgium was undertaken in close co-operation with, and with the financial support of, ONDRAF-NIRAS, the Belgian Agency for Radioactive Waste and Enriched Fissile Materials. I'm grateful to G. Volckaert and his team at SCK for providing me with the opportunity to perform experiments at their underground research facility and work with a talented team of researchers. In particular, I have had the chance to collaborate closely with Pierre De Cannière. Working with him has been a fruitful experience. He has been extremely cooperative in providing all the data and information necessary for this work. I greatly appreciate his contributions to our joined publication and thank him for his hospitality during the days I spent at the underground facility. I must also thank Hugo Moors, F. Vandervoort, L. Van Ravestyn, M., Van Geet, and X. Sillen for their support and for their assistance during the experiments. I am also grateful to Helenius Rogaar, Thomas Keijzer , Theo Saat and all the other members of the TRIAS project Committee for many interesting and helpful discussions, particularly during our meetings every six months. Of course, I must also thank the members of my committee for the in-depth reading of this text and the various constructive suggestions.

In Nessersluis, Groot Mijdrecht I have a few persons to thank. I would like to express my sincere thanks to Mr Pronk and his family for allowing me to transform their back grassland in a experimenting field site. They were always too kind and helpful. Equally, to the people from DWR that allowed also experimenting in their terrain. My sincere gratitude goes to the brothers van Schank and their ferry. They both always managed that I cross the Amstel River even if the ferry was not working. Special thanks to John van Schank that assisted me several times with my heavy instruments and that put me in the car of any neighbor every time that I missed my bus.

I would like to thank administrative and technical staff members of the VU who have been more than kind to advise and help in their respective roles. Among them, Heleen Heijstee at the Hydrology and Geo-Environmental Sciences Department who has been always ready to help. The computer Help Desk team for their continuous support. I greatly appreciate Barbara Spruits, Mr Arnold Bonan and Marc Matitaputtij from the Personnel Office for the generous time assisting me in all administrative and personnel matters. I would like to express my special thanks to Mr Bonan for being a great soul. He and Mr Matitaputtij are always ready to help with a smile. All the friends, those in the distance and those with

whom I shared an enjoyable social life in these years. It is virtually impossible to mention all of them; however there are few I consider my family in this country. Yenory, Katie, Volker, Ayleen, Paty, Cristhian, Marcela, Freddy, Marta, Andrea and Yuko. I'm grateful for their continuous support, encouragement and great long-lasting friendship. The time I spent with them will remain as a very good memory of my life. Now is time to speak about you, Elmer. From the beginning of my PhD in Amsterdam you were an unconditional friend. Always there, ready to help, cheerful, bringing support, spreading happiness and most important constantly listening. I thank you for helping me to keep going (in all aspects personal and professional) and for making easier my staying at the VU. I'm glad to continue having your invaluable support until these days, the most difficult days of the PhD. But mostly I'm immensely happy to think that even though this stage of my life is finishing you will continue being by my side. Last, but not least, I would like to dedicate this thesis to my dearest family, I am indebted to my parents (Cristina and Jose) and sisters (Patricia and Sandra). You gave me the strength and will to bring this task to an end. Without your support and advice throughout these years I could have not make it. The daily conversation with my mother and occasional talks to my sisters and father kept the distance between Colombia and the Netherlands very short. You made the best of each visit to Colombia and managed to give me confidence and strength to depart again. You were always there in all the difficult moments, worrying and caring. I'm very thankful for your love, patience, and understanding. Gracias de verdad!

Chapter 1

Introduction

1.1 Background and Rationale

Clay-rich deposits are usually considered as natural protective covers in regional aquifers because of their low permeability (Fetter, 1992). In the absence of water conductive features, these deposits provide the low-flow environment required for waste containment. In such conditions where advection is negligible, diffusion is clearly the dominant transport process. Moreover, clay minerals retard the movement of contaminants a.o., by ion exchange, sorption, and ultra-filtration. Due to the slow flow and transport processes occurring within them, clay rich deposits may still reflect former environmental conditions from periods that date back thousands of years (e.g. Post, 2004). Data obtained from clay-rich deposits are therefore a very useful tool in paleohydrological development studies. Comprehensive understanding of the physical and chemical processes controlling the water and solute transport in low-permeability materials such as clays and shales is therefore essential both for assessing their suitability as barriers and to understand the processes and factors that control the hydrogeological evolution of groundwater systems.

A number of studies have characterized transport parameters for clay-rich formations over a large range of scales (e.g. Brace, 1980; Corbet and Bethke, 1992; Neuzil, 1993, 1994; McKay et al., 1993, 1998; Wassenaar and Hendry, 1999; Hendry et al., 2000; van der Kamp, 2001) and have successfully used these parameters in transport models. With few exceptions, only the hydraulically-driven flow of water and associated advective-dispersive transport have been considered. That is, the constitutive relations expressed by Darcy's law and Fick's law were used to describe fluid and solute flows driven by gradients in hydraulic head and concentration, respectively. However, clays and shales may act as semi-permeable membranes that, in addition to the primary flows, allow for the occurrence of secondary or coupled flows (e.g Kemper, 1960, 1961; Young and Low, 1965; Olsen, 1969, 1972; Greenberg et al., 1973; Fritz and Marine, 1983; Mitchell, 1993) such as chemical osmosis in which fluid flow is induced by a solute concentration gradient and ultrafiltration, or the preferential retardation of solute with respect to the solvent.

In media with semi-permeable membrane properties, osmosis drives fluid flow from regions of low to regions of high concentration, thereby tending to raise fluid pressure where

concentrations are high and to decrease them where they are low. A number of laboratory studies have demonstrated that clays and shales exhibit membrane properties (e.g. Kemper and Rollins, 1966; Letey and Kemper, 1969; Kemper and Quirk, 1972; Olsen, 1972; Walter, 1982; Barbour and Fredlund, 1989; Whitworth and DeRosa, 1997; Keijzer, 2000; Cey et al., 2001; Malusis and Shackelford, 2004; Oduor, 2004).

Chemical osmosis and ultrafiltration phenomena are also thought to occur in sedimentary basins, being responsible for the generation of anomalous pore pressures and salinities (e.g. Hanshaw and Bredehoeft, 1968; Kharaka and Berry, 1973; Fritz and Marine, 1983).

Studies that clearly indicate that osmosis is significant in geological environments are scarce and only two studies have been published to date. The first investigation described by Neuzil (2000) comes from the osmosis *in-situ* experiment in four boreholes placed within the Cretaceous-age Pierre Shale in South Dakota. Most recently, at the final stage of this PhD research, the second study was published (Noy et al., 2004), reporting on experimental data from *in-situ* tests in the Jurassic-age Opalinus Clay in Switzerland. This clay formation is being considered as a host rock for radioactive waste disposal. The latter study reflects the recent interest of developers and designers of underground radioactive waste containment facilities in the possible implications of chemical osmosis operating within clay layers.

A considerable amount of literature exists on the theory of membrane properties of clays. Much of it concerns how the semi-permeable behavior is affected by clay porosity, clay geochemistry and ion-solid interaction properties (Kemper and Rollins, 1966; Groenvelt and Bolt, 1969; Bresler, 1973; Hanshaw and Coplen, 1973; Kharaka and Berry, 1973).

Discontinuous formulations (flows cast in terms of differential values of pressure and concentration across the membrane) have been extensively used to infer and quantify the membrane properties from laboratory ultrafiltration/osmosis experiments conducted under steady-state conditions (Hanshaw and Coplen, 1973; Keijzer, 2000; Cey et al., 2001). Continuous transport formulations have been increasingly derived allowing simulation of transient flow and transport conditions within membranes (Mitchell et al., 1973; Greenberg et al., 1973; Barbour and Fredlund, 1989; Soler, 2001; Malusis and Shackelford, 2002a; Manassero and Dominijanni, 2003; Noy et al., 2004; Oduor, 2004).

Although the experimental evidence (mainly laboratory studies) and the transport formulations are numerous, and clearly demonstrate the relevance of osmotic phenomena in clays, there is a lack of integrated studies involving laboratory experiments, in-situ experiments and theoretical investigations. It is important to establish the significance of osmotic phenomena operating in geological environments. The effects of osmosis can influence the results of innumerable studies ranging from pollution, salt-water intrusion and waste-containment to the understanding the hydrogeological evolution of sedimentary basins. The study of Neuzil (2000) clearly indicates that shales may behave as semi-permeable membranes and may be able to generate pressures up to 20 MPa. The potential for osmosis to occur exists in both shallow and deep sedimentary basins. However, it is unclear if shallow, little consolidated natural clays exhibit a similar behavior. Although laboratory studies on osmosis carried out on natural (remolded or undistorted) clay samples are conclusive and suggestive, the direct applicability of these results to the field situation may not be always appropriate. Current mathematical models have been mainly applied to laboratory work on

osmosis. These models mostly deal with steady state conditions and do not directly address the expected effects of osmosis on deep geological environments or on groundwater flow. For those reasons, more convincing evidence coming from osmosis *in-situ* experiments and more predictive modelling involving osmotic phenomena are needed.

1.2   Objectives

This study is part of a larger project called: *Chemically and Electrically Coupled Flow Transport in Clayey Soils and Sediments*. The object of this project is to quantify the role of chemically and electrically coupled transport in clayey soils and sediments and to try to establish its relevance for the distribution and emission of contaminants and water. The project is an interdisciplinary research involving laboratory work, field investigation and numerical modelling. Three universities in the Netherlands (University of Utrecht, University of Delft and Vrije Universiteit of Amsterdam) were involved. The results of this research project are compiled in three PhD theses. Bader (2005) worked on the development of a continuous transport model that takes into account chemical osmosis and electro-osmosis. Heister (2005) focused on the performance of laboratory experiments to quantify the effect of induced electrical potentials on the transport of water and ions in clays. This manuscript represents the third thesis produced in this cooperative effort. The focus of this PhD research is on field investigation of osmotic phenomena. The objective of the work, as formulated at the start of the project, was to provide field evidence for osmotic phenomena of clayey sediments and to quantify membrane properties from *in-situ* tests. Additionally, numerical modelling was initially proposed to assess the significance of the inferred membrane properties for flow and transport in groundwater systems. Of these two objectives, the first has received far more attention than the second. The main topic of this manuscript is, therefore, field experiments and *in-situ* measurement of membrane behavior and membrane properties of clays. Both shallow, unconsolidated clays and deep, strongly consolidated clays have been investigated. The focus is on natural clays and chemical osmosis phenomena. Numerical modelling has also been primarily applied in the context of field experiments.

1.3   Thesis Outline

Chapter 2 of this thesis provides a review of the basic concepts of osmotic phenomena and the theoretical concepts of chemical osmosis and semi-permeable membrane behavior of clays. Additionally, a brief retrospection of previous laboratory studies and field investigations is given.

The design and testing of instrumentation and the assessment of different procedures for field measurements of osmotic behavior of clays, were an indispensable part of this study. Chapter 3 is concerned with instrumentation for *in-situ* field testing. Existing methods for pore pressure measurements, hydraulic testing and hydrochemical sampling of low permeability sediments are reviewed. Methods more suitable for osmosis testing are selected and the design of our newly developed instrument is presented. The developed instrumentation and other existing instruments were utilized to perform osmosis *in-situ* tests on the Holocene

estuarine Calais Clay in the Netherlands. In Chapter 4 the results obtained from these tests are presented and discussed. Additionally, existing piezometers were used to perform two in-situ experiments in the Boom Clay at the Underground Research Laboratory (URL) in Mol, Belgium. The tests and the experimental data obtained are described and investigated in Chapter 5. At this facility, there is a particular interest in knowing wether osmotically-driven flows can generate high pore pressures that could affect the clay barrier due to the release of large amounts of nitrate-bearing bituminized radioactive waste.

Finally, the theory of semi-permeable membrane behavior is applied through numerical modelling. A continuum model that has been developed as part of the project research (Garavito et al., 2002; Kooi et al., 2003; Bader and Kooi, 2005) has been utilized. The model evaluates directly the temporal and spatial evolution of concentration, pressure and efficiency within the membrane; and the strong dependence of the efficiency of the membrane on the local concentration. In Chapter 6 a description of the mathematical model is given. Also presented in the chapter, are the results of transient simulation of the data obtained from an osmosis laboratory tests in bentonite reported by Keijzer (2000) and the osmosis *in-situ* tests in the Pierre Shale Neuzil (2000) and the Boom Clay (this study). These modelling results were also reported as research articles. Further, transient modelling is used in Chapter 7 to asses the role of osmosis in the generation of overpressures found in the Triassic-age Dunbarton Basin (Marine and Fritz, 1981).

References

Bader, S., 2005. Osmosis in groundwater; chemical and electrical extensions to Darcy's law. Ph.D. thesis, Delft University of Technology, Delft, the Netherlands.

Bader, S., Kooi, H., 2005. Modelling of solute and water transport in semi-permeable clay membranes: Comparison with experiments. Advances in Water Resources (28), 203–214.

Barbour, S., Fredlund, D., 1989. Mechanisms of osmotic flow and volume change in clay soils. Canadian Geotechnical Journal (26), 551–562.

Brace, W., 1980. Permeability of crystalline and argillaceous rocks. International Journal of Rock Mechanics and Mining Sciences 17, 241–245.

Bresler, E., 1973. Anion exclusion and coupling effects in non-steady transport through unsaturated soils. Soil Sci. Soc. Am. Proc. (37), 663–669.

Cey, B., Barbour, S., Hendry, M., 2001. Osmotic flow through a Cretaceous clay in southern Saskatchewan, Canada. Canadian Geotechnical Journal (38), 1025–1033.

Corbet, T., Bethke, C., 1992. Disequilibrium fluid pressures and groundwater flow in the Western Canada Sedimentary Basin. Journal of Geophysical Research 97 (B5), 7203–7217.

Fetter, C., 1992. Contaminant hydrogeology. Macmillan Publishing Company New York.

Fritz, S., Marine, I., 1983. Experimental support for a predictive osmotic model of clay membranes. Geochimica et Cosmochimica Acta (47), 1515–1522.

Garavito, A., Bader, S., Kooi, H., Richter, K., Keijzer, T., 2002. Numerical modeling of chemical osmosis and ultrafiltration across clay membranes. Development in Water Sciences 1, 647–653.

Greenberg, J., Mitchell, J., Witherspoon, P., 1973. Coupled salt and water flows in a groundwater basin. Journal of Geophysical Research 78 (27), 6341–6353.

Groenvelt, P., Bolt, G., 1969. Non equilibrium thermodynamics of the soil water system. Journal of Hydrology 78, 358–388.

Hanshaw, B., Bredehoeft, J., 1968. On the maintenance of anomalous fluid pressures. II. Source Layer at depth. Geological Society of America Bulletin 79, 1107–1122.

Hanshaw, B., Coplen, T., 1973. Ultrafiltration by a compacted clay membrane: II. Sodium ion exclusion at various ionic strengths. Geochimica et Cosmochimica Acta (37), 2311–2327.

Heister, K., 2005. Coupled transport in clayey materials with emphasis on induced electrokinetic phenomena. Ph.D. thesis, Universiteit Utrecht, The Netherlands.

Hendry, J., Wassenaar, L., Kotzer, T., 2000. Chloride and chlorine isotopes as tracers of solute migration in a thick, clay rich. Water Resources Research (36), 285–296.

Keijzer, T., 2000. Chemical osmosis in natural clayey material. Ph.D. thesis, Universiteit Utrecht, The Netherlands.

Kemper, W., 1960. Water and ion movement in thin films as influenced by the electrostatic charge and diffuse layer of cations associated with clay mineral surfaces. Soil Science Society of America , 10–16.

Kemper, W., 1961. Movement of water as affected by free energy and pressure gradients. I Application of classic equations for viscous and diffuse movements to the liquid phase in finely porous media II. Experimental analysis of porous systems in which free energy and pressure gradients act in opposite directions. Soil Science Society of America Proceedings , 260–265.

Kemper, W., Quirk, J., 1972. On mobilities and electric charge of external clay surfaces inferred from potential differences and osmotic flow. Soil Science Society of America , 426–433.

Kemper, W., Rollins, J., 1966. Osmotic efficiency coefficients across compacted clays. In: Soil Science Society of America 30. pp. 529–534.

Kharaka, Y., Berry, A., 1973. Simultaneous flows of water and solutes through geological membranes: I. Experimental investigation. Geochimica et Cosmochimica Acta (37), 2577–2603.

Kooi, H., Garavito, A., Bader, S., 2003. Numerical modelling of chemical osmosis and ultrafiltration across clay formations. Journal of Geochemical Exploration (78-79), 333–336.

Letey, J., Kemper, W., 1969. Movement of water and salt through a clay water system: Experimental verification of Onsager reciprocal relation. Soil Science Society of America , 25–29.

Malusis, M., Shackelford, C., 2002a. Theory for reactive solute transport through clay membrane barriers. Journal of Contaminant Hydrology 59, 291–316.

Malusis, M., Shackelford, C., 2004. Predicting solute flux through a clay membrane barrier. Journal of Geotechnical and Geoenvironmental Engineering 130, 477–487.

Manassero, M., Dominijanni, A., 2003. Modelling the osmosis effect on solute migration through porous media. Geotechnique (53), 481–492.

Marine, I., Fritz, S., 1981. Osmotic model to explain anomalous hydraulic heads. Water Resources Research 29 (17), 73–82.

McKay, L., Balfour, D., Cherry, J., 1998. Lateral chloride migration from a landfill in a fractured clay rich glacial deposit. Ground Water 36 (6), 988–999.

McKay, L., Cherry, J., Gilham, R., 1993. Field experiments in a fractured clay till. I. Hydraulic conductivity and fracture aperture. Water Resources Research 29 (4), 1149–1162.

Mitchell, J. K., 1993. Fundamentals of soil behavior., 2nd Edition. John Wiley and Sons, New York.

Mitchell, J. K., Greenberg, J., Whiterspoon, P., 1973. Chemico-Osmotic Effects in Fine-Grained Soils. Journal of the Soil Mechanics and Foundations Division, ASCE (SM4), 307–322.

Neuzil, C., 1993. Low fluid pressure within the Pierre Shale: a transient response to erosion. Water Resources Research 29 (7), 2007–2020.

Neuzil, C., 1994. Characterization of flow properties, driving forces and pore water chemistry in the ultra-low permeability Pierre Shale, North America. In: Workshop on Determination of Hydraulic and Hydrochemical Characterisation of Argillaceous Rocks. OECD Documents Disposal of Radioactive Waste. Nottingham, UK., pp. 65–74.

Neuzil, C., 2000. Osmotic generation of "anomalous" fluid pressures in geological environments. Nature (403), 182–184.

Noy, D., Horseman, S., Harrington, J., Bossart, P., Fisch, H., 2004. An Experimental and modelling study of chemico-osmotic effects in the Opalinus Clay of Switzerland. In: Heitzmann, P. ed. (2004) Mont Terri Project - Hydrogeological Synthesis, Osmotic Flow. Reports of the Federal Office for Water and Geology (FOWG), Geology Series (6), 95–126.

Oduor, P., 2004. Transient modeling and experimental verification of hyperfiltration effects. Ph.D. thesis, Department of Geological and Petroleum Engineering, University of Missouri-Rolla.

Olsen, H., 1969. Simultaneous fluxes of liquid and charge in saturated kaolinite. Soil Science Society of America Proceedings , 338–349.

Olsen, H., 1972. Liquid movement through kaolinite under hydraulic, electric and osmotic gradients. American Association of Petroleum Geologists Bulletin (56), 2022–2028.

Post, V., 2004. Groundwater salinization processes in the coastal area of the Netherlands due to transgressions during the Holocene. Ph.D. thesis, Vrije Universiteit Amsterdam, The Netherlands.

Soler, J., 2001. The effect of coupled transport phenomena in the Opalinus Clay and implications for radionuclide transport. Journal of Contaminant Hydrology (53), 63–84.

van der Kamp, G., 2001. Methods for determining the in situ hydraulic conductivity of shallow aquitards - an overview. Hydrogeology Journal (9), 5–16.

Walter, G., 1982. Theoretical and experimental determination of matrix diffusion and related solute transport properties of fractured tuffs from Nevada test site. Los Alamos National Laboratory report LA-9471-MS.

Wassenaar, L., Hendry, M., 1999. Improved piezometer construction and sampling techniques to determine pore water chemistry in aquitards. Ground Water 37 (4), 564–571.

Whitworth, T. M., DeRosa, G., 1997. Geologic Membrane Controls on Saturated Zone Heavy Metal Transport. New Mexico Water Resources Research Institute Report 303.

Young, A., Low, P., 1965. Osmosis in argillaceous rocks. American Association of Petroleum Geologists Bulletin (49), 1004–1008.

Chapter 2

Chemical Osmosis and Osmotic Phenomena

Chemical osmosis has been invoked as explanation for anomalous hydraulic heads and salinities observed within sedimentary basins. It has been suggested that osmosis has the potential to modify groundwater heads across clay layers and thereby groundwater flow patterns. Understanding of chemical osmosis phenomena and semi-permeable membrane behavior of clays is fundamental to evaluate the significance of chemical osmosis in the geological environment. This chapter provides the basic concepts of osmotic phenomena and the theoretical concepts of chemical osmosis and semi-permeable membrane behavior of clays. In addition, previous laboratory studies and field investigations are reviewed.

2.1 Chemical Osmosis

Osmotic phenomena refer to water and solute transport processes that occur when transport of solute molecules or ions is restricted by the porous medium relative to that of water molecules. A porous medium which exhibits such behavior is referred to as a membrane. Chemical osmosis and reverse osmosis/ultrafiltration are osmotic phenomena.

Chemical osmosis is the flow of solution through a semi-permeable membrane due to a difference in fluid chemical composition on either side of the membrane. The flow occurs from dilute solution to concentrated solution. The driving force for this movement is the chemical gradient across the membrane. However other forces may also cause fluid flow as shown in Table 2.1.

Figure 2.1a schematically illustrates the basic features of the simple, classical laboratory experiments that are used to demonstrate the osmotic phenomenon. Two closed reservoirs containing solutions of different concentration are separated by a semi-permeable membrane. Initially the hydraulic gradient across the membrane is zero. Due to osmosis, flow of solution (from low to high concentration) causes a rise in pressure/head in the reservoir containing the concentrated solution (osmotically-induced pressure) and a reduction in the other reservoir (osmotically-induced pressure drop). An opposing hydraulic counter flow is induced. The net flow of solution continues until osmotic equilibrium is reached in which case the counter flow is equal to the osmotically-induced flow.

If the membrane is ideal (impermeable for solute), the equilibrium osmotically-induced

Table 2.1: Coupled Flow Phenomena modified after Mitchell (1993) and Keijzer (2000).

Flow	Gradient			
	Hydraulic	**Temperature**	**Electrical**	**Chemical**
Fluid	Hydraulic Flow **Darcy's Law**	Thermo-osmosis	Electro-Osmosis	Chemical-Osmosis
Heat	Heat Convection	Thermal Conduction **Fourier's Law**	Peltier Effect	Dufour Effect
Electric Charge	Streaming Current	Seebeck Effect	Electro Current **Ohm's Law**	Diffusion current
Ion	Ultrafiltration	Soret Effect	Electro-phoresis	Diffusion **Fick's Law**

differential pressure is highest and persists indefinitely. This theoretical osmotic pressure difference ($\Delta\pi$) between two solutions can be estimated from the solution properties on either side of the membrane using the Van't Hoff's equation (Fritz and Marine, 1983, e.g):

$$\Delta\pi = \frac{RT}{v} \ln \frac{a_{H_2O}^{low}}{a_{H_2O}^{high}} \tag{2.1}$$

where R is the universal gas constant (J/mol K), T is the temperature (K), v is the molar volume of water (m^3/mol) and a_{H_2O} is the water activity in the solution.

As already mentioned, flow may result also from other driving forces than chemical gradients across the membrane (Table 2.1): hydraulic gradients (hydraulic flow), electrical gradients (electro-osmosis) and/or thermal gradients (thermo-osmosis) (Mitchell, 1993). The different types of flow are usually referred to as coupled flows.

The theory for coupled flows and the corresponding transport formulations have been derived from non-equilibrium thermodynamics (Katchalsky and Curran, 1965). This theory is a phenomenological, macroscopic theory that provides a basis to describe systems that are not in equilibrium. The theory considers the different types of flow (water, solute, electric charge and heat) that are associated with several types of driving forces (Table2.1). Chapter 6 provides a description of the theory as well as a review of the existing formulations.

In situations where driving forces other than chemical gradients cause fluid flow through a membrane, restricted advective transport of solute leads to accumulation of solute on the inflow side of the membrane, due to the sieving behavior of the membrane. This is referred as to reverse osmosis or ultrafiltration (Horseman et al., 1996).

2.2 Membrane Behavior and Clay materials

By definition, a semi-permeable membrane rejects solutes relative to the solvent. Solute rejection is caused by particle size and/or electrical restrictions.

Membrane behavior in low permeability clayey materials is mainly due to the electrical properties of the minerals that constitute the geological material. Descriptions of how this

works at the pore level have been given by Fritz (1986); Mitchell et al. (1973); Kemper and Rollins (1966); Groenevelt and Bolt (1969); Bresler (1973); Hanshaw and Coplen (1973) and Marine and Fritz (1981).

The follow description of the origin of membrane behavior is mainly based on the work by Marine and Fritz (1981). Several clay minerals are characterized by a net negative surface charge (charge deficiency) caused by broken bonds and substitution of low valence cations within the lattice. The charged mineral, in the presence of a solution, adsorbs cations and few anions (to maintain electrical neutrality) constituting a mobile, predominately positively charged layer near the clay particles (Figure 2.2). The concentration of positive charges diminishes away from the surface up to a point where it becomes the same as the pore water solution. The resultant charged surface and the predominant positively charged layers define what is known as the Gouy double layer. Double layer thicknesses are of the order of tens of nanometers or less. In sandstone this thickness is insignificant in relation to the pore
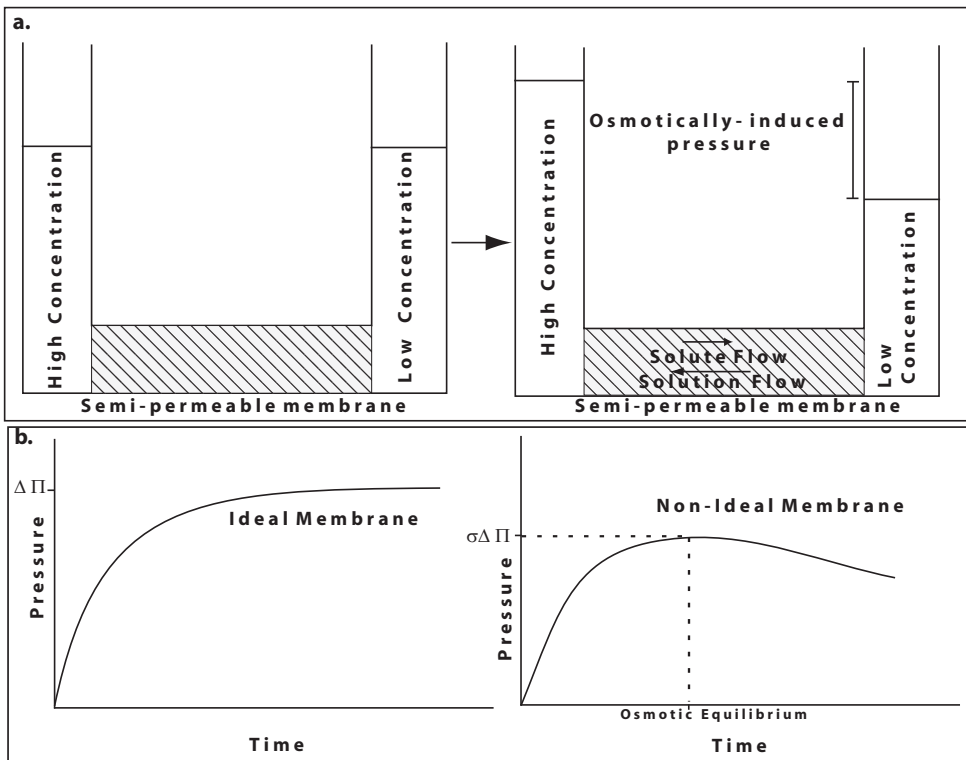
Figure 2.1: a. Schematic illustration of typical laboratory osmosis experiments. For the case of ideal membrane, solute flow is zero and solution flow corresponds only to water. b. Illustration of osmotically-induced pressure evolution for ideal and non-ideal membranes

15
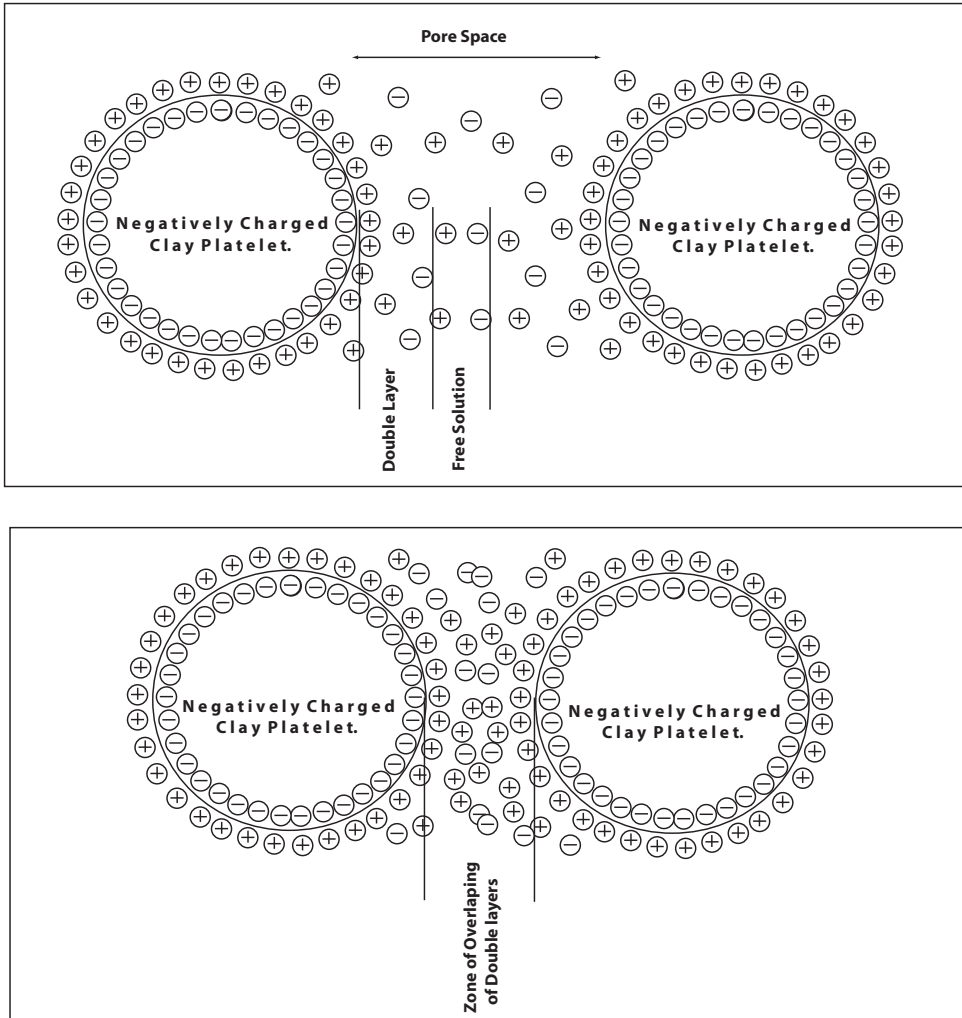
Figure 2.2: Schematic illustration of non-overlapping (top) and overlapping (bottom) double layers between clay platelets.

size. Hence the majority of ions in the ambient solution in sandy sediments pores are not affected by the double layers. In contrast, in clay-rich sediments, double layer thicknesses are comparable to the pore size leaving little or no solution in the pores that is uninfluenced by the double layers.

The salt exclusion properties of clay membranes (restriction of both anions and cations) result from the overlapping of double layers when the clay has been sufficiently compacted.

Compaction causes an increase in concentration of positive charges and a decrease in concentration of negative charges in the double layers compared to the pore water solution (Figure 2.2). Hence, when a solution strives to pass through the pores, anions tend to be repelled by the net negative charge on the platelets. Movement of cations is also restricted as they tend to remain with their anionic counterpart to maintain electrical neutrality in the external solution. Water, by contrast, moves without restriction across the structure (Fritz, 1986; Horseman et al., 1996). According to Fritz (1986) the pore spaces of an ideal membrane contain no free salt, the only solutes present are cations. By contrast in a non-ideal membrane there is free salt within the pore spaces.

2.3   Membrane Ideality

Ideal membranes completely prevent the passage of solutes and permit exclusively the passage of water through it. This type of membrane may not exist in natural low permeability environments; only commercial, artificially-made polymer membranes exhibit ideality. Clayey mineral membranes are non-ideal membranes since they allow restricted diffusion and advection of salt through the membrane.

The degree of solute restriction is not only established by the degree of compaction. The efficiency of a membrane depends on many characteristics of the material and factors and conditions within it (e.g. external solution concentration). A considerable amount of literature exists on the theory of membrane properties of clays. A brief review will be presented later in this chapter. Much of the literature concerns studies of how membrane efficiency is affected by clay properties such as porosity and geochemistry and ion-soil interaction parameters such as exchange capacity, salt exclusion factors and thickness and concentration of the solution between the negatively-charged clay platelets.

The magnitude of the osmotically-induced pressure in osmosis experiments varies with the degree to which there is solute restriction. If a porous medium without membrane properties is placed between the reservoirs in a similar experimental set-up as shown in Figure 2.1a, solute transport is not hindered and no differential pressure Δp due to osmosis develops. In case an ideal membrane is placed, the flow is limited to the solvent (water) and a maximum differential pressure Δp is developed equal to $\Delta \pi$. If a non-ideal membrane is in between the reservoirs, the membrane partially restricts the solute transport; and solution flows across the membrane. In this case, Δp will be smaller than $\Delta \pi$. Figure 2.1b illustrates the pressure evolution (build-up, equilibrium and post-equilibrium behavior) across the semi-permeable membrane (ideal and non-ideal) for the experimental set-up shown in Figure 2.1a.

The extent to which a low-permeability material acts as a membrane is indicated by the efficiency of the membrane or reflection coefficient σ. Katchalsky and Curran (1965) have defined σ as the ratio of the the osmotically-induced hydraulic pressure and the osmotic pressure at equilibrium:

$$\sigma = (\frac{\Delta p_{os}}{\Delta \pi})_{J_v=0} \tag{2.2}$$

where Δp_{os} is the osmotically-induced pressure difference, $\Delta\pi$ is the osmotic pressure difference and J_v is the flux of solution. The osmotic efficiency ranges from 0 for materials without semi-permeable membrane properties, to 1 for ideal membranes.

2.4 Laboratory Studies

Qualitative and quantitative evidence for osmotic flow processes has been found extensively in the laboratory using small (few mm thick), remolded samples of purified or processed clays (Kemper, 1961; Olsen, 1972; Kharaka and Berry, 1973; Fritz and Marine, 1983; Barbour and Fredlund, 1989; Fritz, 1986; Keijzer, 2000) and undisturbed natural clay samples (Young and Low, 1965; Walter, 1982; Whitworth and DeRosa, 1997; Cey et al., 2001; Noy et al., 2004; Oduor, 2004). Most of these studies have also focused on aspects as membrane composition and thickness, and effects of compaction and solution concentration (salinity) on the efficiency of the membranes.

Laboratory work performed by Olsen (1972), Kharaka and Berry (1973), Kharaka and Smalley (1976) and Fritz and Marine (1983) showed that clayey materials act more efficiently as membranes when they are compacted. The degree of compaction necessary for membrane behavior depends on the thickness of the double layer. The thickness is inversely proportional to the ionic strength of the pore fluid and the valence number of the cation forming the mobile layer (Alexander, 1990).

Membrane ideality increases with decreased pore water concentration (Kemper, 1961; Berry, 1969; Groenevelt and Bolt, 1969; Hanshaw and Berry, 1969; Bresler, 1973; Kharaka and Berry, 1973; Fritz, 1986). The efficiency of exclusion of different solutes is not the same due to differences in ionic charge. Experimental work indicates that the degree of ion restriction of the membrane is specific for different constituents of the solutions. Different types of ions have different mobility and are retarded with respect to others when passing through the membrane. Kharaka and Berry (1973) presented experimental laboratory results on the membrane efficiencies obtained with different clays and shales and the relative retardation of cations and anions. The results showed that geological membranes act in a specific way for each different dissolved species. The retardation sequences found for monovalent and divalent cations at laboratory conditions were: $Li < Na < NH_3 < K < Rb < Cs$ and $Mg < Ca < Sr < Ba$. Monovalent cations were in general retarded with respect to divalent cations. The general sequence for anions found was: $HCO_3 < I < B < SO_4 < Cl < Br$. Furthermore, fractionation of the stable hydrogen and oxygen isotopes of the water molecules passing across montmorillonite membranes has been reported (Hanshaw and Coplen, 1973; Benzel and Graf, 1984).

Observations by Kharaka and Berry (1973) and Fritz (1986) have shown that the degree of salt exclusion of a clay membrane is a function of the cation-exchange capacity (CEC). Fritz (1986) observed that the membrane efficiency of high CEC materials like smectite, which posses a high surface charge density, is less affected by pore water salinity. Efficiency exhibited is higher for this type of material and lower for membranes with lower CEC such as kaolinites. According to Malusis and Olsen (2003) the presence of sodium occupying the cation exchange complex enhances the semipermeable behavior.

The experimental work by Benzel and Graf (1984) showed that membrane thickness doesn't influence the efficiency of the membrane.

Mitchell et al. (1973) evaluated the chemico-osmotic consolidation of different low permeability materials. These authors measured the loss in pore volume as water is drawn out from the clay due to osmosis. Major losses were reported for bentonite.

The membrane efficiencies measured in the laboratory vary within a large range of values depending on the experimental conditions, material and solutions used. Minimum and maximum efficiency values reported for bentonite ranged between 4% and 84% and for smectite between 21% and 52% .

Literature on laboratory experimental work is extensive and the reported findings may be used to indicate the potential semi-permeable membrane behavior of low permeability geological formations. The above review of laboratory studies suggests that smectite-rich geological formations are likely to exhibit the strongest membrane behavior. It also suggests that smectite-rich clay sediments within fresh groundwater systems, may exhibit membrane behavior even at relatively small degrees of compaction.

However, the extent to which inferred relationships are applicable to field studies is questionable because laboratory conditions usually differ from subsurface conditions. Laboratory experiments involve the use of samples made of commercially-available clays or remolded sediments, which are not representative for heterogeneous geological deposits. Similarly, solutions that are used in laboratory experiments are usually artificial and not representative of the sediment pore water. An exception is the laboratory study conducted by Cey et al. (2001)who used natural groundwater. Furthermore, the pressure gradients used in laboratory experimental work are usually as much as six orders of magnitude higher than the gradients present in the subsurface (Alexander, 1990).

2.5   Evidence from Field Investigations

Compared to results from laboratory measurements, evidence for osmotic phenomena obtained from field studies tends to be more circumstantial. It is mainly based on observations of anomalous fluid pressures and fluid concentrations that could not be readily explained by more conventional hydrological processes (Berry and Hanshaw, 1960; Hanshaw and Hill, 1969; Kharaka and Berry, 1973; Marine and Fritz, 1981; Graf, 1982; Fritz and Marine, 1983; Horseman et al., 1996; Neuzil, 1995, 2000). A short description of the results and conclusions of some of these studies is given below.

Hanshaw and Hill (1969) studied and reported on the hydrology and geochemistry of two interconnected basins: the Paradox Basin (extending through Utah, Colorado and New Mexico) and the San Juan Basin (North Western New Mexico). Within the Cretaceous strata of the San Juan basin anomalous low pressures were observed. Further observations showed the occurrence of brines and inexplicable high pressures in the Pensylvanian and Misissipian Paleozoic aquifers in the Paradox Basin. Based on these observations, Hanshaw and Hill (1969) suggested the existence of an osmotic flow system acting within the entire upper part of the Cretaceous strata of the San Juan Basin in which the Paleozoic aquifer units of the Paradox Basin act as the outflow receptors of the membrane system.

Kharaka and Berry (1974) studied the regional hydrogeology and hydrochemistry of the Kettleman North Dome oil field in California. The Miocenic Temblor formation contains most of the oil and gas in the field and was subdivided into five sand units, each separated by at least 15 m of shale beds. The water from the Temblor formation was determined to be meteoric in origin, and its elevated concentration relative to meteoric water is attributed mainly to hyperfiltration through the shale membranes. The chemistry of the pore water of a given sand unit exhibited membrane effluent characteristics with respect to the unit stratigraphically below. The overall chemical compositions of water in the Temblor showed also membrane effluent characteristics and followed the retardation sequences found in the laboratory by Kharaka and Berry (1973) (see section 4). Hydrogen isotopic fractionation was demonstrated and this could only be attributed to osmosis.

Fritz (1986) investigated high observed pressures in two wells drilled in the Triassic-age Dunbarton Basin, and identified them as a good example of osmotically-induced potentials. The heads found in these two wells (192m and 140m above sea level), drilled into the low permeability sediments, are well above the local water table developed in the overlying Cretaceous coastal plain sediments (58m above sea level). Marine and Fritz (1981) calculated the osmotic equilibrium head from the solution concentration of water produced by each well and concluded that it approximates the observed head in the wells. Based on these findings they suggested that the low permeability sediments behave nearly as an ideal membrane. In Chapter 7 the Dunbarton Basin will be described in more detail and numerical modelling of this case is presented.

Although observational evidence in studies like the ones discussed here is intriguing and rather convincing, several key questions remain. It is generally unclear to what extent these observations are indeed produced by coupled flows, or are the product of other mechanisms. More conventional geological processes or mechanisms (thermal effects, mineral diagenesis, tectonic compression, gas migration, erosion, etc) could explain the anomalies observed (Neuzil, 2000). Further, conditions suitable to maintain osmotically-induced fluxes and to prevent the associated pressures from dissipating (heterogeneity, leakage) should prevail.

The first "direct" experimental evidence for osmosis at the field scale has been obtained by Neuzil (2000) at a site in the Cretaceous-age Pierre Shale in South Dakota. Waters of different salinity were added to four boreholes. Two boreholes received water with high salt concentration (35 g/l), one received a duplicate of the expelled pore water (3.5 g/l) and one received de-ionized water. During nine years water levels and borehole TDS were monitored. Differences in well responses provided strong evidence for contributions by chemical osmosis in wells with the more saline waters. Heads in the boreholes with saline water increased to a maximum of 2m compared to the one with duplicate pore water. By analyzing the pressure and TDS readings after nine years, which were assumed to correspond to osmotic equilibrium, Neuzil (2000) calculated membrane properties of the Pierre Shale (reflection coefficient σ). The calculated efficiencies for higher and lower concentrations were close to 4% and 14% respectively. The experiment of Neuzil (2000) is described in more detail in Chapter 6.

Recently, Noy et al. (2004) reported results obtained from direct experimental *in situ* evidence for osmotic phenomena in the Jurassic-age Opalinus Clay in Switzerland. The

research programme at Mont Terri consisted of laboratory tests on samples, *in situ* experiments in a borehole at the Mont Terri Rock Laboratory and a theoretical study supported by mathematical modelling. For the *in situ* experiments water within a sealed borehole was equilibrated with the Opalinus Clay pore water followed by a sudden water exchange (fresh or hypersaline brine). Due to the induced chemical gradient Noy et al. (2004) observed a significant pressure increase (several meters of water) that persisted for several months. The reflection coefficient of the Opalinus Clay was inferred by matching the pressure response data to the theoretical model equations. Low efficiencies for higher and lower water concentrations were found (3.6% and 8% respectively).

2.6   Quantitative Theoretical Framework

A considerable volume of literature exists on the theory of membrane properties of clays. Much of it concerns how membrane efficiency is affected by clay porosity and geochemistry and by ion-solid interaction properties like exchange capacity, salt exclusion behavior and thickness and concentration of the solution between the negatively charged clay platelets (Kemper and Rollins, 1966; Groenevelt and Bolt, 1969; Bresler, 1973; Hanshaw and Coplen, 1973; Kharaka and Berry, 1973). In these studies, relationships have been developed that are mostly based on the Donnan membrane equilibrium concept, the Teorell-Meyer- Siever theory and the Gouy double layer theory (see Keijzer (2000) for a review). Some of these models are described in detail by Horseman et al. (1996) and by Keijzer (2000). A number of models were used and compared by Keijzer (2000) to predict the reflection coefficient of commercial bentonite. In the following section some of the models are briefly explained. Particularly the relationship presented by Bresler (1973) is adopted later in the present study for simulations.

Kemper and Rollins (1966) and Bresler (1973) assumed that anion exclusion occurs over the entire water layer and that anions and cations are uniformly distributed on the external surfaces of the clay according to the planar diffusive double layer theory. These authors presented the dependence of efficiency on the salt exclusion factor (function of the external solution equilibrium concentration) and the thickness of the water film between overlapping double layers. The osmotic efficiency coefficient σ according to Bresler (1973) is strongly dependant on the water film thickness b and on the equilibrium concentration of the monovalent anion. This relationship is used later in Chapter 6.

Groenevelt and Bolt (1969) also calculated the salt exclusion as a function of the double layer properties. These authors assumed that the ion distribution in the double layer follows the corrected Gouy-Chapman theory (Keijzer, 2000). Accordingly, salt exclusion doesn't occur over the entire thickness of the water layer but only within that part that is known as the mobile water layer. Hanshaw and Coplen (1973) and Marine and Fritz (1981) developed a theory to explain and quantify salt sieving effects by means of the Donnan membrane equilibrium concept and the Teorell-Meyer-Siever theory. In particular Marine and Fritz (1981) redefined and modified these concepts and together with laboratory-derived results developed a theory that relates the reflection coefficient to porosity and the mean concentration of the solutions on either side of the membrane.

References

Alexander, J., 1990. A review of osmotic processes in sedimentary basins. British Geological Survey, Report no. WE/90/12.

Barbour, S., Fredlund, D., 1989. Mechanisms of osmotic flow and volume change in clay soils. Canadian Geotechnical Journal (26), 551–562.

Benzel, W., Graf, D., 1984. Studies of smectite membrane behavior - Importance of latter thickness and fabric at 20°C. Geochimica et Cosmochimica Acta (48), 1769–1778.

Berry, F., 1969. Relative factors influencing membrane filtration effects in geological environments. Chemical Geology , 295–301.

Berry, F., Hanshaw, B., 1960. Geological field evidence suggesting membrane properties of shales. In: International Geological Congress. Report of the twenty first session Norden, Copenhagen, Denmark. p. 209.

Bresler, E., 1973. Anion exclusion and coupling effects in non-steady transport through unsaturated soils. Soil Sci. Soc. Am. Proc. (37), 663–669.

Cey, B., Barbour, S., Hendry, M., 2001. Osmotic flow through a Cretaceous clay in southern Saskatchewan, Canada. Canadian Geotechnical Journal (38), 1025–1033.

Fritz, S., 1986. Ideality of clay membranes in osmotic processes: a review. Clays and Clay minerals (34), 214–223.

Fritz, S., Marine, I., 1983. Experimental support for a predictive osmotic model of clay membranes. Geochimica et Cosmochimica Acta (47), 1515–1522.

Graf, L., 1982. Chemical osmosis, reverse osmosis, and the origin of subsurface brines. Geochemica et Cosmochemica Acta 46, 1431–1448.

Groenevelt, P., Bolt, G., 1969. Non-equilibrium thermodynamics of the soil water system. Journal of Hydrology (7), 358–388.

Hanshaw, B., Berry, F., 1969. Natural membrane phenomena and subsurface waste emplacement. In: Underground waste management and environmental implications. Memoirs American Association Petroleum Geologists (18), 308–317.

Hanshaw, B., Coplen, T., 1973. Ultrafiltration by a compacted clay membrane: II. Sodium ion exclusion at various ionic strengths. Geochimica et Cosmochimica Acta (37), 2311–2327.

Hanshaw, B., Hill, G., 1969. Geochemistry and Hydrodynamics of the Paradox basin region Utah, Colorado and New Mexico. Chemical Geology (4), 263–294.

Horseman, S., Higgo, J., Alexander, J., Harrington, J., 1996. Water, gas and solute movement through argillaceous media. Nuclear Energy Agency, Organization for Economic Cooperation and Development, report CC 96-1 Paris.

Katchalsky, A., Curran, P., 1965. Non equilibrium thermodynamics in bio-physics. Harvard University Press.

Keijzer, T., 2000. Chemical osmosis in natural clayey material. Ph.D. thesis, Universiteit Utrecht, The Netherlands.

Kemper, W., 1961. Movement of water as affected by free energy and pressure gradients. I Application of classic equations for viscous and diffuse movements to the liquid phase in finely porous media II. Experimental analysis of porous systems in which free energy and pressure gradients act in opposite directions. Soil Science Society of America Proceedings , 260–265.

Kemper, W., Rollins, J., 1966. Osmotic efficiency coefficients across compacted clays. In: Soil Science Society of America 30. pp. 529–534.

Kharaka, Y., Berry, A., 1973. Simultaneous flows of water and solutes through geological membranes: I. Experimental investigation. Geochimica et Cosmochimica Acta (37), 2577–2603.

Kharaka, Y., Berry, A., 1974. The influence of geological membranes on the geochemistry of subsurface waters from Miocene Sediments at Kettleman North Dome in California. Water Resources Research (10), 313–327.

Kharaka, Y., Smalley, W., 1976. Flow of water and solutes through compacted clays. American Association of Petroleum Geologists Bulletin (60), 973–980.

Malusis, M.A., S. C., Olsen, H., 2003. Flow and transport through clay membrane barriers. Engineering Geology 70, 235–248.

Marine, I., Fritz, S., 1981. Osmotic model to explain anomalous hydraulic heads. Water Resources Research 29 (17), 73–82.

Mitchell, J. K., 1993. Fundamentals of soil behavior., 2nd Edition. John Wiley and Sons, New York.

Mitchell, J. K., Greenberg, J., Whiterspoon, P., 1973. Chemico-Osmotic Effects in Fine-Grained Soils. Journal of the Soil Mechanics and Foundations Division, ASCE (SM4), 307–322.

Neuzil, C., 1995. Abnormal Pressures as hydrodynamic phenomena. American Journal of Science (295), 742–786.

Neuzil, C., 2000. Osmotic generation of "anomalous" fluid pressures in geological environments. Nature (403), 182–184.

Noy, D., Horseman, S., Harrington, J., Bossart, P., Fisch, H., 2004. An Experimental and modelling study of chemico-osmotic effects in the Opalinus Clay of Switzerland. In: Heitzmann, P. ed. (2004) Mont Terri Project - Hydrogeological Synthesis, Osmotic Flow. Reports of the Federal Office for Water and Geology (FOWG), Geology Series (6), 95–126.

Oduor, P., 2004. Transient modeling and experimental verification of hyperfiltration effects. Ph.D. thesis, Department of Geological and Petroleum Engineering, University of Missouri-Rolla.

Olsen, H., 1972. Liquid movement through kaolinite under hydraulic, electric and osmotic gradients. American Association of Petroleum Geologists Bulletin (56), 2022–2028.

Walter, G., 1982. Theoretical and experimental determination of matrix diffusion and related solute transport properties of fractured tuffs from Nevada test site. Los Alamos National Laboratory report LA-9471-MS.

Whitworth, T. M., DeRosa, G., 1997. Geologic Membrane Controls on Saturated Zone Heavy Metal Transport. New Mexico Water Resources Research Institute Report 303.

Young, A., Low, P., 1965. Osmosis in argillaceous rocks. American Association of Petroleum Geologists Bulletin (49), 1004–1008.

Chapter 3

Selection and Development of Instrumentation for Osmosis *In-Situ* Testing

Direct evidence of osmotic processes operating at the field scale is scarce. It is therefore not surprising that there are no standard, tested procedures and methods for field measurements of osmotic behavior of clays. In this chapter the instrumentation is described that has been used in this study to carry out field measurements of osmotic properties of clays in the subsurface. The field experiments that were conducted with these instruments are presented in Chapters 4 and 5. Considerable effort has been put in both the selection of existing instruments that might be potentially suitable for field testing and the design and development of new instruments. Part of this chapter is therefore devoted to elucidate the selection process and to provide the rationale for the design that was ultimately adopted.

3.1 General Considerations

Providing direct evidence for osmotic processes operating within a clay layer is time consuming and complex because of the low permeabilities involved (Neuzil, 2000). For this study the design and development of instrumentation and a testing methodology that allow for in-situ measurements of parameters required to quantify membrane properties are needed. The experimental design to be used should strike an optimal balance among experiment duration, ability to monitor water chemistry and the magnitude of the osmotically-induced pressure. Until now, laboratory studies have limited experiment duration by using remolded samples of limited thickness (only few mm thick) and experimental pressure gradients that greatly exceed in-situ pressure gradients (Neuzil, 1986; Alexander, 1990). Normally, laboratory studies are conducted in a set-up similar to the one displayed in Figure 2.1a : a remolded semi-permeable clay membrane separating two closed reservoirs containing different aqueous solutions. Within the reservoirs pressure/flow responses and water chemistry are monitored or controlled. Experimental conditions vary depending on the type of test. Ultrafiltration tests imply application of high hydraulic gradients (exceeding osmotic pressure) across the semi-permeable membrane. Chemical osmosis tests require an initial hydraulic equilibrium condition.

At the field scale, two high permeability layers (e.g. aquifers) acting as reservoirs and a

separating clay layer may resemble the typical laboratory experimental configuration. However major differences and practical complexities are involved if testing is to be carried out in such a set-up. First, perturbation of the natural conditions can not be avoided. Second, imposition of the required chemical gradient and/or pressure controls (e.g. initial equilibrium condition for osmosis tests or imposed hydraulic gradient for ultrafiltration tests) become difficult in practice. Third, flow or pressure responses should be measured within the layers acting as membrane or reservoirs. In order to observe these responses, some conditions must prevail to ensure that osmotic fluxes are maintained and that its fast dissipation due to salt diffusion across the membrane is prevented (Fritz, 1986). Thus, the low permeability formation acting as the membrane should be rather continuous to avoid leakage. Further, observation of osmotically-induced pressures in the reservoir receiving the induced flux (e.g. an aquifer) would become only possible if this layer is surrounded by impervious material: in this way pressure is allowed to build-up and to be maintained.

A more practical alternative seems to be the utilization of the methods and instrumentation conventionally used for hydraulic characterization of aquifers and aquitards (boreholes, wells, piezometers and push-in probes). In this case the instrument itself plays the role of the reservoir containing the high/low concentration water and it is placed in direct contact with the clay that contains lower concentration pore water. Monitoring of both hydrochemistry and pressures can be more easily carried out within the instrument. Below, first a review of existing methods for hydraulic measurements and hydrochemical monitoring/sampling is presented. For each method the advantages/disadvantages are explored.

3.1.1   Hydraulic Measurements and Characterization Methods in Tight Formations

Both laboratory and field measurement methods exist to determine hydraulic parameters (hydraulic conductivity and specific storage) of compacted clays. However, because of the difficulties in field tests, most of the measurements on low permeability sediments are conducted in the laboratory (permeameters and consolidation tests). Controversy exists about the applicability of laboratory experimental results to field studies (Neuzil, 1986; Alexander, 1990; Horseman and Higgo, 1994; van der Kamp, 2001). Laboratory techniques only allow the investigation of small samples of sediments and typically use hydraulic gradients of many orders of magnitude higher than those found in the field. In contrast, in-situ methods allow testing of larger volumes of sediment material that may incorporate secondary features such as macro-pores and cracks that are not represented in laboratory experiments.

In-situ testing methods used for determining the properties of tight formations fall into several categories: infiltrometers, lysimeters, borehole testing and push-in devices (David, 1989; Stienstra and van Deen, 1994). In this chapter only in-situ techniques will be briefly described, particularly borehole testing and push-in devices which are useful for in-situ osmosis testing.

Borehole Tests. Borehole tests that are commonly used to characterize aquifer properties also appear to be a common technique for hydraulic characterization of low-permeability natural deposits. However, due to the low permeability of these materials the conventional
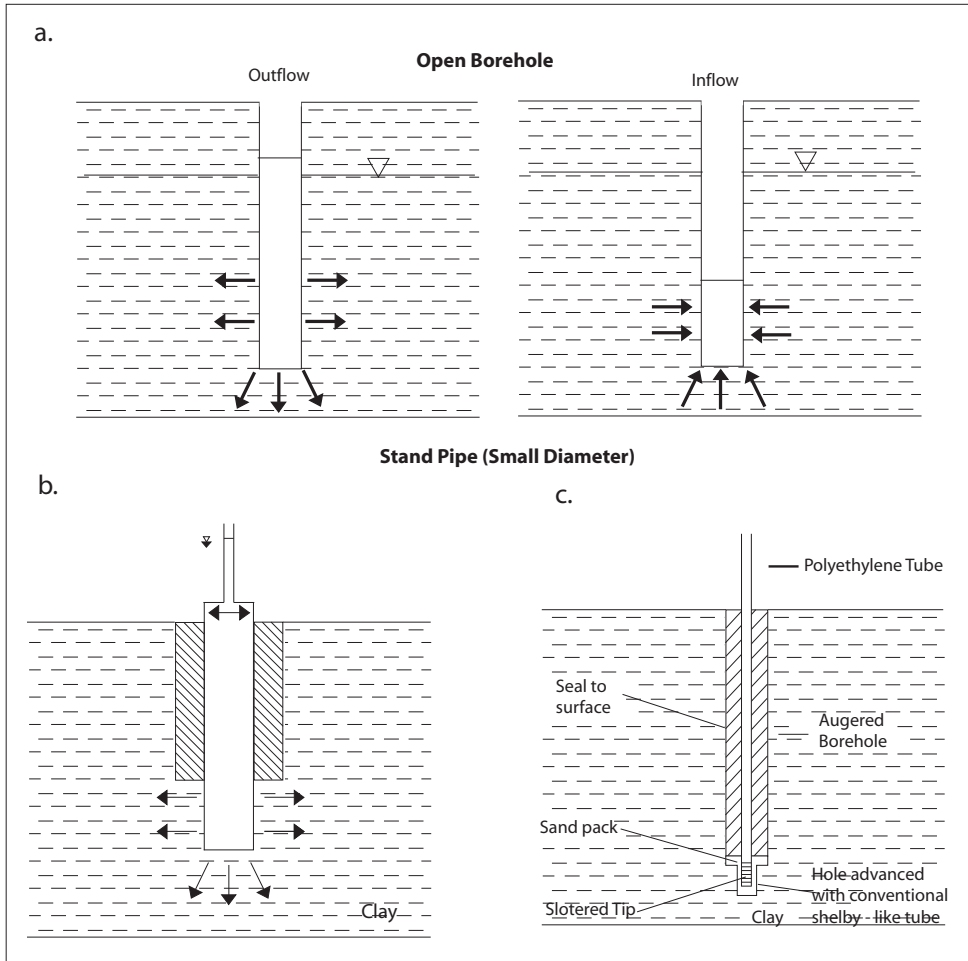
Figure 3.1: Schematic diagram of open borehole testing: a. Conventional outflow and inflow tests in large diameter boreholes. b. Small diameter pipe is used only where the expected water level change takes place (David, 1989). c. Small diameter pipe testing; polyethylene tube (0.64cm diameter) used by McKay et al. (1993)

.

measurement of hydraulic heads is problematic. Low permeability and large well bore storage make the head changes occur extremely slowly, rendering direct observations impractical (Neuzil, 1986).

Conventional methods have been modified in several ways to overcome those problems (Neuzil, 1986; David, 1989; Stienstra and van Deen, 1994; van der Kamp, 2001). Table

Table 3.1: In-situ methods for characterizing tight formations and their suitability for osmosis testing

Technique/Test	Advantage	Disadvantage
Borehole Testing		
Slug test (Figure 3.1)	Easy installation Simple performance	Very long response time
Constant Head Permeability test.	Easy installation	Complex performance
Shut-in test (Figure 3.2)	Short response time	Small volume tested Leakage
Push-in Devices/ Porous devices (Figure 3.3)	Quick measurements	Small volume tested Trapped air

3.1 summarizes the conventional borehole testing methods to characterize aquifers and the advantages/disadvantages when used in aquitards. The contents of the table are based on the reviews of Neuzil (1986), David (1989) and van der Kamp (2001). In this section slug tests and shut-in tests are presented in greater detail and compared.

Slug tests (Figure 3.1a) are also commonly known as falling/rising head tests or borehole/piezometer hydraulic conductivity tests. They are carried out by causing an instantaneous water level change relative to the equilibrium background level and observing its falling/rising with time in an open standpipe/piezometer. This type of test is considered very useful when estimating the large-scale permeability of aquitards although fracture permeability may not be identified (van der Kamp, 2001). Only a small volume near the piezometer intake is influenced by the test and the estimated conductivity is only representative for that volume. Furthermore, for very low permeability formations without fractures the response time to a disturbance is usually very long (months). The response time depends on how fast the water flows between the borehole and the formation as well as the storage within the standpipe.

Several methods exist that considerably shorten the duration of borehole tests (van der Kamp, 2001; Bredehoeft and Papadopulos, 1980; Neuzil, 1986; McKay et al., 1993, 1998; Wassenaar and Hendry, 1999). Decreasing the piezometer diameter is an alternative to conventional testing (Figures 3.1b and c). Observation of pore fluid pressure changes within closed and pressurized piezometers or tested intervals allows as well for the determination of the vertical permeability in relatively short periods of time.

The shut-in test (Figure 3.2) is an alternative method for evaluating tight formations and is a variation of the conventional slug test. Instead of imposing a head change and observing its falling in a standpipe, the borehole/pipe is filled with water to the surface and pressurized

using an additional amount of water. Thereafter the borehole is shut-in and the change in head/pressure is monitored. The change in pore fluid pressure is usually measured continuously with pressure transducers. The method has as advantage that the field test can be conducted within a relatively short period of time. The response time in this test is reduced since the storage in the borehole is due to the water and system compressibility, while in the open standpipe it is due to the water level changes within it. One of the difficulties of this method is that although time response is reduced a proportionally smaller volume of rock is tested. Tests with a short duration can be influenced by the material immediately adjacent to the borehole. This material is most likely to be damaged by drilling the borehole and/or emplacing of the instrument. Other disadvantage of the shut-in tests is that any leakage (through packers or sealing materials) can cause an artificial fall in pressure, resulting in erroneously estimated values for the permeability. In the same way, if air or gas is trapped in the shut-in volume, the effective compressibility will increase and therefore the response time will be longer. More importantly, the effective compressibility is not accurately known in that case.

Bredehoeft and Papadopulos (1980) presented the shut-in test as an alternative to the conventional slug test. Based on an analytical solution they compared the head decay for both methods (Figure 3.4) for hydraulic and well parameters listed in Table 3.2.

The figure shows for instance that for 80% head decay the time required for a pressurized test is four hours while for the conventional test the duration of the test is three and a half years. Bredehoeft and Papadopulos (1980) also demonstrated that a reduction of the radius of the standpipe for the open test to 0.78 mm would be required to shorten the response time
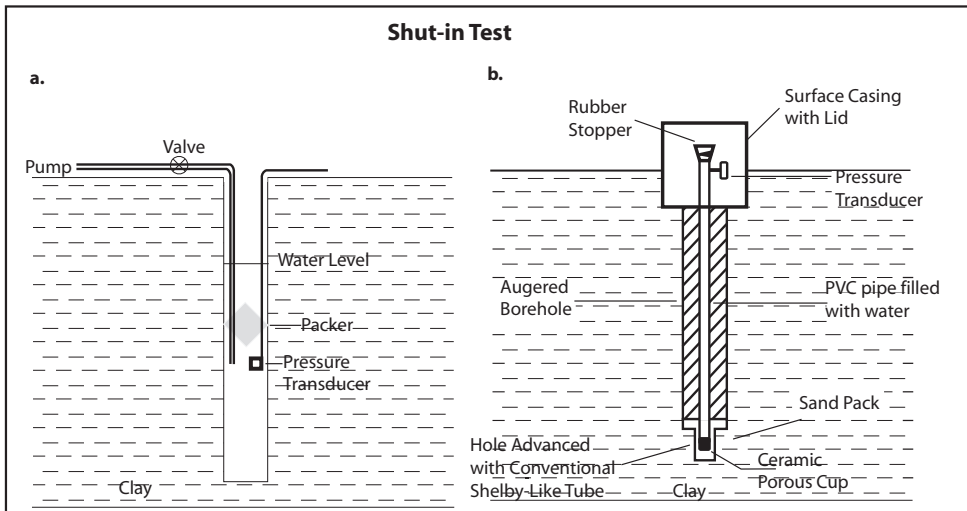

Figure 3.2: Representation of Shut-in borehole testing: a. using packers (Bredehoeft and Papadopulos, 1980), and b. piezometer using transducers (McKay et al., 1993).

Table 3.2: Parameters used by Bredehoeft and Papadopulos (1980) in illustrative example to compare results between slug test, shut-in test and small-diameter pipes test

Parameter	Dimension
Transmissivity tested interval	$10 \cdot 10^{-11}$ (m^2/s)
Storage Coefficient tested interval	$4 \cdot 10^{-4}$
Thickness tested interval	10m
Radius of well in tested interval	0.1m
Compressibility of water	$4 \cdot 10^{-10}$ (m^2/N)
Density of water	1000 (kg/m^3)
Radius of standpipe	0.02 m
Length of standpipe	90 cm

to that of the shut-in test.

Porous Probes/Push-in Devices. Porous probes (Figure 3.3) have been widely used for pore pressure measurements in saturated non-compacted clay (Wolff, 1970; David, 1989). These devices can be pushed or driven into the clay sediment. Changes in pressure within the porous probe usually are monitored with pressure transducers. Slug or constant head tests can be also performed using porous probes. Torstensson (1984) presented a device that has been utilized in moderately compacted clay sediments: the BAT permeameter/probe (Figures 3.6 and 3.7). In section 3.2.4 a detailed description of the BAT-permeability system is provided since the instrument is useful for osmosis in-situ testing.

3.1.2 Methods for Characterizing Pore-Water Chemistry in Tight Formations

Several methods for characterization and monitoring of pore-water chemistry are available. The selection of any specific method depends on the type of data that are required. It is important to make a distinction among the different types of water and their distribution in the clay/system: absorbed water, interlayer water and pore water. Direct comparison of results from the various methods is complex. Simultaneous use of several methods could be necessary to have a comprehensive understanding of the hydrogeochemistry of the system (Bath, 1994). Nowadays international projects such as ARCHIMEDE ARGILE (Horseman and Higgo, 1994) and the Mont Terri Geochemical Project (Noy et al., 2004) have the objective of hydrochemical characterization of mudrocks (potential host rocks for ra-
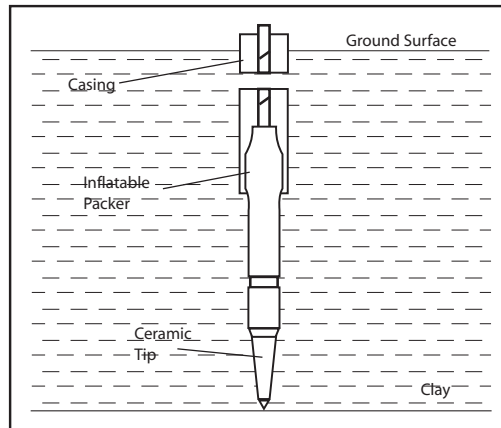
Figure 3.3: Illustration of a porous probe, taken from Wolff (1970).

dioactive waste containment) including comparison of techniques and results. Among the most commonly utilized pore water characterization techniques are squeezing and leaching of sediment samples and piezometer sampling. In this chapter reference is made only to piezometer sampling which is a common technique employed for hydrochemical monitoring.

Piezometer Sampling. Water samples from piezometers placed in aquitards are more representative of the in situ pore water in natural conditions than water extracted from cores. Sampling of undisturbed in-situ pore water using piezometers is time consuming due to the low permeability and the slow flow rate into the piezometer. Reducing the diameter of the well is not only advantageous for permeability measurements, it also enhances the hydrochemical sampling. Compared to larger diameter observation wells the amount of formation water necessary for flushing is less. Standpipes with a few millimeters diameter (12 mm: 4 times smaller than the standpipes often used for monitoring) have been tested with good results in a thick clay-rich glacial till in Sakatchewan, Canada (McKay et al., 1998; Wassenaar and Hendry, 1999). Due to the very low hydraulic conductivity of aquitards the water recovery is slow and therefore the temporal sampling strategy was adjusted to that recovery rate.

Water samples collected from filters placed in aquitards have shown chemical contamination due to contact (for extended periods of time) with the sealing materials used during

piezometer installation (Wassenaar and Hendry, 1999). This problem may be avoided with careful piezometer design and the use of inert sealing materials.

Several closed boreholes equipped with specific monitoring instrumentation (Eh, pH) and that collect pore water periodically, have been recently utilized with success in the hydrogeochemical studies of the Opalinus Clay in Switzerland (Noy et al., 2004) and the Boom Clay in Belgium (Merceron and Mossman, 1994). Nevertheless squeezing and leaching of cores provided additional information in these studies.

3.2   Chemical Osmosis In-Situ Testing Instrumentation

The membrane properties of low permeability materials have been widely studied in the laboratory, but not in field studies. At the initial phase of this project in 2001, the only study reporting on direct measurements of clay-membrane properties was the one presented by Neuzil (2000). Later during the project Noy et al. (2004) reported on results obtained for in-situ measurements aiming to asses the semi-permeable membrane behavior of the Opalinus Clay. The final instrumentation for in-situ osmosis tests was therefore designed and constructed based on the existing testing methods presented in section 1.1 , the experience
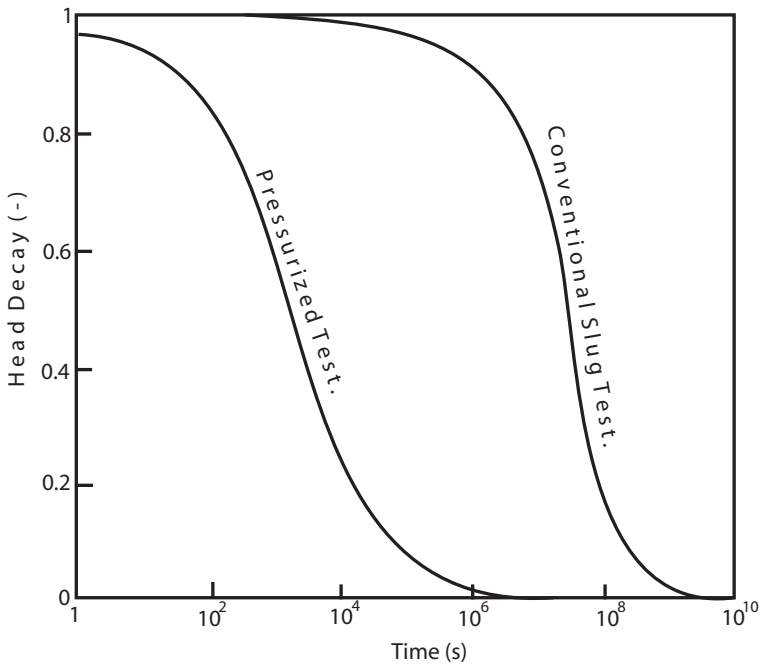

Figure 3.4: Head or water level decay in well system during pressurized and conventional slug tests, after Bredehoeft and Papadopulos (1980).

of Neuzil (2000) and results of experiments with bentonite that are briefly described later.

3.2.1   Neuzil's Experiment

In-situ measurements of both fluid pressures together with total dissolved solids changes have been obtained for the first time for a Cretaceous-age Pierre Shale in South Dakota (Neuzil, 2000). A detailed description of the experiment in the Pierre Shale is found in Chapter 6. In this section only the experiment configuration and testing methodology are briefly presented. For the experiment, four 14 cm-diameter boreholes were drilled and a large diameter (6 cm) PVC casing slotted at the bottom was installed. Clean sand was used for the contact area between the clay and the screen. In the upper part of the construction, aggregate-free cement was used as a sealing material. The clean sand pack was isolated from the cement by shale cuttings and powdered bentonite. Due to the low pore pressure of the shale, an initial condition of hydraulic equilibrium (prerequisite of chemical-osmosis testing) was not achieved. Four tests were conducted. One conventional slug test using a solution that replicated the shale pore water concentration and three modified slug tests using solutions of different concentrations. The test was modified with respect to a conventional slug test since rather than imposing only an instantaneous water level change at the beginning of the test, a salt concentration gradient was also imposed (between borehole and the shale). Two piezometers were filled with high salinity water, one with an approximate duplicate of the shale pore water and one with de-ionized water. With the initial condition of hydraulic disequilibrium, comparison of responses for the different water types was crucial to isolate the osmotic effect. Furthermore, the use of large diameter piezometers in this low permeability-shale made the test response time extremely slow and non-practical for normal testing cycles (nine years until osmotic equilibrium seemed to have been reached).

3.2.2   Preliminary Laboratory Testing of Small-Diameter Standpipe Concept

Based on the experience of Neuzil (2000), we initially opted to continue working with open piezometers and the same testing methodology. However in order to reduce the duration of the experiment significantly the configuration was modified by introducing a small-diameter standpipe in a similar set-up to the one displayed in the Figure 3.1b. The large-diameter piezometer constitutes the high concentration water reservoir and is placed within the clay section to be tested. The small-diameter standpipe is attached to the reservoir only where the presumed water level change is expected to occur. In this way duration of the experiment shortens and the induced chemical gradient dissipates slower. Preliminary tests using this configuration on saturated bentonite and other clays were conducted in the laboratory. The tests were performed using scaled-down versions of the field instrument described above. A small-scale stainless steel filter (4 cm diameter, 18 cm long) attached to a small-diameter glass standpipe (2 mm diameter) was placed into continuously saturated commercial bentonite. Water level changes were monitored within the standpipe. The small-scale system did not include an option to monitor water chemistry. Prior and during the test the bentonite was saturated with fresh water. The filter/glass standpipe is pre-filled with high

NaCl concentration water and pushed into the bentonite. The experimental conditions for this preliminary test (dimensions of the filter and standpipe, quality of water used, amount of bentonite, etc) were determined using numerical modelling (See model details in Chapter 6). A significant osmotic effect in a reasonable period of time (2.5 cm water column in 15 days) was predicted. Problems with filling the filter (filling through glass standpipe) and leakage along the sides of the instrument were encountered. Additionally, air was trapped in the reservoir section during its insertion into the clay. A new instrument was designed and built to correct for these deficiencies (removable standpipe and one additional opening in the filter to allow air to escape). In spite of improvements, the virtually unlimited swelling capacity of the bentonite made experimenting difficult. For that reason, different types of clay (artistic clay, clay from excavation site and Calais Clay) were also tested. Preliminary tests with the new instrumentation and new clay material showed improved performance (maintaining an initial water level in the standpipe was possible), however the leakage was only partially solved. It was concluded that a full solution to the leakage problems was most likely possible by placing the filter deeper into fully and permanently saturated more compacted clay. These conditions could possibly be attained directly in the field without replicating them at small scale. Although the small scale experiments were not very successful they were useful for the improvement of the instrument and for the determination of certain conditions favorable for field testing.

3.2.3 Piezometer System for Field Testing

The piezometer for in-situ testing was constructed in such a way that it may be used both in open (small-diameter standpipe) and closed reservoir (shut-in) configuration (Figure 3.5). When experiment duration is considered, shut-in systems seem to be more efficient than small-diameter standpipes (Bredehoeft and Papadopulos, 1980). Equilibrium pressure is reached in a shorter time and fast enough to avoid dissipation of the induced chemical gradient. Additionally filling up of the instrument with solution is easier in a piezometer without attached small-diameter standpipe as experienced with small-scale tests.

The instrument basically consists of a stainless steel pipe with a 40 cm long filter section of stainless steel screen. A lid in the top that may be placed/removed by screwing allows the filling of the instrument with solution. When the small-diameter stand pipe configuration is used, changes in head are monitored in the glass stand pipe itself. The design was constructed such that the small-diameter glass standpipe can be attached to the top of the stainless steel pipe. The filter section and piezometer/reservoir are relatively large diameter to increase the amount of solute in the piezometer and to limit effects of diffusion. Diffusion reduces any chemical contrast between the instrument and the clay rather quickly, muting or making osmotic effects undetectable. When the instrument is used in the "shut-in" configuration, changes in fluid pressure are monitored by utilizing sensors. Fluid pressure changes are measured with pressure transducers. Unfortunately, the instrument configuration makes it difficult to sample the borehole fluids without disturbing the pressure. Thus, monitoring of concentration changes without sampling is done by measuring electrical conductivity (EC) with a sensor containing a conductivity cell (range 0-80 mS/cm). The top lid itself has sev-
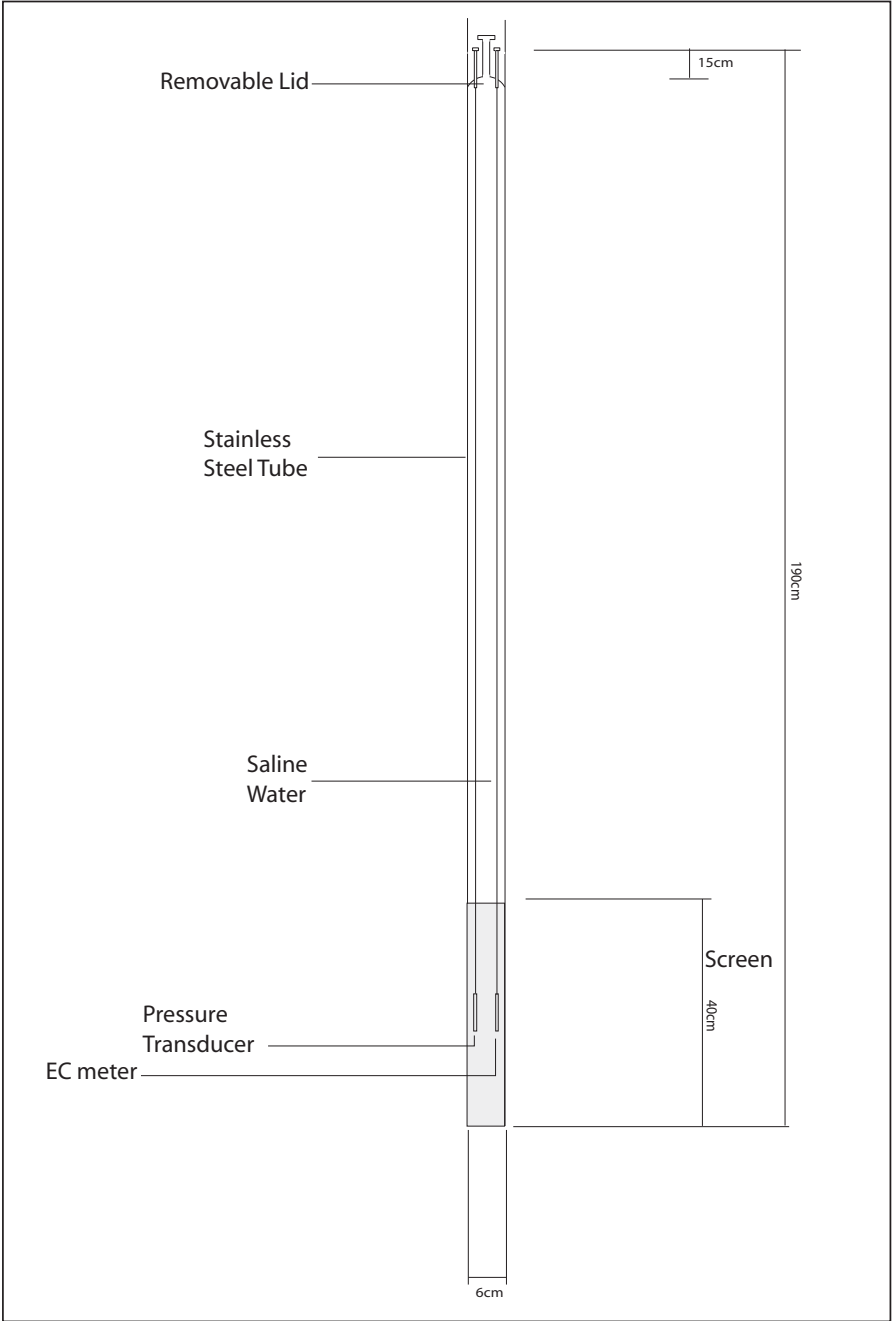
Figure 3.5: Experimental design built and used for in-situ evaluation of osmosis.

eral openings where the standpipe is placed or the cables for the transducers pass through. One additional opening allows air to escape during filling. A support rod is attached to the center of the lid. The rod is mainly used for guiding the cables of the sensors and to fix their position within the instrument. The length of the rod is such that the sensors are positioned in the middle of the filter-screen. During an experiment simultaneous measurements of fluid pressure (hydraulic head) and fluid salinity (EC) variations are made. Performance of this type of tests, requires special attention for the presence of trapped air after shutting-in the system and any leakage that might lead to erroneous pressure recordings. The instrument dimensions where chosen so that the instrument is suitable to use in a shallow clay formation (Calais Clay top not more than 1 m deep) that was selected for osmosis in-situ experiments (see Chapter 4). Additionally, calculations of response time were done (response for a shut-in test expected within 12 hours) using the analytical solution introduced by Bredehoeft and Papadopulos (1980).

In-situ testing in this study was conducted by using the design described above. Additionally, existing instrumentation such as the BAT probe and a piezometer used at the Underground Research Laboratory (URL) in Mol, Belgium were used. The piezometer used at the URL will be described in Chapter 5.

3.2.4   BAT Probe and BAT Permeability Systems

The BAT-permeability system for in situ measurement of the hydraulic conductivity (or permeability) is an extension of the BAT-system (porous probe composed of a filter porous tip and a electronic pressure transducer that allows accurate and efficient measurements of the pore pressure in the soil (Figure 3.6). The permeability measuring set (Figure 3.7) consists of a test adapter that is equipped with a double-sided hypodermic needle and a gas/water container. The test can be carried out either as an inflow test (at the beginning of the test the pressure within the container is set to be lower than the pore pressure in the clay) or an outflow test (the container is partly filled with water and partly filled with compressed gas such that the pressure in the container is higher than the pore pressure in the clay). Additionally, an inflow test automatically incorporates sampling of pore water for further chemical analysis. The arrangement for an outflow test can also be used for the controlled injection of a tracer liquid into the soil. The spreading of this liquid can be checked by repeated sampling in filter tips installed at different distances from the point of injection. A typical set-up for permeability measurements with a BAT probe is described next and depicted in Figure 3.7. The filter tip is pushed or driven in to the soil and the pore pressure in the soil is monitored with the BAT system prior to the beginning of the permeability test. The aim of this monitoring prior to the actual permeability test is to characterize the background pore pressure and to allow some time for equilibration. Subsequently, the adapter is lowered into the extension pipe. The adapter is automatically connected to the filter tip by means of the double-sided hypodermic needle. Upon connection the pressure in the filter tip quickly equilibrates with that in the container. As water flows in/out the filter tip pressure changes are recorded within the container with the aid of the BAT system. The BAT pts-software allows inversion modelling of the pressure data to obtain permeability.
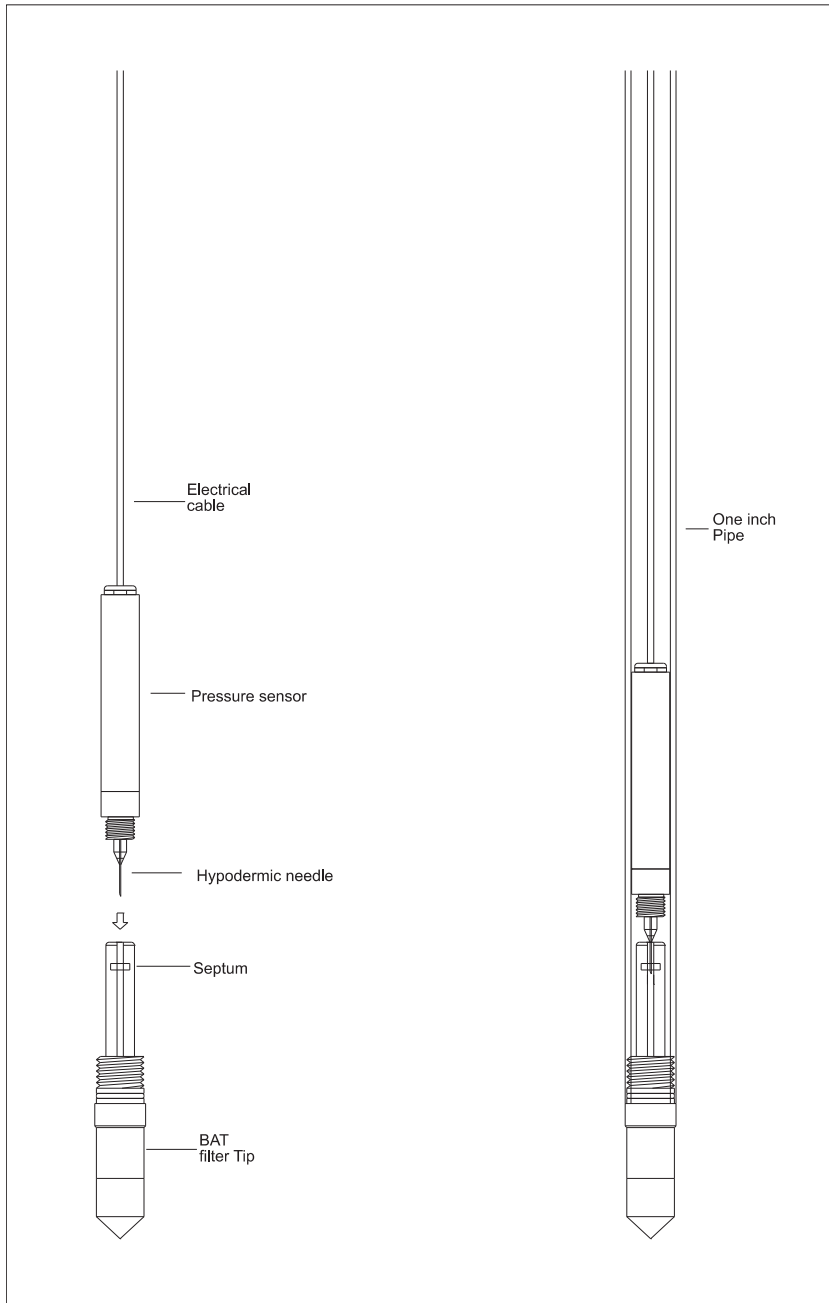
Figure 3.6: Configuration of the BAT system for pore pressure measurements. At the right, the connection system of the pressure sensor to the BAT system tip is displayed.
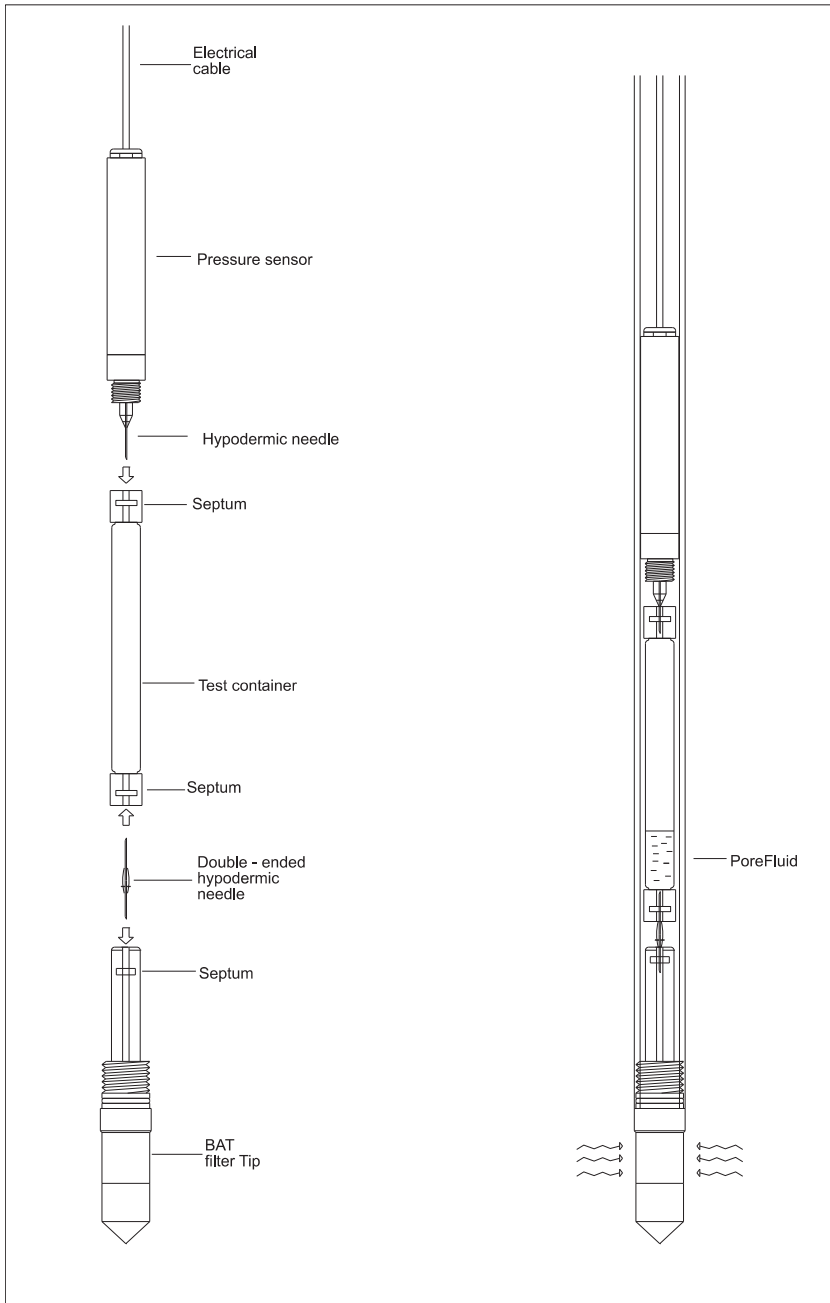
Figure 3.7: Configuration of the BAT permeability system for hydraulic conductivity determinations. At the right, an inflow test is illustrated.

The advantage of this device is that quick measurements can be performed. Smearing of the soil along the probe during installation and the small volume of tested soil may appear as the main inconveniences. In-situ testing aiming to evaluate semi-permeable membrane behavior of clays using this device has a clear advantage: it allows experimenting with different water types within short periods of time. However with this device monitoring of the water concentration is not possible.

With the methods and instruments presented in the sections above, assurance of an initial hydraulic equilibrium condition necessary to perform the conventional osmosis tests is not as simple as it is in the laboratory. In the case of slug tests an initial hydraulic disequilibrium condition is inherent to the test. Performance of shut-in tests may result in initial hydraulic disequilibrium conditions, due to the low permeability of the clayey sediments. Long periods of time are required before hydraulic equilibration and ultimately the osmotic processes will be operating and even dissipating before equilibration occurs. The initial disequilibrium condition implies that not only osmotic processes are taking place but also hydraulic effects associated to disequilibrium are present. For analysis, it is therefore necessary to isolate the osmotic effects from the hydraulic effects. Isolation can be done by comparison of the results of simultaneous tests using different water types (similar approach as the one used by Neuzil (2000)). A test using a pore water duplicate running parallel to the tests using different water concentrations is essential for further data analysis. Moreover, if initial hydraulic gradients are larger than the osmotic pressure ultrafiltration processes may be induced at the beginning of the test.

References

Alexander, J., 1990. A review of osmotic processes in sedimentary basins. British Geological Survey, Report no. WE/90/12.

Bath, A., 1994. Hydrochemical characterization of argillaceous rocks. In: Workshop on Determination of Hydraulic and Hydrochemical Characterisation of Argillaceous Rocks. OECD Documents Disposal of Radioactive Waste. Nottingham, UK., pp. 77–87.

Bredehoeft, J., Papadopulos, S., 1980. A method for determining the hydraulic properties of tight Formations. Water Resources Research (16), 233–238.

David, E., 1989. In-situ hydraulic conductivity tests for compacted clay. Journal of Geotechnical Engineering 115 (9), 1205–1226.

Fritz, S., 1986. Ideality of clay membranes in osmotic processes: a review. Clays and Clay minerals (34), 214–223.

Horseman, S., Higgo, J., 1994. Summary report on the workshop on Determination of Hydraulic and Hydrochemical Characterisation of Argillaceous Rocks. In: Workshop on Determination of Hydraulic and Hydrochemical Characterisation of Argillaceous Rocks. OECD Documents Disposal of Radioactive Waste. Nottingham, United Kingdom, pp. 7–14.

McKay, L., Balfour, D., Cherry, J., 1998. Lateral chloride migration from a landfill in a fractured clay rich glacial deposit. Ground Water 36 (6), 988–999.

McKay, L., Cherry, J., Gilham, R., 1993. Field experiments in a fractured clay till. I. Hydraulic conductivity and fracture aperture. Water Resources Research 29 (4), 1149–1162.

Merceron, T., Mossman, J., 1994. The Archimede-Argile project: Acquisition and regulation of the water chemistry in a clay formation. In: Workshop on Determination of Hydraulic and Hydrochemical Characterisation of Argillaceous Rocks. OECD Documents Disposal of Radioactive Waste. Nottingham, UK, pp. 105–118.

Neuzil, C., 1986. Groundwater flow in low permeability environments. Water Resources Research (22), 1163–1195.

Neuzil, C., 2000. Osmotic generation of "anomalous" fluid pressures in geological environments. Nature (403), 182–184.

Noy, D., Horseman, S., Harrington, J., Bossart, P., Fisch, H., 2004. An Experimental and modelling study of chemico-osmotic effects in the Opalinus Clay of Switzerland. In: Heitzmann, P. ed. (2004) Mont Terri Project - Hydrogeological Synthesis, Osmotic Flow. Reports of the Federal Office for Water and Geology (FOWG), Geology Series (6), 95–126.

Stienstra, P., van Deen, J., 1994. Field data collection techniques - Unconventional sounding and sampling methods. In: Proceedings of the 20 year jubilee symposium of the Ingeokring. Engineering Geology of Quaternary sediments. Delft, The Netherlands., pp. 41–56.

Torstensson, B., 1984. A new system for groundwater monitoring. Ground Water Monitoring Review. 4 (4), 131–138.

van der Kamp, G., 2001. Methods for determining the in situ hydraulic conductivity of shallow aquitards - an overview. Hydrogeology Journal (9), 5–16.

Wassenaar, L., Hendry, M., 1999. Improved piezometer construction and sampling techniques to determine pore water chemistry in aquitards. Ground Water 37 (4), 564–571.

Wolff, R., 1970. Field and laboratory determination of the hydraulic diffusivity of a confining bed. Water Resources Research 6 (1), 194–203.

Chapter 4

Chemical Osmosis field measurements in the Calais Clays, Polder Groot Mijdrecht, The Netherlands

Up to now chemically and coupled-flow transport investigations have been mainly performed through laboratory experimental work and theoretical studies. Integrated studies combining results of field and laboratory experiments and the basic theoretical framework are needed to understand the role of osmosis in groundwater flow and solute transport and to incorporate this process into practical studies (*e.g.* pollution, salt intrusion and waste disposal barriers). At present there is particularly a lack of field investigations. In this chapter results of several osmosis in-situ tests are presented. Tests were performed with different instrumentation and different methods on the Holocene estuarine Calais Clay in the Netherlands.

4.1   Hydrogeological Setting of Polder Groot Mijdrecht

The field site that is selected to carry out the osmosis experiments is located in Nessersluis, in the northwestern part of the Polder Groot Mijdrecht (Figure 4.1 a and b). Groot Mijdrecht is a deep polder (ca 6 m below NAP = Dutch Ordnance date = approximately mean sea level) with an area of about 20 km^2 and is situated about 15 km south of Amsterdam. The polder is formed in the late 19th century by reclamation of a lake that was created artificially by excavation of peat for fuel.

The subsurface of the polder consists of a layer of about 150 m of medium-grained fluvial sand of Pleistocene age which forms an aquifer with a transmissivity of about 4000 m^2/day. The aquifer is separated into an upper and a lower aquifer by a clay layer with a thickness of 5 - 15 m at a depth of about 50 m NAP. The lower boundary of the aquifer system consists of a sequence of marine sand and clay layers of Early Pleistocene age. These marine layers are filled with brackish water; the fluvial layers are partly brackish, the salt content originating from leakage from the deeper marine deposits and from salinisation during Holocene marine transgressions. These transgressions, caused by sea level rise, began with the forming of a peat layer which has been consolidated and has now a thickness of about 1 m. The peat is covered by a sequence of clay and clayey sand with a thickness

that increases from 1 m in the east to 7 m in the west of the polder. These low permeability layers were deposited in a brackish lagoonal and estuarine environment. They were covered by peat that reached an elevation of 5 m above mean sea level. This peat has now almost completely been removed in the present polder, but is still present at the surface in the surrounding area. The Holocene forms a low permeability confining layer on the Pleistocene aquifer (with a controlled water table at about 0.5 m below the surface). The water table is maintained by a dense drainage system. The average vertical permeability of the confining layer is in the order of 10^{-3} m/day. The Holocene clay deposits used to be indicated in the past as 'Old Clay' or 'Calais Clay'; we will stick to this old stratigraphic name because of references in earlier reports. Table 4.1 presents the average hydrogeological characteristics.

The hydrogeology of the polder was studied by Singh and Boekelman (1990) and Boekelman (1991) in the framework of their analysis of the fresh/salt groundwater distribution. The average annual precipitation and evapotranspiration are about 800 mm and 550 mm respectively, so that the precipitation excess is about 250 mm. The polder receives an annual subsurface inflow from the surrounding higher land and surface water areas of more than 1000 mm which reaches the surface through upward leakage. All excess water is drained by a dense network of ditches from which the water is lifted and transported by pumping to the river Amstel. Part of the upward seeping groundwater is brackish, particularly in the centre of the polder where the deepest flow lines bring water with a high chloride content to the surface. This upwelling groundwater reaches chloride concentrations of more than 5000 ppm and forms a cone of brackish groundwater. The polder is flushed with water from the river Rhine. The occurrence of $NaHCO_3$ water at the edge of the polder indicates a process of desalination of original saline or brackish water by infiltrating fresh $Ca(HCO_3)_2$ water from the surrounding higher areas, including the river Amstel and the lake Vinkeveense Plassen.

Table 4.1: Geohydrological parameters of the northern part of the polder Groot Mijdrecht after Singh and Boekelman (1990)

Average thickness of Holocene confining layer	5m
Specific vertical flow resistance of confining layer	2500 d
Thickness of first and second aquifers	160 m
Transmissivity of first + second aquifer	5500 m^2/d

4.1.1 Field Site Characterization

The Calais Clay in the polder Groot Mijdrecht was selected for osmosis in-situ testing. These clay deposits have certain features that make them attractive for this type of experiments. Several sub-layers consist of rather pure and homogeneous clay and are at shallow depth so that experimental equipment could easily be installed and monitored. Moreover,
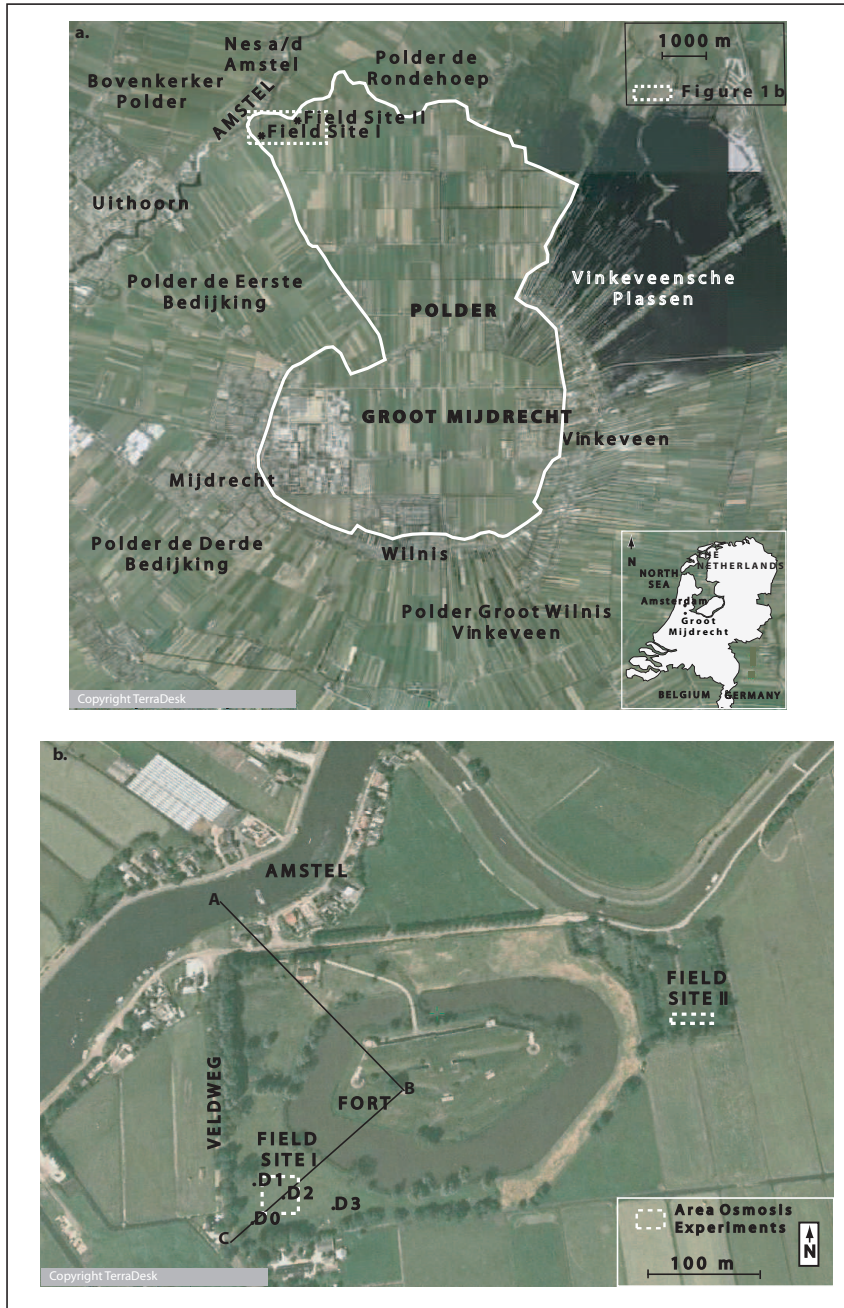
Figure 4.1: a. Map showing the Polder Groot Mijdrecht and the location of the field sites. b. Field sites and location of the drilled cores D0, D1, D2 and D3 and areas of osmosis experiments.
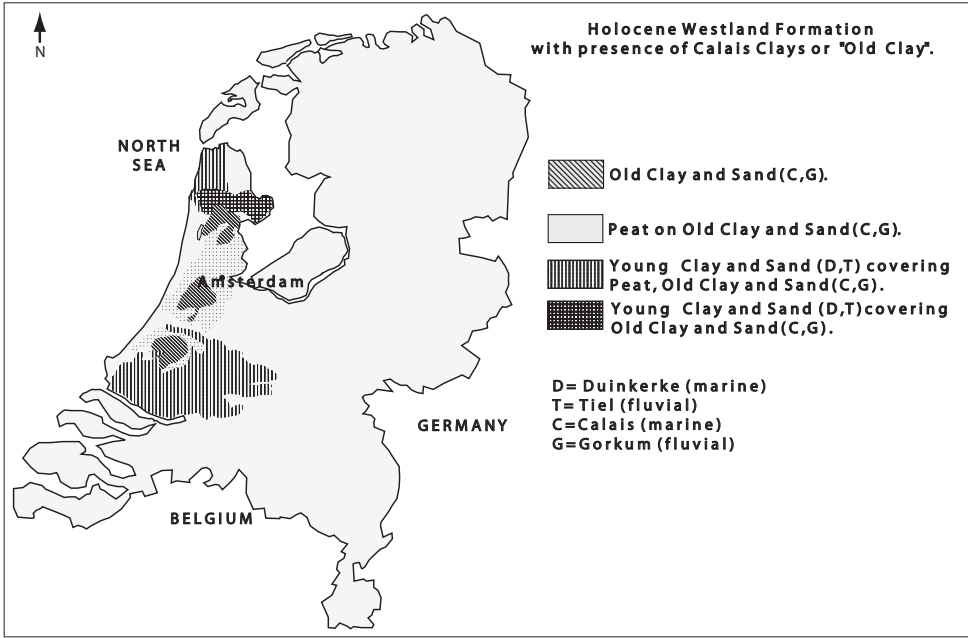
Figure 4.2: Distribution of Calais Clay in the Netherlands within the Holocene (Zagwijn et al., 1987).

this type of clay sediment extends throughout the western part of the Netherlands (Figure 4.2) so that the characterization of its semi-permeable membrane behavior can be of use in various theoretical and practical applications, including the study of the present salt and fresh groundwater distribution and prediction of future changes in the interface, and problems with containment of waste repositories and proliferation of contaminants.

Two field test-sites were selected in the northwestern margin of the polder (Figure 4.1b), close to an old fortress that is surrounded by a canal with a slightly higher level than the water table at the test site (Figure 4.4). This polder corner is surrounded by the river Amstel, the level of which is few decimeters below NAP. The sites are on grass land with sheep grazing. The surface is at an elevation of about 6 m below NAP and is surrounded by shallow drainage ditches. Fresh Calais Clay was identified at a depth of 6.2 m below NAP; four cores D0, D1, D2 and D3, were drilled to investigate the lithological properties and succession of the different sub-strata. This showed that the clay layer has a thickness between 1.5 and 3 m and that within this deposit intercalations of sandy clay and peat are present. Detailed coring revealed the lithological succession (Figure 4.3). Similar features were found in a core drilling at site II. The topsoil above the clay consists of peaty and non-ripened clayey material which is irreversibly desiccated and has an acid sulphuric horizon of at least 10 cm thickness. Sulphate has been produced by oxidation of pyrite (FeS_2) minerals that occur abundantly in the marine clays.

The hydraulic head distribution and pore pressures were determined at different depths as part of a preliminary survey (Figure 4.5). The measurements were carried out in piezometers with a diameter of 2.5 cm and a filter length of 20 cm, and by using the BAT probe system (description in Chapter 3). The piezometers were installed into two shallow boreholes at depths of 6.8 and 6 m below NAP (center of filter). Hydraulic heads of -5.65 and -5.52 m relative to NAP were measured respectively. Pore water pressure was measured with the BAT probe at 6.8 m , 7.2 m and 8.2 m below NAP where pressure heads of 0.9, 1.3 and 1.9 m were measured respectively. Relative to NAP these pressure heads correspond to the following hydraulic heads: -5.8, -5.9 and -6.3. Figure 4.5 displays all measurements as hydraulic heads. Both shallow measurements show the existence of downward flow and not upward seepage through the confining layer as was observed earlier by Boekelman (1991). However, the inference of Boekelman (1991)was based on the comparison of observations
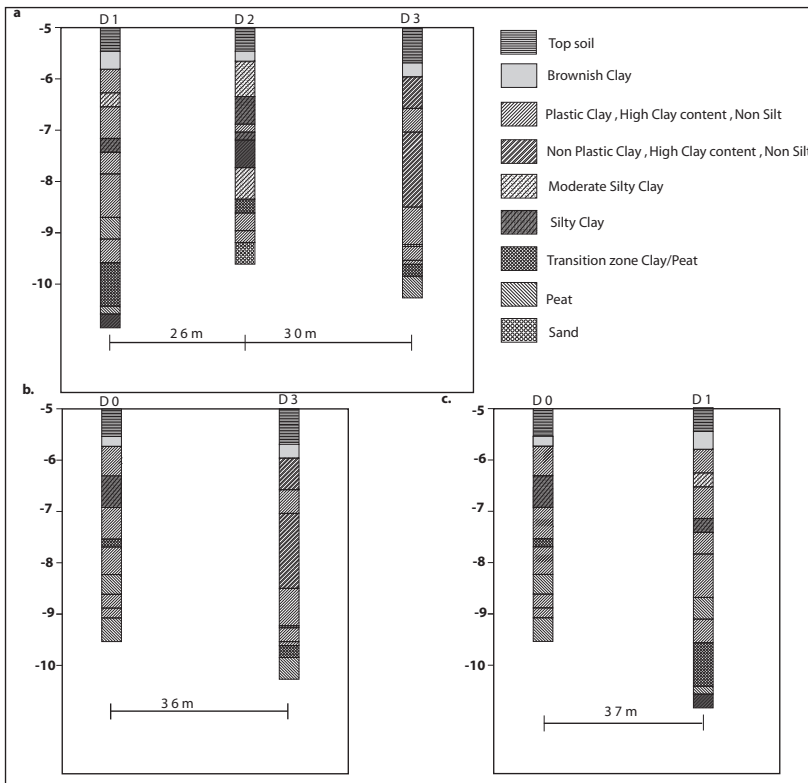

Figure 4.3: Shallow geological profiles (D0, D1, D2 and D3) showing lithological sequences within the holocene cover layer at field site I.

coming from the first and second aquifers and holocene cover layer.

Additionally, pore pressures were recorded continuously and parallel to the six-day osmosis experiments. Monitoring was carried out at 6.8 m below NAP with a pressure transducer in a open pipe piezometer (PZ) and a pressure sensor inserted directly in the clay (PT). Figure 4.5 shows the 6-day data time series of pressure that were obtained concurrently with the osmosis experiments (see next section). The results are comparable with those of previous measurements as mentioned in the previous paragraph. They show a decreasing head from -5.84 at day-1 to -5.92 after day-6 in the test of July; and of -5.78 at day-1 to -5.84 after day-6 in the September test. Small day and night fluctuations are most probably caused by evapotranspiration during day time.

Analyses of water samples that were extracted by squeezing and centrifugation from clay samples at different depths demonstrated that pore water is brackish and dominated by NaCl, with 1207 mg/l chloride, corresponding to an EC of 4 mS/cm. Figure 4.6 displays the chemical composition and the EC of the pore water. The EC value and composition do not change significantly with depth within the clay layer.

Permeability tests and pore water sample collection was carried out using the BAT probe permeability system (see Chapter 3). Testing depths within the clay were 6.8, 7.2 and 8.2 m below N.A.P. Results indicate that the permeability of the clay is similar at all depths and ranges from $1.42 \cdot 10^{-9}$ m/s ($1.2 \cdot 10^{-4}$ m/day) to $1.47 \cdot 10^{-9}$ m/s ($1.3 \cdot 10^{-4}$ m/day). The permeability of the investigated clay layer is thus almost a factor 10 lower than the average permeability of the Holocene (Table 4.1) which consists of a sequence of clay and sandy clay. The EC of the pore water collected with the BAT permeability system was 4.1 mS/cm.

4.1.2 Laboratory Measurements on Calais Clay

As part of the cooperative project, Heister (2005) at the University of Utrecht has performed laboratory measurements on Calais Clay. The aim of this research was to quantify the effects of induced electrical potential gradients on the transport of water and ions. Electrical potential gradients were induced by means of hydraulic pressure gradients and salt concentration gradients. Measurements were performed on commercially available bentonite and two natural clay (Calais Clay and Boom Clay) samples mounted on a flex wall permeameter. Heister (2005) has performed an initial characterization of the clay. The sample employed was taken from the Field Site I. The sample was fully saturated and taken under anoxic conditions. However immediately after sampling the clay was exposed to aerobic conditions. Heister (2005) reported the formation of sulphate precipitate during air drying in the laboratory. Sample properties of the Calais Clay were determined after a storage period of 17 months. Heister (2005) found that the oxidized Calais Clay sample consists of a mixture of illite, smectite and kaolinite. Compared to the other two samples, the Calais Clay has the lowest content of clay minerals the lowest CEC and the highest impureness. Nevertheless Heister (2005) assumed that all the clays could show semi-permeability behavior and concluded that all the clays were suitable for coupled flow phenomena testing. The laboratory results of Heister (2005) showed that the oxidized and acidified Calais Clay did not exhibit semi-permeable membrane behavior. Simultaneously to the characterization
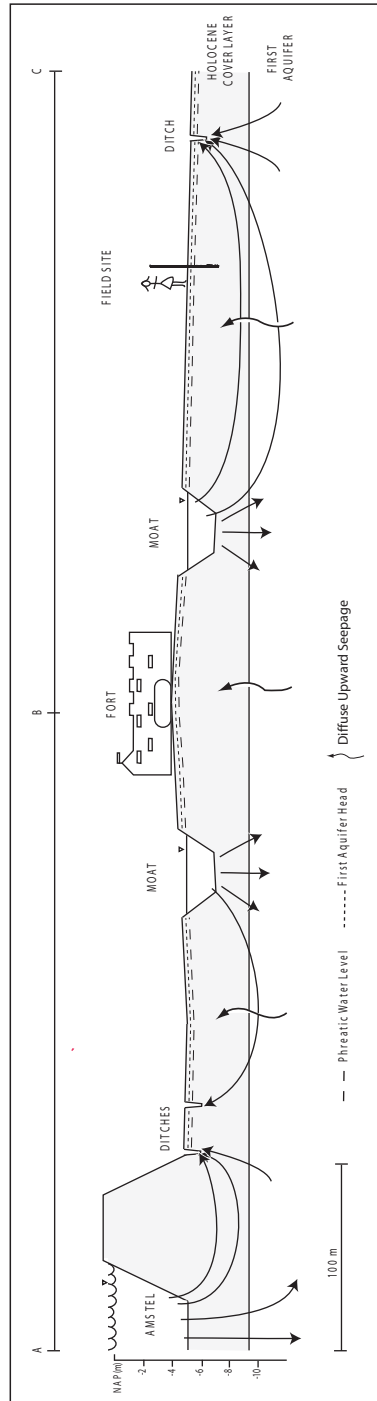
Figure 4.4: Schematic hydrogeological section showing the local groundwater flow patterns in the vicinity of the field tests sites. The relatively high water level of the Amstel river causes infiltration into the first aquifer and seepage to drainage ditches just behind the dike. Similarly, the water level in the moat is slightly higher than the surrounding drainage ditches and possibly of the piezometric head (Boekelman, 1991) in the first aquifer, causing water to infiltrate. The drainage ditches receive precipitation excess and seepage from the moat and from the first aquifer, the fields in between the ditches are subject to a continuous diffuse upward seepage.
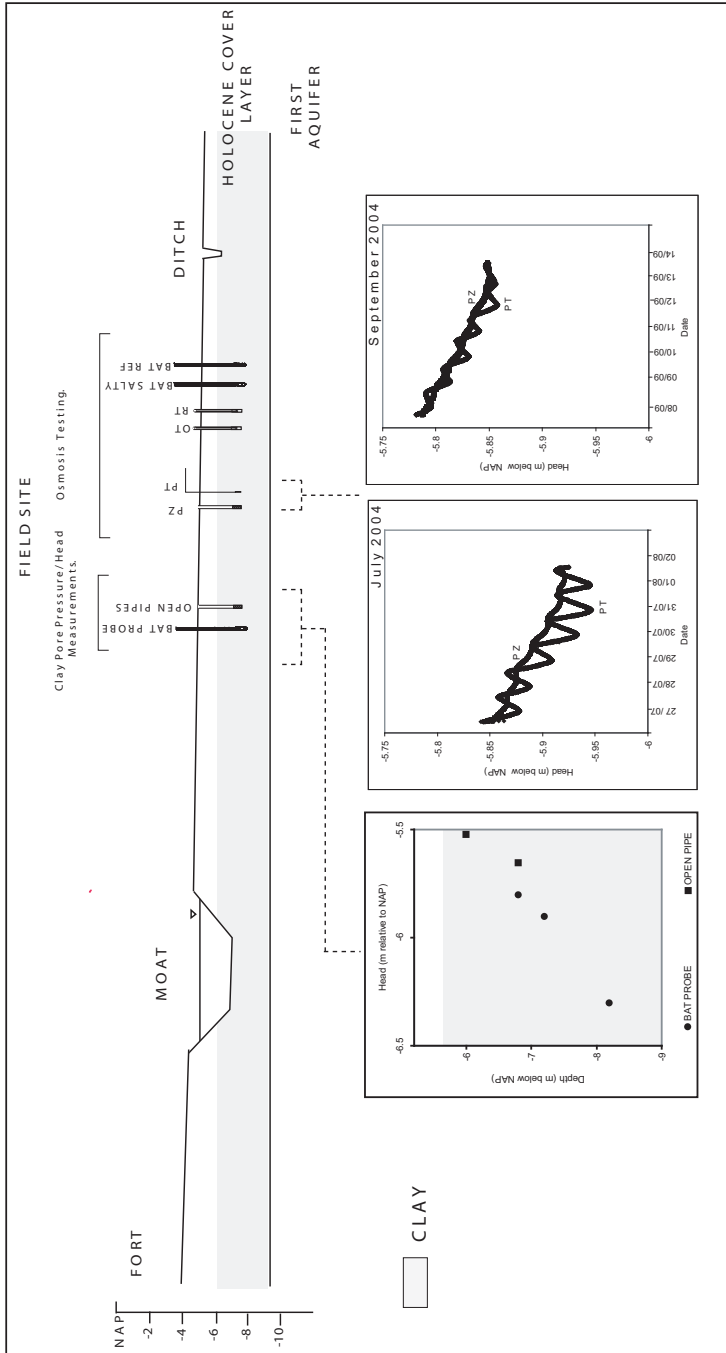
Figure 4.5: Experimental field site description and head measurements.

and measurements of Heister (2005) our osmosis *in-situ* testing campaign was carried out.

4.1.3   Osmosis Experiments Using the Shut-in Filter

A number of osmosis experiments were conducted with the closed reservoir configuration filter (Figure 4.7) described in Chapter 3.

The experiments were carried out at approximately 6.8 m below N.A.P. (position of the sensors), ensuring that the 40 cm length filter is within a plastic clay zone and that the clay is fully saturated at this depth. Each experiment lasted around 4 days and consisted of two simultaneous tests: one with saline water within the filter (osmosis test, OT) and one with a pore water duplicate within the filter (reference test, RT).

The saline water used in the OT has a concentration which corresponds to an osmotic pressure of 26 m (relative to the pore water) . This value was calculated from equation (2.1) using $R = 8.31447$ J/mol K, $T = 298K$, $v = 1.8 \cdot 10^{-5}$ m^3/mol. The water activities for high and low concentrations were calculated using the equation $a_{H_2O} = 1 - 0.017fm$ (Keijzer, 2000); where f is the number of moles of ions into which 1 mole of the electrolyte dissociates (-) and m is the molality of the solution (mol/kg).

The values of σ for saline solution and pore water concentrations are 0.2 % and 2 % respectively according to Bressler's relationship (assuming a typical value of thickness of the water film for a non-compacted clay of 120 Å. Thus, a pressure build up of the order of
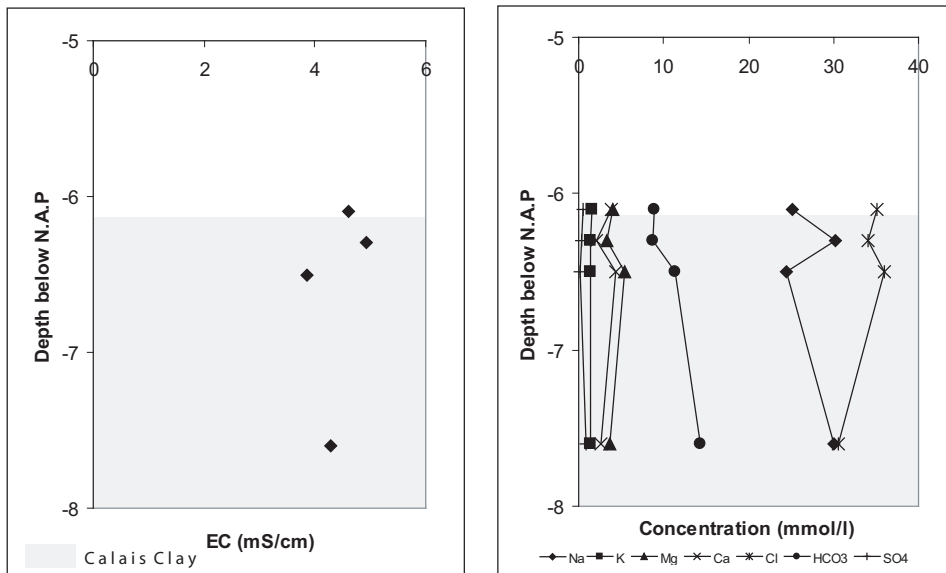
Figure 4.6: Chemical composition and EC profiles of pore water of the Calais Clay at the field location.Pore water was obtained by core squeezing.

tens of cm of water due to osmosis was expected.

For setting-up the test, a hole was pre-drilled through the top soil to the top of the clay. From that depth on the device is pushed into the clay. Pushing the instrument is possible because the Calais Clays are soft, plastic non-consolidated sediments. In this way, a good contact between the clay and the screen is achieved. Use of packing material (sand or bentonite) around the instrument was not required. A very coarse packing material could lead to leakage. Bentonite may act also as semi-permeable membrane inducing pressure gradients that interfere with the measurements. Two rubber plugs were installed around the filter to prevent (if it existed) leakage along the filter walls.

Monitoring began after over-filling (with nearly 5 liters of solution) each instrument. Subsequently, the sensors (wired through the closing lid and connected to the logger) were lowered. The closing lid was screwed closing the system, however a small opening remained open to allow trapped air to escape. The system was over filled one more time through these small opening and shut-in. The initial pressure was higher than the pore pressure and the response, therefore, resembled a slug test. The solutions utilized were prepared based on the chemical analysis performed on pore water from the squeezed sediments (Figure 4.6). Thus, the solution utilized for RT was a close duplicate of the pore water; while the solution prepared for OT was 5 times more concentrated for all solutes (that resulted in a solution with an EC of nearly 16 mS/cm).

Many experiments were conducted before readings were obtained that seemed free of instrumental errors, non-optimal installation or monitoring procedures. Response differences between OT and RT were indeed observed; however the significance of these differences was not clear. First, pressure decay for both tests (OT and RT) occurred relatively fast (nearly 10 hours for equilibration). However, OT and RT were not conducted simultaneously (hours or even a week apart) and sensor position within the reservoir was not identical for both tests. Therefore, isolation of osmotic effects (extraction of a differential signal between OT and RT) was not possible. Secondly, it was not clear if observed anomalies in pressure response were due to secondary effects. Changes in atmospheric pressure and rainfall during the experiment might have caused additional observed pressure variations (phreatic water level changes or infiltrated rain water may be reflected in the background pore pressure of the clay). Thirdly, a number of the tests initially performed showed an extremely slow pressure response, indicating that probably air was trapped (one of such measurements is shown in Figure 4.8). Subsequently several improvements were made to overcome some of the problems. OT and RT were carried out as simultaneous as possible; differences in timing were less than 5 minutes. Additionally, several complementary measurements were performed (*e.g.* open pipe PZ and pressure transducer PT inserted directly in the clay) to have a better idea of background pore pressure behavior of the Calais Clay sediments. The final procedure used is described in Figure 4.9.

The data obtained for one of the osmosis experiments is presented in Figures 4.10 and 4.11. Recordings were performed every minute. The pressure curves for OT and RT show a rapid initial decay (few hours) to the value of the background pore pressure. If osmosis were to occur, the pressure decay of OT would be expected to be retarded with respect to the pressure decay of RT, the difference corresponding to the osmotic induced pressure.
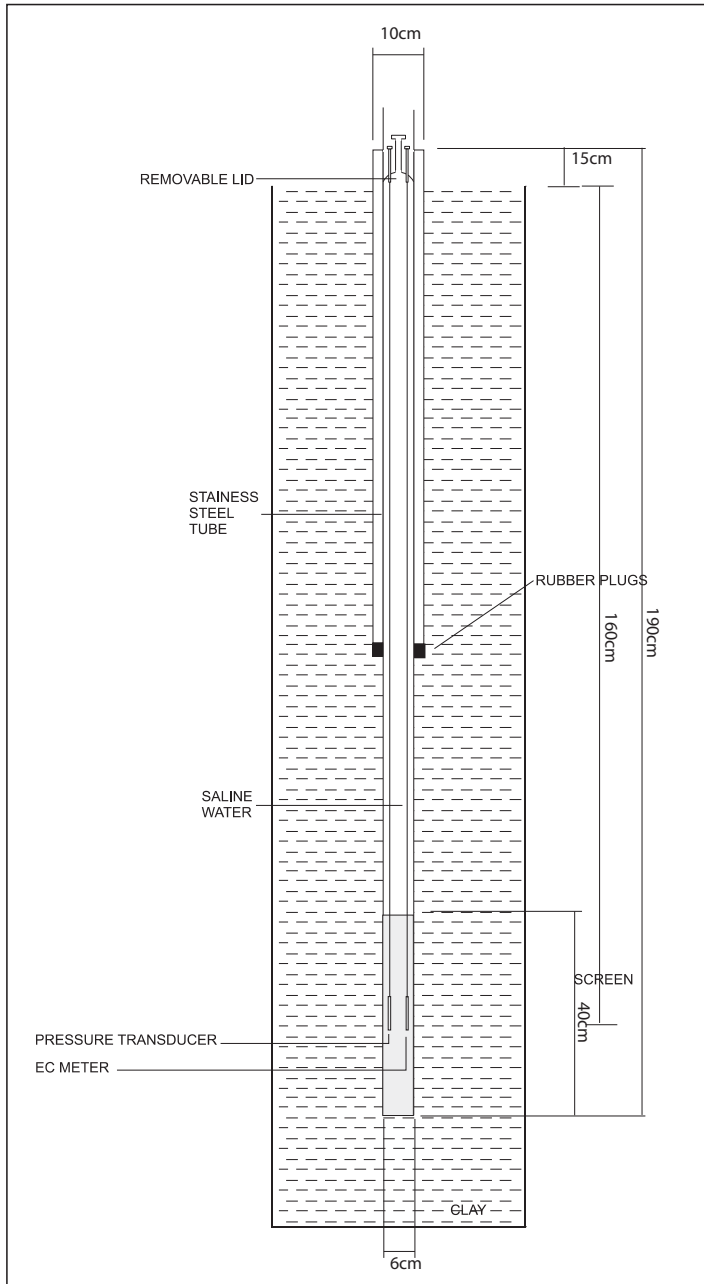
Figure 4.7: Experimental design built and used for in-situ evaluation of osmosis. The filter is located at approximate 6.8 m below N.A.P into the clay.
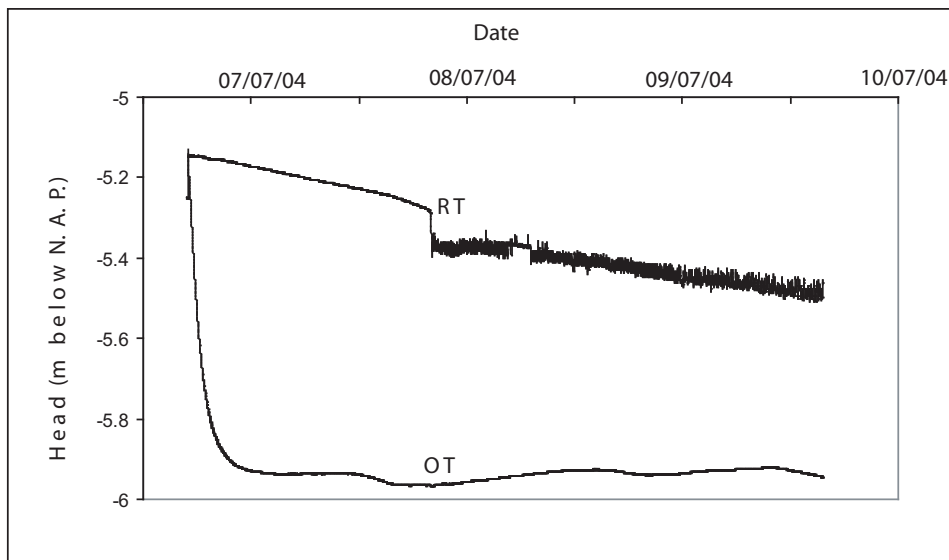
Figure 4.8: Results obtained from one osmosis experiment in which the anomalous pressure decay in the reference test RT is most likely due to trapped air within the reservoir.

However, during the experiment both tests showed the same rate of decay; and once the background pressure was reached the pressures in OT and RT followed the behavior of the pore pressure in the clay (same as PT and PZ). Figure 4.11 shows that EC decreases during the test. However, this decrease occurs slowly and even at the moment at which pressures have equilibrated a significant chemical gradient is still present and osmotically-induced pressures are not generated. These results suggest that in the Calais Clay, osmotic effects are too small to be detected with such an experiment and/or that the Calais Clay doesn't exhibit membrane properties.These findings will be discussed later in this chapter. First additional experiments with the BAT probe system will be presented.

4.1.4 Osmosis Experiments Using the BAT Probe System and BAT Permeability System

As discussed in Chapter 3 the BAT probe and BAT permeability systems can be utilized to conduct quick pore pressure measurements on low permeability sediments. The BAT probe system (pore pressure measurements) and the BAT permeability system (inflow and outflow permeability tests) were utilized in the Calais Clay for osmosis testing using different types of water .

Preliminary Test. A preliminary osmosis test using the BAT probe system (only pore pressure measurement) was performed. One filter tip of the probe was pre-saturated with

saline water (same solution used for OT) and a second one with distilled water. Subsequently, the probe was pushed into the soil at 6.5 m below N.A.P. The pressure in the system after pushing it in was not controlled. The pressure decayed in both tests, and was recorded for a short interval of time until it had stabilized (2 hours). A difference in pressure evolution using the two different water types was observed. The pressure decay in the distilled water test was slower than the decay in the saline water test. This behavior appears to be opposite to what is expected if osmosis occurs: Osmotic flow is expect to delay the pressure decay in the saline reservoir. There were uncertainties about the initial conditions of the test and the natural hydraulic regime within the clay. Initial conditions don't ensure equilibrium, the tips were pushed in the soil and the test started immediately. Furthermore, few minutes for monitoring pressure changes within the clay may not provide sufficient information since they may reflect only the changes in pressure induced by placement of the instrument in the soil. Experiments with the BAT probe were repeated using the the BAT-permeability system
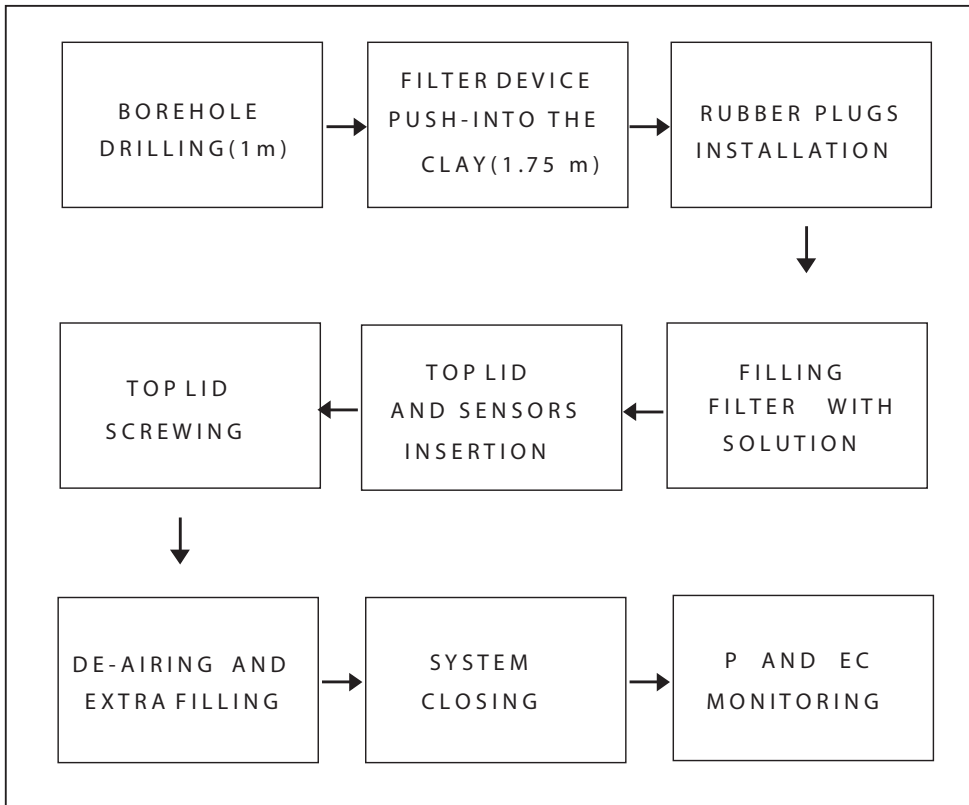
Figure 4.9: Procedure followed to perform an osmosis/reference test using the closed reservoir filter configuration
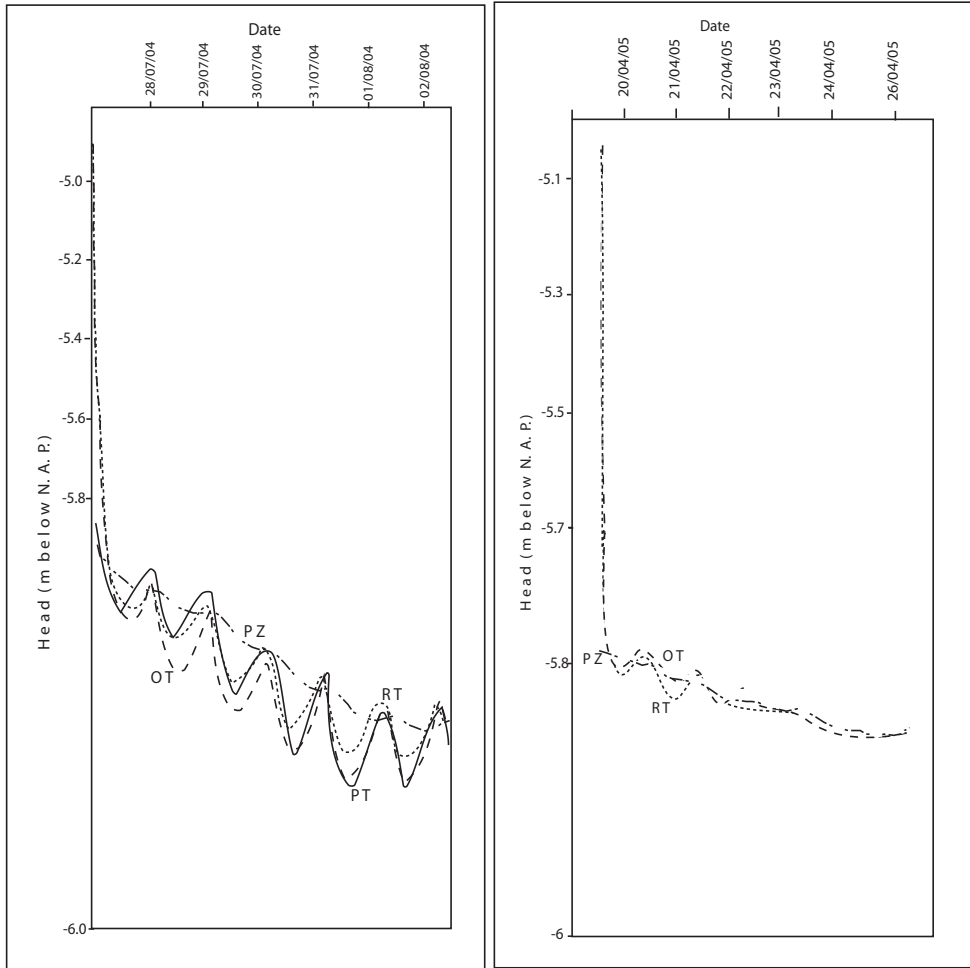
Figure 4.10: Pressure decay within the closed system for two osmosis tests OT and reference tests RT. Also shown in the figure are the pressure recordings of an open pipe PZ and a pressure transducer PT placed in the clay (only for one test).

configuration that allows a better control of initial conditions as will be described next.

Inflow Permeability Tests. Inflow permeability tests using different solutions to pre-saturate the filter tip of the probe were performed at different depths. The filter tip was pre-saturated and flushed using the solution prepared for OT (16mS/cm) and the solution RT that replicates pore water concentration (4mS/cm). The filter tip is pre-saturated, pushed down to the desired depth and immediately connected to a test container, in which vacuum has been applied, allowing pore water flow into the system. Observations showed that the
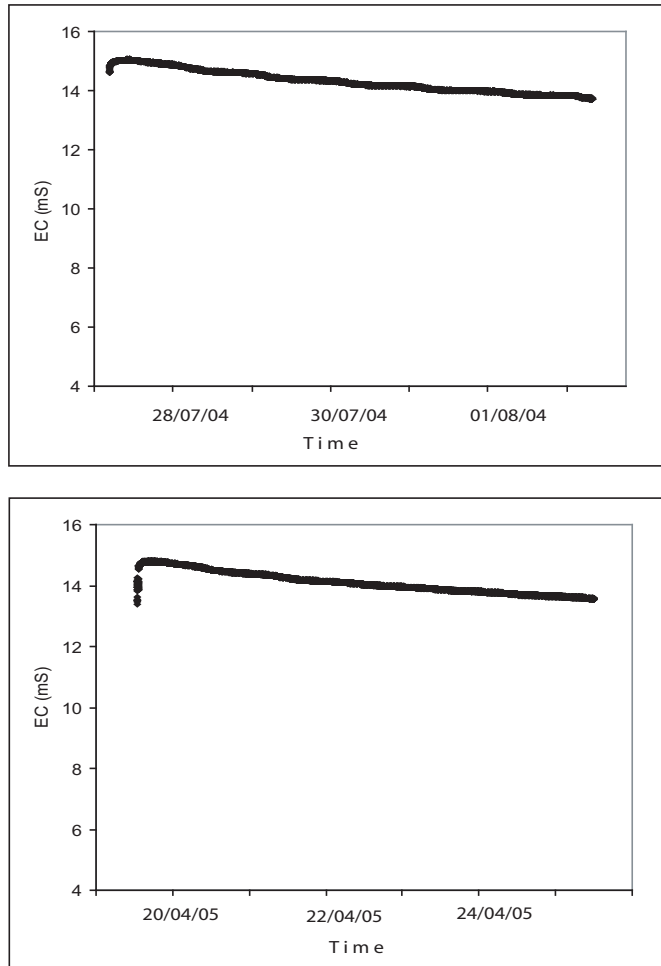
Figure 4.11: Continuous recording of electrical conductivity within the closed system for the osmosis tests OT. The minimum value of y- axis corresponds to the pore water EC value (4 mS/cm). Initially the EC slightly increases since after pushing the filters into the clay, pore water from the clay enters the filter and mixes with the added solution. The sensor is located where mixing takes place, and therefore the EC recorded is lower than 16 mS/cm.

pressure and time responses of the two water types are very different. Figures 4.12 a and b show the results of this tests. The pressure response curves in the saline water tests differ in shape from the conventional curves in permeability testing. Inversion of the curves to estimate permeability using the standard BAT-permeability-system software yields higher values for the test using pore water $(1.5 \cdot 10^{-10}$ m/s) and lower apparent permeability for the

saline solution tests ($6.7 \cdot 10^{-10}$ m/s). Final EC values within the container after the saline solution tests were around 9mS/cm.

The lower apparent permeability of the OT and the deviation from a normal pressure response curve (Figure 4.12 c) are consistent with osmotic behavior. With osmosis the pressure build-up of OT would be expected to be accelerated with respect to the pressure build-up of RT. However with this type of tests, inflow of pore water into the pre-saturated filter tip occurs immediately after pushing. The small volume of saline solution that saturates the ceramic filter tip is quickly displaced by pore water flowing into the container; allowing little time for any osmotic effect to fully develop. Only at the beginning of the test and for few minutes the saline solution is in contact with the clay. During this interval of time the largest concentration gradient exists. If osmosis occurs, pore water from the clay would be driven into the filter tip and therefore the pressure build up initially should be speeded up for the OT test with respect to the RT test. However, when observing the experimental data a different response is noticed. During the first minutes the pressure build up for OT and RT occurs at the same rate. Only at a later stage of the experiment the pressure build up speeds up for OT test. This effect can not be explained by osmosis and together with the lower apparent permeability inferred for OT may also suggest that changes in the permeability of the clay occurred due to contact with the saline solution. Added uncertainties exist as the tests (OT and RT) were not performed simultaneously. Therefore direct comparison of OT and RT for osmotic effects isolation is not the most adequate.

One more inflow test with saline solution 2.5 times more concentrated than the pore water of the Calais Clay has been carried out (OT h). Results obtained were very similar to those obtained for the OT test, and are displayed in Figure 4.12.

Outflow Permeability Tests. To ensure a longer contact between the saline solution and the clay, outflow tests were carried out. The general procedure followed for an outflow test has already been described in Chapter 3. The tests were performed consecutively using two different solutions (same solutions used in OT and RT tests) to fill and pressurize the glass container. Two filter tips were pre-saturated with pore water. Then, the filters were pushed into the clay (6.8 m below NAP) and left for few days to hydraulically equilibrate with the clay. Initially the RT tests were performed in each filter. A volume of 35 ml of solution (pore water duplicate) was added to the glass container. The container is closed, connected to the pressure sensor and pressurized with Nitrogen gas at a pressure of 1.2 bar (absolute including atmospheric pressure). Figure 4.13 displays the pressure evolution after pressurization. Once pressurized the container is assembled in the system (see Figure 3.7) and the system is connected to the filter tip. Upon connection the pressure instantaneously drops and from that moment on continues falling at a different rate. This behavior was observed in the two filters and it is shown in detail in Figures 4.13b and d. The pressure decay occurs rather quickly, and after a few hours seems to have stabilized. After the RT tests the filter tips are left within the clay. A few days later the OT experiments are executed. The procedure followed is the same with the difference that the solution in the glass container corresponds to the saline solution used previously for OT tests. Results are also displayed in Figure 4.13. Similarly to RT tests the pressure decays and stabilizes within a few hours and the instantaneous pressure drop upon connection is also observed. However different
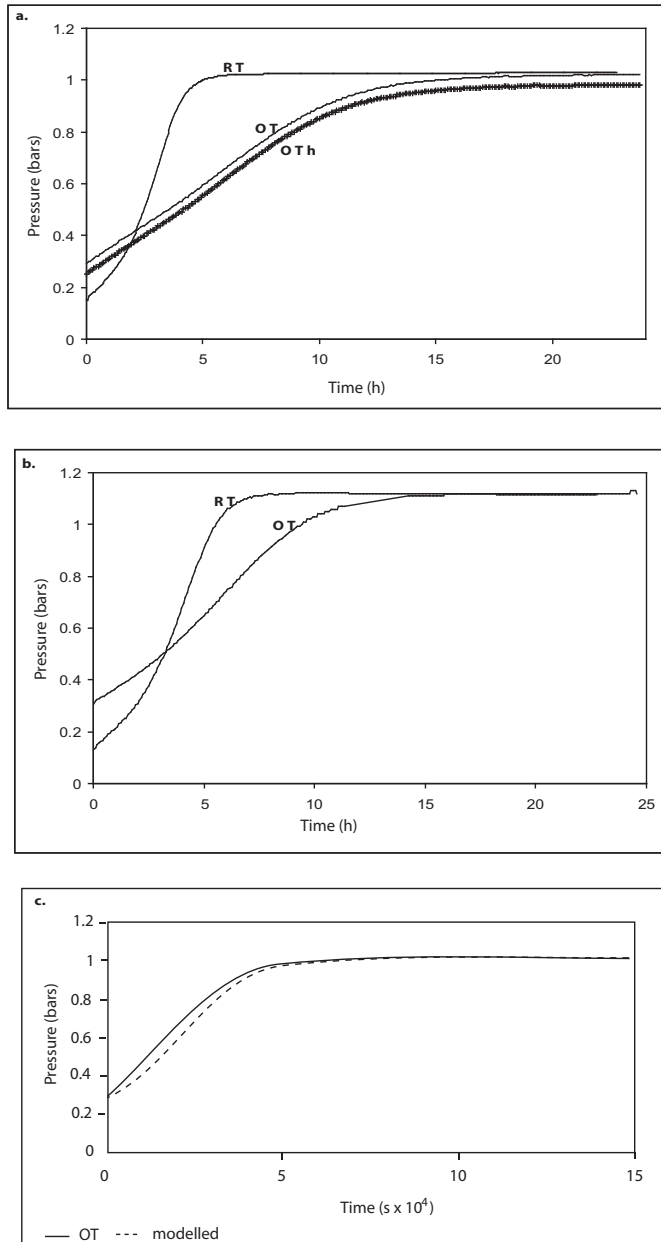
Figure 4.12: Pressure curves for inflow permeability tests carried out with the BAT probe and using different concentration solutions to pre- saturate the filter tip: a. 6.8 m below NAP. b. 7.2m below NAP. c. Modelled and measured response for the OT test at 6.8m below NAP.

response features can be distinguished. After connection with the filter tip the pressure decay occurs slower in the OT tests. As for a slug test both pressures should decay and reach the equilibrium background level, however the final pressure is higher for both OT tests. These features are consistent with osmotic behavior. The pressure decay of OT tests is delayed with respect to RT tests as pore water flow from the clay would be induced by the concentration gradient. If there exists an osmotically-induced pressure, this pressure could be maintained for a long period of time. This could be an explanation for the difference in final pressures. Unfortunately the pressure recordings were not long enough to register the complete decay to the "equilibrium background pressure". Additionally other uncertainties exist that make it difficult to judge if the observed differences are caused by osmosis. First, the four tests were not carried simultaneously, but consecutively. Thus, osmotic effects can not be isolated and/or quantified from the data of OT and RT. Second, there existed not only differences in timing, but also differences in initial pressures. Pressure can be controlled within the reservoir prior to connection, but after connection pressures drop to a different value in each test. Third, the natural hydraulic regime within the clay at the time of the experiments was unknown.

4.2   Results Discussion

Although we have not observed any semi-permeable membrane behavior of the Calais Clay, the newly designed instrument and procedures used seem to be adequate to measure the necessary parameters to evaluate osmotic properties of a shallow clay formation. Nevertheless, several questions regarding mainly procedures still remain open. As this instrument is pushed into the clay, it is inherent that smearing around the instrument occurs and that the pressure is perturbed. Smearing causes mechanical disturbance of the material surrounding the instrument and most likely pore pressure perturbation. Due to the low permeability of the clay sediments, the pressure perturbation probably takes long to dissipate (days). In our case we fill the instruments with the solutions immediately after installation and do not allow any time for dissipation. The reason to do so, is to avoid that water coming from the clay enters the instrument and mixes with the prepared solutions. On the other hand, the perturbation effect should be reflected in both OT and RT and therefore it is also subtracted when isolating the osmotic effect. As the instruments are manually pushed, each test may have been affected differently. The effect of smearing on the osmotic efficiency in the same region is unknown. Besides smearing, pushing may contribute to the formation of air bubbles around the screen as the bottom of the instrument is flat and not pointy as the conventional push-in devices. Trapped air while filling the instrument is another factor that may influence the response of the system. Solutions are poured into the piezometers from the top of the instrument and trapping at least some air is difficult to avoid.

When using the BAT probe permeability system, outflow tests appeared to be the best procedure for osmosis experiments. As for the newly designed instrument, the BAT instrument is also placed within the clay by pushing. Similarly, it is not known what is the effect of smearing on the osmotic efficiency and on the individual tests. With this instrument, only the pressure can be constantly monitored. EC or concentration values can be measured only
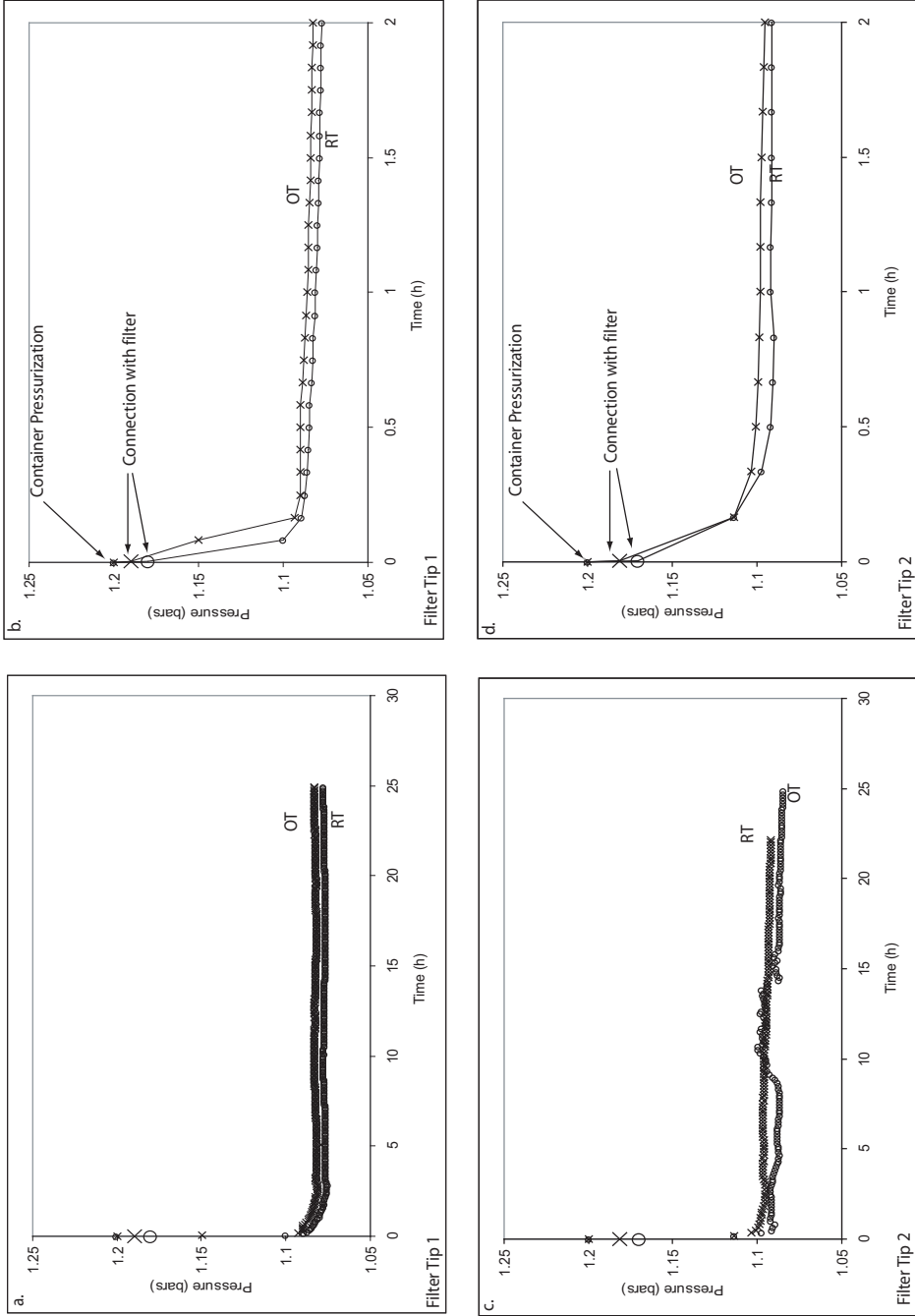
Figure 4.13: Pressure curves for outflow permeability tests carried out with the BAT probe using different concentration solutions to pressurized the glass container. Tests were carried out in two filter tips at 6.8 below NAP. Figures on the right correspond to the first two hours of the experiments shown left.

at the beginning and at the end of the permeability tests. We encountered several limitations for the interpretation of the results obtained with this device. There was only one BAT probe available and therefore it was not possible to perform the OT and RT tests simultaneously for direct comparison. Furthermore, the natural hydraulic regime within the clay at the time of the experiments could not be measured as was done for the tests with the newly designed instrument. Nevertheless, results obtained from OT and RT were compared and differences where observed. With the data available, the significance of those differences is still not clear and an unambiguous conclusion can not be drawn on the existence of osmotic effects.

The results obtained with the newly designed instrument, seem to confirm the results found by Heister (2005). We did not observe any semi-permeability membrane behavior in the Calais Clay using these instruments and procedures. It is important to note that Heister (2005) measured clay properties and experimented on oxidized Calais Clay samples. However in the field situation conditions are different (anaerobic) and some characteristics of the Clay may differ from those measured in oxidized Calais Clay. According to Heister (2005) the lack of semi-permeability of the oxidized Calais Clay can be attributed to several factors: first the measured cation occupation of the exchange complex showed that sodium occupation is extremely low. Secondly, Heister (2005) concluded that the oxidation of the Calais Clay causes modification on the minerals due to the very low pHs. Modification of the mineral surfaces translates into changes of semipermeability properties (diffuse double layers do not overlap for instance).

In-situ osmosis experiments were always performed on fully saturated Calais Clay under more anoxic conditions. We initially estimated an osmotically-induced pressure of tens of centimeters. The value was estimated using Bresler's relationship and assuming a value for thickness of the water film. It is possible that we are overestimating the efficiency of the membrane and/or that the value of thickness of the water film is not adequate for the Calais Clay. A sample of the clay (at the same depth of osmosis tests) was taken and handled under anaerobic conditions for analysis, in order to 1) check if under these anaerobic conditions the Clay exhibits similar characteristics to those of the oxidized Calais Clays, and 2) have a better value of thickness of the water film.

The analysis was carried out by the Laboratory for Colloid Chemistry, Department of Microbial and Molecular Systems, Faculty of Bio-Engineering Systems at the Katholieke Universiteit Leuven in Belgium. The parameters measured were pH, particle density, cation exchange capacity, specific surface area, carbonate content and organic matter. The results are compiled in Table 4.2. The table lists the methods used for the determination of the properties of the anaerobic Calais Clay, as well as the values obtained for the different parameters. The fourth column lists the values reported by Heister (2005) for some parameters.

Differences in parameters for oxidized and non-oxidized Calais Clay can be detected immediately. The extremely low pH and carbonate content reported by Heister (2005) clearly show that acidification occurred during the oxidation of the clay.

Results for CEC and cation occupation differ slightly, but in general it is observed that the Calais Clay has a low CEC and that Ca^{2+} and not Na^+ is the dominant cation on the exchange complex. This has important implications for osmotic behavior. As already men-

Table 4.2: Chemical analysis of Calais Clay

Parameter	Determination Method*	Anaerobic sample *	Oxidized Sample Heister (2005)
pH	Soil-water (1:1) solution	7.9 ± 0.02	3
Particle Density	Pycnometer	2.72 ± 0.16 g/cm^3	
Cation Exchange Capacity	Cs-CEC	19.3 ± 0.2 cmol$_c$/kg	14 ± 0.4 cmol$_c$/kg
Cation Occupation Ca^{2+}		9.46 ± 0.12 cmol$_c$/kg	11.6 ± 0.4 cmol$_c$/kg
Cation Occupation Mg^{2+}		4.61 ± 0.13 cmol$_c$/kg	9 ± 0.2 cmol$_c$/kg
Cation Occupation Na$^+$		2.89 ± 0.07 cmol$_c$/kg	3.5 ± 0.2 cmol$_c$/kg
Cation Occupation K$^+$		1.72 ± 0.04 cmol$_c$/kg	1 ± 0.0 cmol$_c$/kg
Specific Surface Area	N$_2$ (BET)	32.7 ± 0.1m^2/g	
Carbonate Content	Acid destruction	5.4 ± 0.1 wt %	0.29 wt %
Organic Matter	Loss on ignition	2.2 ± 0.6 %	

tioned, ideality increases with increased CEC and the dominance of Na$^+$ in the exchange complex, enhances the semi-permeable behavior.

Furthermore, the Cs-CEC found is typical for illite clay minerals, meaning that the predominant clay mineral is probably illite. Mineralogical analysis of Heister (2005) suggest that the main phases detected in the X-ray diffractograms are illite, smectite, kaolinite and quartz.

With the value of specific surface area it is possible to calculate the thickness of the water film (see equation (6.3)). The calculated value (109 Å) is not very different from the one we adopted for the membrane efficiency predictions (120 Å). Using Bressler's relationship the new calculated efficiencies are for pore water concentration 2.2 % and for the saline solution 0.2 % . Based on this result still a pressure build up of tens of centimeters would be expected. However, the low CEC, low Na$^+$ occupying the exchange complex and the possible dominance of illite in the Calais Clay may cause the Calais Clay to exhibit a poor semi-permeable membrane behavior. This presumption can not be conclusive as we observed some differences between OT and RT tests using the BAT probe. Nevertheless at this point it is not ceratin if those differences can be attributed to osmosis or not.

References

Boekelman, R., 1991. Geoelectrical survey in the polder "Groot-Mijdrecht". In: W. de Breuck, Hydrogeology of salt water intrusion: A selection of SWIM papers. Verlag Heinz Heise. pp. 363–378.

Heister, K., 2005. Coupled transport in clayey materials with emphasis on induced electrokinetic phenomena. Ph.D. thesis, Universiteit Utrecht, The Netherlands.

Keijzer, T., 2000. Chemical osmosis in natural clayey material. Ph.D. thesis, Universiteit Utrecht, The Netherlands.

Singh, S., Boekelman, R., 1990. Behaviour of groundwater of the polder Groot-Mijdrecht. In: Mededeling van de Vakgroep Gezondheidstechniek en Waterbeheersing. Delft University of Technology, Faculty of Civil Engineering, Sanitary Engineering and Water Management, Section Hydrology.

Zagwijn, W., Beets, D., van den Berg, M., van Montfrans, H., van Rooyen, P., 1987. Geologie. - Atlas van Nederland, 13: 23. Staatsuitgeverij.

In Situ Chemical Osmosis Experiments in the Boom Clay at the Underground Research Laboratory (URL) at Mol, Belgium

The development of underground storage concepts for radioactive waste containment targets deep clay-rich formations as potential host rocks. Due to their low permeability these deposits may constitute an excellent natural barrier against the transport of radionuclides towards the biosphere. In Belgium, the Boom Clay (an over-consolidated marine Oligocene deposit) has been considered for that purpose. For more than twenty years this clay formation has been under investigation aiming to asses its suitability as host rock. Studies on the compatibility of Boom Clay with large amounts of nitrate-bearing bituminized radioactive waste have recently raised a particular interest for osmosis-induced effects in this formation. In this chapter two chemical osmosis experiments performed *in situ* in the clay are presented. Modelling and analysis of the data are presented in Chapter 6.

5.1   Introduction

Clay rich deposits are usually considered as natural protective covers in regional aquifers because of their low permeability. In the absence of water conductive features, these deposits provide the low-flow environment required for waste containment. In such conditions, diffusion is the dominant transport process. Moreover, clayey materials retard the movement of contaminants a.o., by ion exchange, sorption, radioactive decay, biodegradation and ultra-filtration (De Cannière et al., 1994; Horseman and Higgo, 1994; Hendry et al., 2000; Cey et al., 2001; Shackelford et al., 2001). The clay formation is therefore a key barrier for ensuring the long-term safety of a disposal system. Comprehensive understanding of the physical and chemical processes controlling the water and solute transport through low permeability argillaceous formations is essential for assessing their suitability as host rocks.

The Boom Clay, an Oligocene over-consolidated marine deposit, is considered as a reference host formation for radioactive waste disposal in the north eastern part of Belgium because of its expected favorable characteristics. The Belgian strategy concerning spent nuclear fuel and nuclear waste considers direct disposal as a possible alternative of manage-
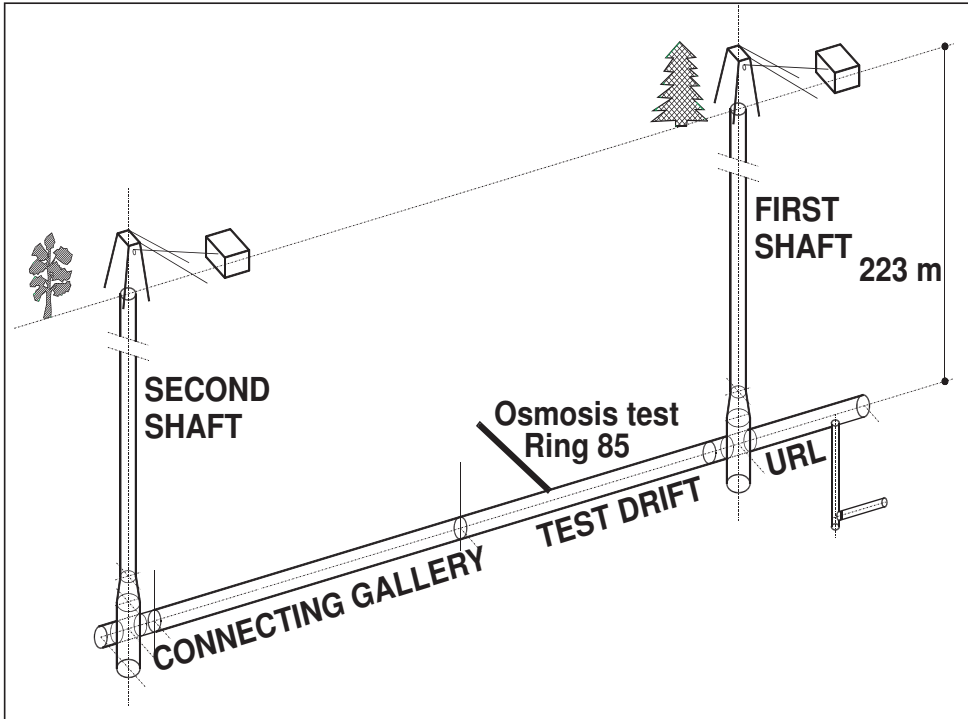
Figure 5.1: HADES Underground Research Facility (URF) at Mol (Belgium). With the courtesy of Euridice EIG.

ment. At an international level, the recommended practice for management is the isolation of high-level and long-life waste from humans and the environment. Safety of disposal of this type of waste in a stable geological formation with appropriate characteristics (ability to efficiently delay the migration of radionuclides) is being assessed by several countries, including Belgium. The long-term safety of such a repository relies on the principle of multiple barriers (engineered and natural barriers placed between the waste and the biosphere for a period of time long enough to allow sufficient decrease in activity of the radionuclides). The geological formation barrier is key in ensuring the long-term safety of the disposal system. For more than 25 years extensive hydraulic, geomechanical and geochemical research projects have been carried out in the Boom Clay at the HADES Underground Research Laboratory (URL) in Mol (Belgium). One of the main objectives of the experiments conducted at the HADES URL has been to characterize the *in situ* hydrogeological conditions, to determine the hydraulic parameters, and to study the mechanisms controlling the chemistry and the composition of the Boom Clay pore water.

At Mol, the Boom Clay is 100 m thick and is located at a depth of 180 m to 280 m. The URL deep disposal facility envisages a network of rectilinear galleries. The main gallery of
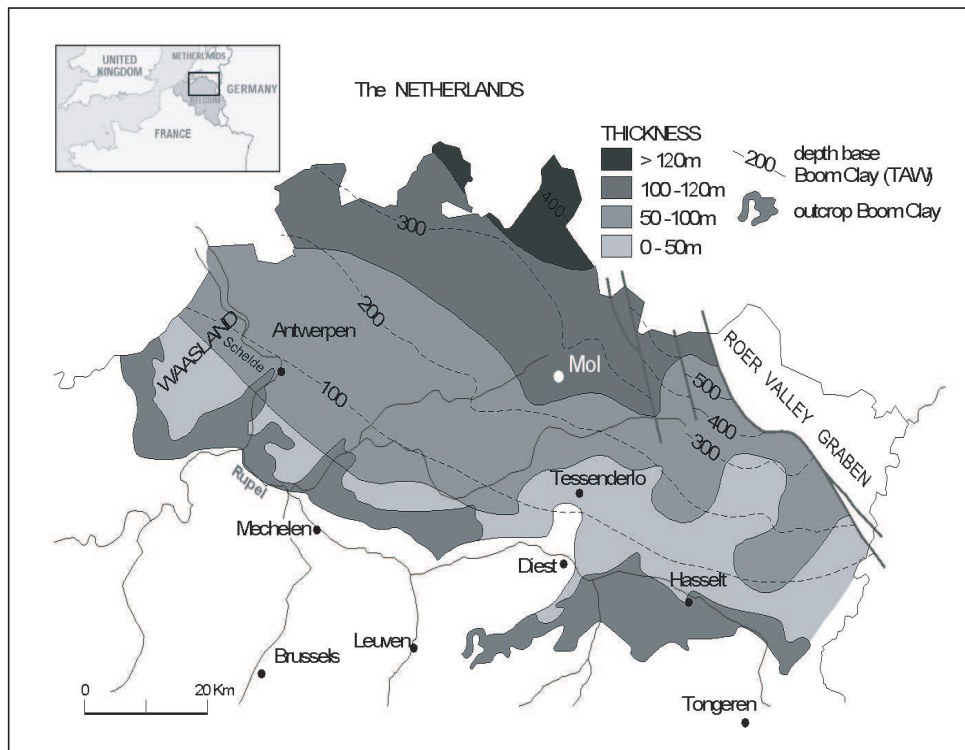
Figure 5.2: Location and outcrop map of the Boom Clay in north-eastern Belgium. Taken from the SAFIR 2 report (ONDRAF-NIRAS, 2001).

the URL is located just above the median plane of the Boom Clay layer, at about -223 m below the ground level (Figure 5.1). Access to the underground is by two shafts with an effective diameter of approximately 6 m and linked at their base by a connecting gallery, 400 m long and 2 m in diameter.

The research and hydrogeological models at regional (north-east Belgium) and local scale (Mol site) aim to quantify the water flow and the transport of radionuclides through the Boom Clay and in the aquifers surrounding the host formation for different scenarios (normal and altered evolutions) (De Cannière et al., 1994; Horseman and Higgo, 1994).

As discussed in chapter 1, direct experimental evidence for osmosis has been obtained *in situ* in the Cretaceous-age Pierre Shale in South Dakota (Neuzil, 2000) and in the Jurassic-age Opalinus Clay at the Mont Terri Rock Laboratory in Switzerland (Noy et al., 2004).

Similar evidence may also be obtained for the Boom Clay. Studies on the compatibility of Boom Clay with large amounts of bituminized intermediate level waste (3200 tons of Eurobitume medium level waste, MLW, produced by the former Eurochemic fuel reprocessing plant at Dessel, Belgium) have recently raised a particular interest for osmosis. Two ques-

tions thus arise: 1. does the Boom Clay exhibit an osmotic behavior, and if so, 2. to what extent is it relevant for the radioactive waste disposal. The second question particularly pertains to potential hydraulic fracturing of the formation: is it possible to create high pore pressures that could damage the near-field of MLW galleries, if osmotically-driven flows are produced by the release of 750 tons of $NaNO_3$ in the formation?

As part of this study, two *in situ* osmosis experiments were conducted in an existing piezometer at the URL. A recently developed chemical- osmosis flow continuum model (Garavito et al., 2002; Kooi et al., 2003; Bader and Kooi, 2005) was applied:

1. to predict and design the osmosis experiments using existing piezometers, and,

2. to model the data obtained from the *in situ* experiment. Model equations and modelling results are presented in Chapter 6.

5.2   The Boom Clay and the HADES URL

The Boom Clay is an Oligocene silty clay of marine origin. The Boom Clay occurs in a rather continuous bed above an undulated east-west line running from the Scheldt estuary (Sint Niklaas region) to the Meuse river (Eisden region) where it crops out (Figure 5.2). The marine clay was deposited during several transgressions that occurred during the Tertiary period (35 to 30 Ma). Two million years ago, at the end of the Tertiary, the saline pore water of the Boom Clay marine deposits was replaced by fresh water of meteoric origin (Wemaere et al., 2000; Marivoet et al., 2000).

Hydraulic and hydro-geochemical characterization of the Boom Clay has been mainly carried out within the framework of the Belgian programme on the deep disposal of nuclear waste and the European ARCHIMEDE - ARGILE project. The ARCHIMEDE - ARGILE project provided understanding of the geochemistry of the clay and the nature of the interstitial water in the argillaceous medium and its evolution. The Boom Clay is a plastic clay (19-26 wt. % of water) of total porosity of 35 to 40 % by volume. The average clay mineral content (phyllosilicates) is 60 wt. % and the clay mineralogy is dominated by Illite/Smectite (I/S) mixed layers (Vandenberghe, 1978; De Cannière et al., 1994; De Craen et al., 2004). The pore water of the Boom Clay at Mol is typically of $NaHCO_3$ type (850 mg L^{-1}) with a low concentration of chlorides (27 mg L^{-1}) (Henrion et al., 1985; Merceron and Mossman, 1994; De Craen et al., 2004). Most of the marine sodium chloride has already diffused out of the clay formation that is surrounded by fresh water aquifers.

Within the SCK·CEN (Belgian Nuclear Research Center) research programme the hydraulic conductivity and anisotropy of the Boom Clay formation at different scales were determined: analysis of clay cores from several boreholes located in north-east Belgium (cm scale); injection and slug tests in boreholes (m scale); and a small test shaft of the HADES facility used as large-scale macropermeameter (decameter scale). The measurements yield coherent values of hydraulic conductivity of the order of 10^{-12} m s^{-1} and confirm the very low permeability of the Boom Clay. The best estimates of the hydraulic parameters are presented in Table 5.1. The anisotropy of the hydraulic conductivity of the Boom Clay is about 2.4 (De Cannière et al., 1994). The extensive geological, geochemical and hydrological research performed makes the Boom Clay one of the better-characterized

Table 5.1: Hydraulic parameters from *in situ* experiments on Boom Clay cores (De Cannière et al., 1994).

Symbol	Parameter	Value$_{min}$	Value$_{max}$
K_h (m s^{-1})	Hydraulic conductivity ∥ to bedding	$4.5 \cdot 10^{-12}$	$5.2 \cdot 10^{-12}$
K_v (m s^{-1})	Hydraulic conductivity ⊥ to bedding	$2.2 \cdot 10^{-12}$	$2.3 \cdot 10^{-12}$
S_0 (m^{-1})	Specific storage coefficient	$9 \cdot 10^{-6}$	$1.8 \cdot 10^{-5}$
D (m^2 s^{-1})	Effective diffusion coefficient	$1 \cdot 10^{-10}$	$4 \cdot 10^{-10}$
b (Å)	Water film thickness	38	53

clay formations (SAFIR 2 Report, 2001).

5.3 The Osmosis *In-Situ* Experiments

5.3.1 Feasibility and Design

The Hades URL has as advantage that it hosts a huge network of piezometers that can be potentially utilized for *in-situ* osmosis tests in the Boom Clay. Only the piezometers of second generation with filters equipped with two water lines were considered because they allow water/saline solution exchange, or injection. *Krebshöge* porous filters are commonly used by SCK·CEN. The typical values for dimensions (three different size filters) are presented in Table 5.2.

The technical feasibility of chemical-osmosis experiments using second generation piezometers has been initially assessed. Scoping calculations were carried out for that purpose. The three available filter sizes and different exchange solution concentrations were evaluated. The filter and concentration that ensure a significant pressure response after the water/saline solution exchange were selected. Although SCK·CEN interest in osmosis is

Table 5.2: *Krebshöge* porous filters commonly used by SCK·CEN.

Filter	Length (mm)	Inner diameter (mm)	Outer diameter (mm)
Smallest	60.0	50.0	55.6
Larger	200.0	124.0	130.0
Largest	760.0	142.2	149.0

mainly focused on $NaNO_3$ solutions, we adopted a $NaHCO_3$ solution, as NO_3^- is practically absent in the clay pore water (see discussion in Chapter 6 for more comprehensive explanation).

The continuum model presented by Kooi et al. (2003); Bader and Kooi (2005) was used for the calculations (see chapters for model equations and simulation details). Parameters used in the model are default parameters for the Boom Clay (Table 5.1). A significant osmotic signal (induced pressure up to 10 m of water) within a reasonable period of time (30 h) was predicted when using the existing smallest piezometer filters and injecting a 0.14 M $NaHCO_3$ solution (10 times more concentrated than the pore water of the clay) at the local pore pressure in the clay. For the largest filters the maximum induced pressure is reached earlier; however the decay is much slower. From these scoping calculations it was concluded that the duration of the experiment (pressure build-up and decay) is very short and that performance of osmosis in-situ tests using the smallest filters was feasible.

5.3.2 Piezometer

Many piezometers are installed in the HADES URL. To perform an in-situ osmosis test, only the second-generation piezometers with filters equipped with two water lines can be used in order to ensure the water/saline solution exchange, or injection previous to system shut-in. The existing piezometers of second generation are mainly made from a supporting hollow casing, and typically the tubing is fabricated in stainless steel. The hollow casing can support multiple filters installed at different distances from the gallery lining. The filter screens have a relatively small size (diameter: 6 cm, length: 10 cm), and are equipped with an annular filter space as small as possible to minimize the dead volume of water.

The boreholes are drilled in different directions: vertical downwards, horizontal (east, or west), and, inclined at 45 degrees downwards. For this reason, in this thesis we refer to distance from the gallery instead of depth. The hollow casing can support multiple filters installed on the casing at different distances from the gallery lining, *e.g.*, 3, 5, 10, 15, 20 m at the best convenience for the experiment. Most of the filters are located far enough in the clay (further than 5 m), out of the excavation disturbed zone (EDZ), out of the plastic irreversible deformation zone existing around the gallery, to avoid geomechanical interferences.

The filter chambers are equipped with two water lines in order to flush the chamber and to replace the solution in the filter for the test solution. The outer and inner diameters of the stainless steel water lines are often 4 mm / 2 mm.

The piezometer selected for the osmosis in-situ testing was installed in 1992 and used by the Bureau de Recherches Géologiques et Minières (BRGM, Orléans) for a cation exchange experiment in the frame of the ARCHIMEDE Project. It is located in the horizontal direction west, at the ring 85 of the Test Drift of the HADES URL. The length of the piezometer is 4 m and its diameter is 60 mm. It is built in stainless steel and it holds three filters at the following depths: 3 m, 3.5 m and 4 m. This piezometer was used in 1993 to perform a cation exchange capacity (CEC) experiment with cobaltihexamine hydrochloride (Co-Hex). The Co-Hex was recirculated at atmospheric pressure through two of the three filters.

The piezometer was constructed in the workshop of BRGM at Orléans according to a

design plan provided by SCK·CEN. However, the "as-built" plans are no longer available at BRGM with the details of possible technical changes made upon construction. Uncertainties exist about the exact inner diameter of the water lines and dimensions of the porous filters. For modelling, it is assumed that the geometry and dimensions of the filters of this piezometer are the same as the *Krebshöge* filters normally used by SCK·CEN.

5.3.3 Osmosis Tests

The procedure followed to carry out the *in situ* osmosis test is described next.

A solution of 0.14 M $NaHCO_3$ corresponding to 10 times the pore water concentration in the Boom clay was used for the osmosis tests. The filter and water exchange system are described in Figure 5.3. A volume of 1 L of solution containing 122.6 g of $NaHCO_3$ was first prepared and transferred into a stainless steel tank of 20 L. Subsequently, 9 L of de-aired deionized water was transferred into the tank. The solution was then equilibrated with CO_2 by bubbling a mixture of argon containing 400 ppm CO_2 and then by pressurizing the container at 6 bar (absolute). Sampling of the tank containing the 0.14 M $NaHCO_3$ solution was done just before the injection to control the injected solution concentration. The water/solution exchange was carried out at the ambient pore pressure of the clay.

The procedure for the 0.14 M $NaHCO_3$ solution exchange was the following: the two isolation valves (inlet and outlet) of the water tank lines going to the filter 03 were opened. The other two valves isolating the "inlet and outlet" water lines of the filter 03 were opened as well, allowing the circuit to be connected. At that moment the water pressure was exactly the same in the connected system.

Subsequently ($t = 0$), the water recirculation gear pump (*Verder*) was turned on and operated at a flow rate of 100 ml min^{-1}. After 10 minutes (time that ensures that the water volume of the filter has been renewed several times) the water recirculation pump was stopped and the two isolating valves of the filter were closed. Then, the two quick connectors were disconnected from the tank water lines.

Water pressure in the three filters of the piezometer was continuously monitored for several weeks. Data acquisition was performed by means of a Yokogawa data logger.

The first *in situ* test (TI) was started in June 2004. The original test plan considered the water/solution exchange at the ambient pore pressure of the clay. However this was not possible. First pressure sensors had to be emplaced. This required opening of the filters leading to a pressure drop in the three filters. As a consequence, the pore water pressure also significantly decreased in the Boom Clay around the filters.

After installation of the pressure sensors, the water tubing were closed again, and the water pressure allowed to build-up. The disturbance did not equilibrate before the start of the osmosis experiment. Thus, the osmosis response is superposed onto the general water pressure recovery.

The monitoring of the water pressure in the three filters within the piezometer started one week before the experiment. The pressure measurements obtained a few hours prior to the experiment are shown in Table 5.3.

A pore water/saline solution exchange was performed ($t = 0$) in the filter 03 (at 3 m
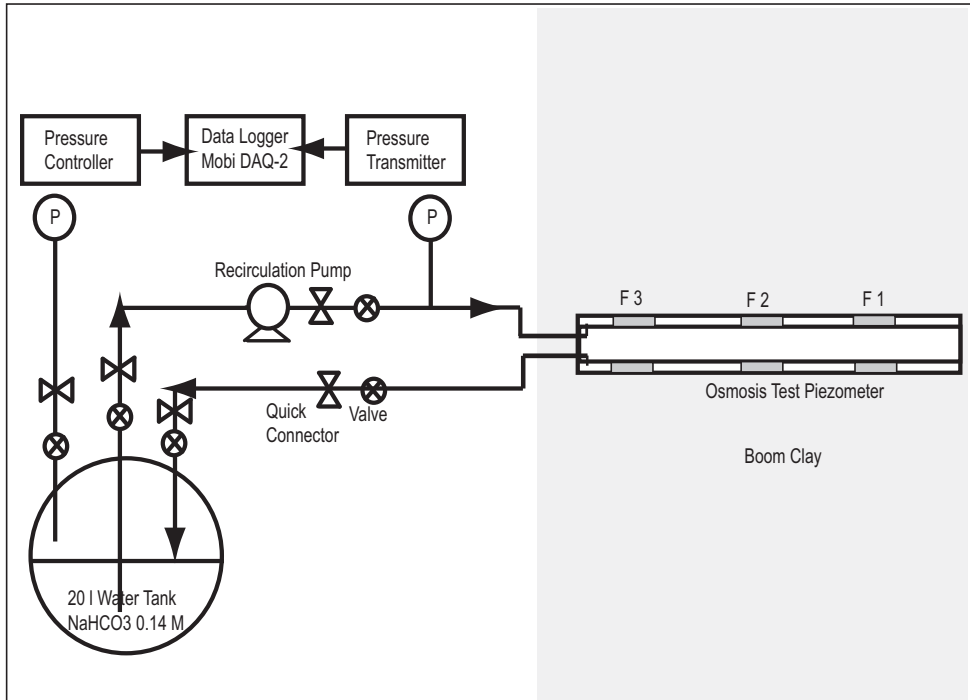
Figure 5.3: Schematic drawing of the water/saline solution exchange system and filter used for the *in situ* osmosis test in the Boom Clay.

Table 5.3: Water pressure and status of the filters before the osmosis test.

Filter	Depth (m)	Pressure (m)	Co-Hex (mg L^{-1})	Status	Selection
03	3.0	55.57	700 to 4000	First candidate	Test 1 and 2
02	3.5	60.89	5570	Disturbed Co-Hex	Discarded
01	4.0	64.88	never used	Filter in reserve	Test 3

from the gallery) at constant hydraulic pressure (5.45 bar = 55.57 m water), *i.e.*, the local water pressure of the clay at the moment of exchange. The water pressure was equilibrated in the 20 L solution tank with that of the piezometer filter (5.45 bar = 55.57 m water) using a *Druck* pressure controller.

During the recirculation of the solution, the water pressure inside the circuit increased to 57.41 m of water because of the pressure gradient imposed by the gear pump. The water

pressure stabilized between 56.59 m and 57.10 m of water just after the disconnection of the tank.

Monitoring of the water pressure in the three filters continued for more than 100 days. The measurements are shown in Figure 5.4. Several phenomena can be recognized in the pressure response of the three filters. Figure 5.4a shows the rise in pressure in all filters before the injection occurred. This reflects the equilibration due to sensor installation. Also shown in Figure 5.4a is the distinct behavior of filter 3 compared to the response of the other filters. Nearly 6 hours after exchange a pressure increase within the filter containing more saline water (filter 3) is detected. The deviation relative to the response that would be anticipated in the absence of osmotic effects consists of a rise in head of about 2 m over the first 30 hours after solution exchange. The rise in head is followed by a gradual decline. The osmotic effect seems to have dissipated after about 15 days. Figure 5.4b displays the response in some detail for the first two days following injection. The figure shows that all filters exhibited a short but rapid rise in head during the first minutes which subsequently rapidly dissipates. This response feature is largest in filter 1 and decreases away from the gallery. The pressure pulse in filter 3 reflects the influence of the pumping during injection. Apparently this pressure pulse is immediately transmitted to the other filters. Most likely this has to do with compression of the clay skeleton but is otherwise not well understood.

The observed increase in pressure is interpreted to be produced by a water inflow from the clay formation into the filter caused by osmosis, and by the pressure recovery due to the initial disturbance.

The second osmosis *in situ* test (TII) was started in February 2005. The experimental conditions were identical to those of TI. The same filter and a solution with the same concentration were used. However, at the beginning of this test, the filter and the clay were in hydraulic equilibrium. The water/solution exchange was performed at the ambient pore pressure of the clay, ensuring therefore an initial equilibrium condition. The pressure response is shown in Figure 5.5. Similar features to those observed for TI are found in this figure. Nevertheless, the pressure pulse due to injection is more pronounced when compared with the pulse observed in TI. Similarly to TI this behavior is also observed in the other two filters and rapidly dissipates. Additionally a general trend of the hydraulic pressure to slightly decrease as a function of time in the three filters is observed (Figure 5.5a). This behavior is not clearly understood and a possible explanation maybe a large-scale geomechanical perturbation induced by the excavation works of the second shaft and of a new connecting gallery. Pressure response in filter 3 differs from the other filters and a pressure build -up of nearly 2 meters relative to the starting pressure is observed. In this case the observed increase in pressure is interpreted to be produced only by a water inflow from the clay formation into the filter caused by osmosis.

5.4   General Discussion

The experimental results obtained *in situ* confirm the occurrence of chemical osmosis in a low-permeability plastic formation such as the Boom Clay. From the observations it appears that the necessary conditions prevail to maintain the osmosis induced fluxes and to

Figure 5.4: a) Pressure evolution in the piezometer for the first osmosis test: filters located at 3 m (filter 3), 3.5 m (filter 2) and 4 m (filter 1) from the gallery. The osmosis test was performed in the filter located at 3 m from the gallery. b) Zoom in of the first hours of the test.

Figure 5.5: a) Pressure evolution in the piezometer for the second osmosis test: filters located at 3 m (filter 3), 3.5 m (filter 2) and 4 m (filter 1) from the gallery. The osmosis test was performed in the filter located at 3 m from the gallery. b) Zoom in of the first hours of the test.

prevent the fast dissipation of osmosis. Analysis and modelling of the experimental data (fully described in Chapter 6) showed that the osmotic efficiency of Boom Clay is high under undisturbed chemical conditions ($\sigma = 41$ % at 0.014 M NaHCO$_3$), but rapidly decreases when the concentration increases ($\sigma = 7$ % at 0.14 M NaHCO$_3$). The semi-permeable membrane behavior of the Boom Clay (high efficiencies) is relevant for the radioactive waste disposal. However, the presently observed osmotically-induced pressure is very low (0.2 bar, or 2 m water column). At this level, the osmotic pressure does not represent a danger of hydraulic fracturing for the host rock. The duration of the osmosis test performed suggests that the shut-in test method is effective for osmosis testing. Long-term monitoring of the changes in concentration may provide additional information useful to better estimate the diffusion coefficient values. To assess the osmotic effect induced by the salts released by intermediate level bituminized waste, the test should also be performed with NaNO$_3$ solutions. Interpretation will be more complex because of the side effects due to the reduction of nitrate and pyrite oxidation during the diffusion of nitrate in the very reducing Boom Clay.

In the first osmosis test (TI), due to time constraints the hydraulic equilibrium could not be fully restored at the start of the experiment. This introduced complexities for the modelling and the isolation of the osmotic effect (see Chapter 6). However, for the second
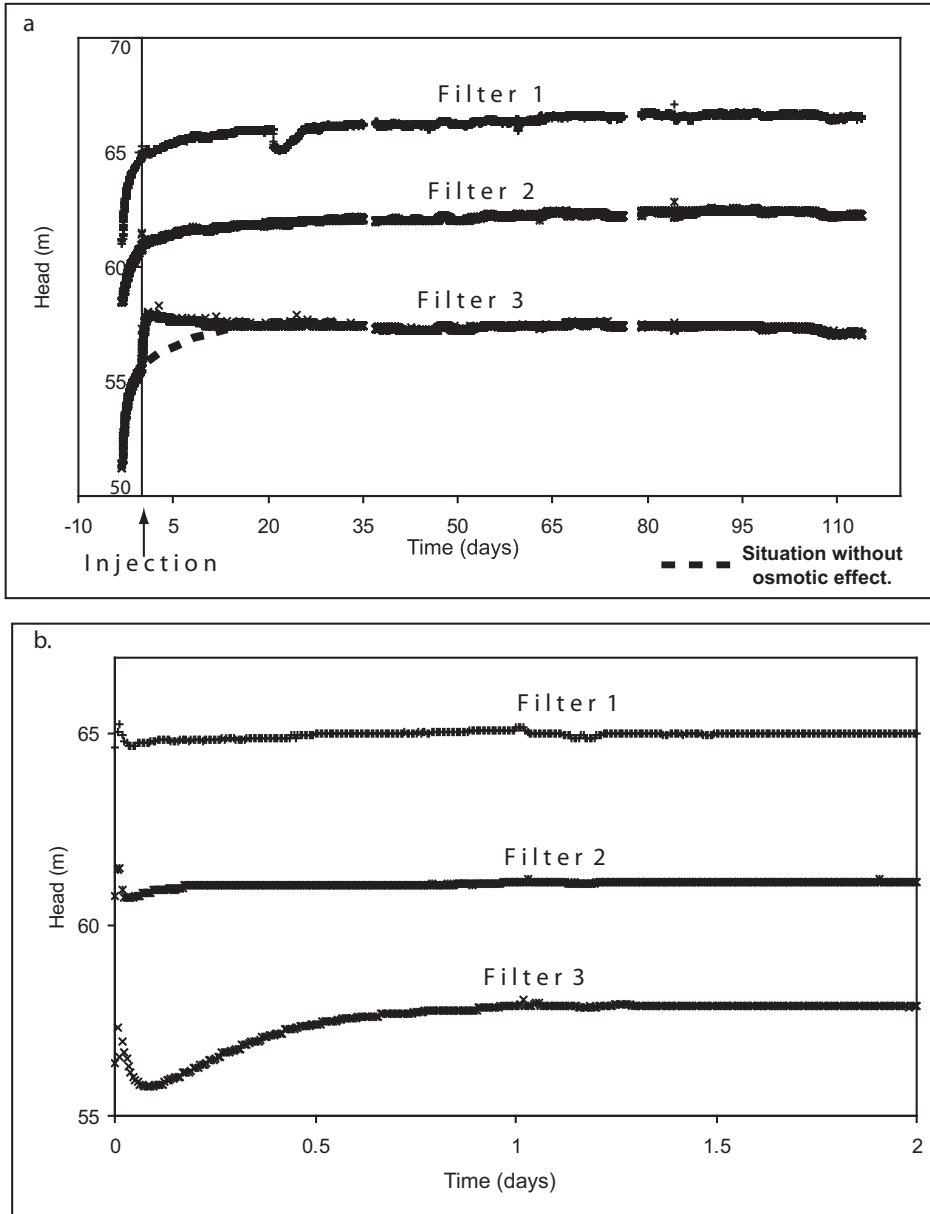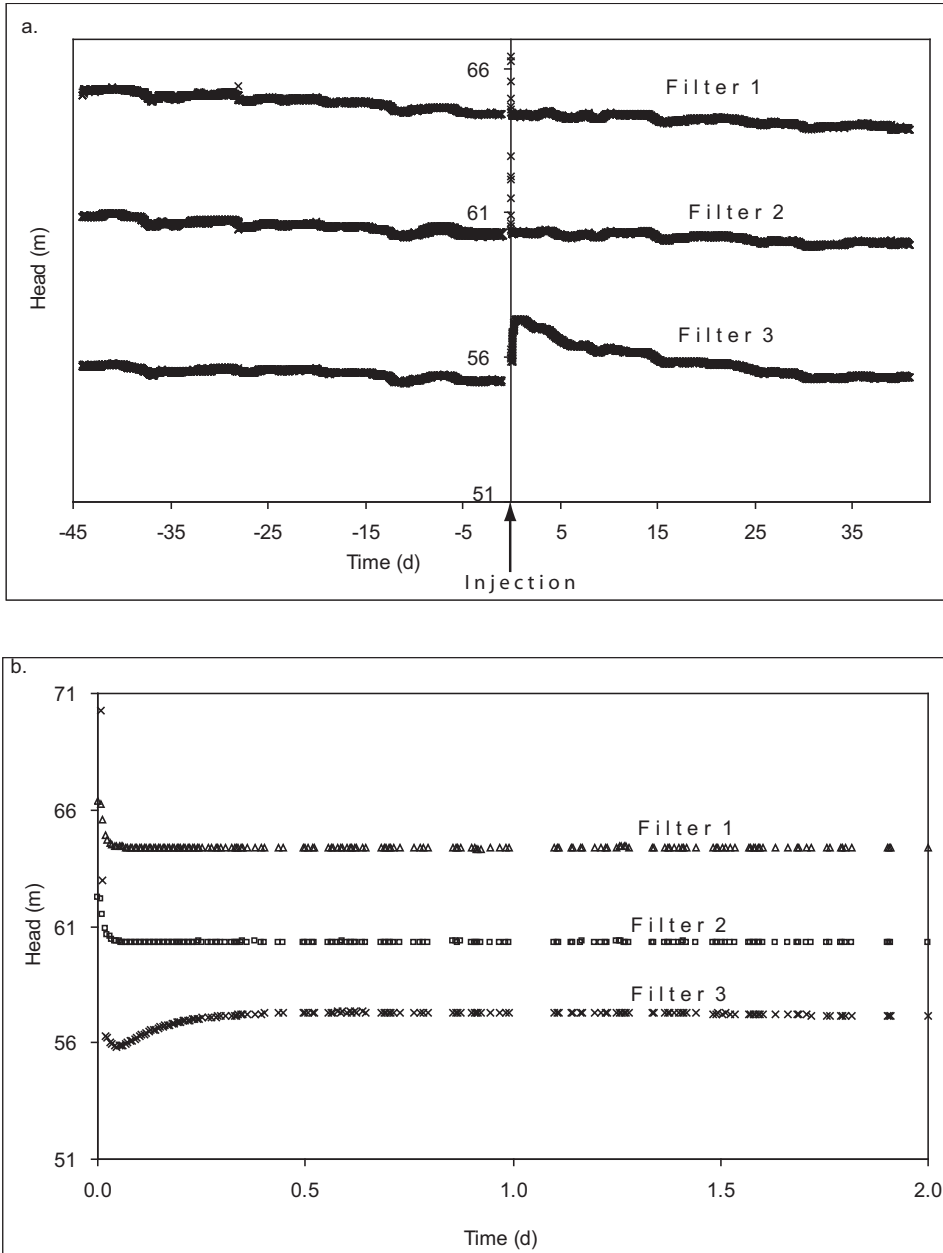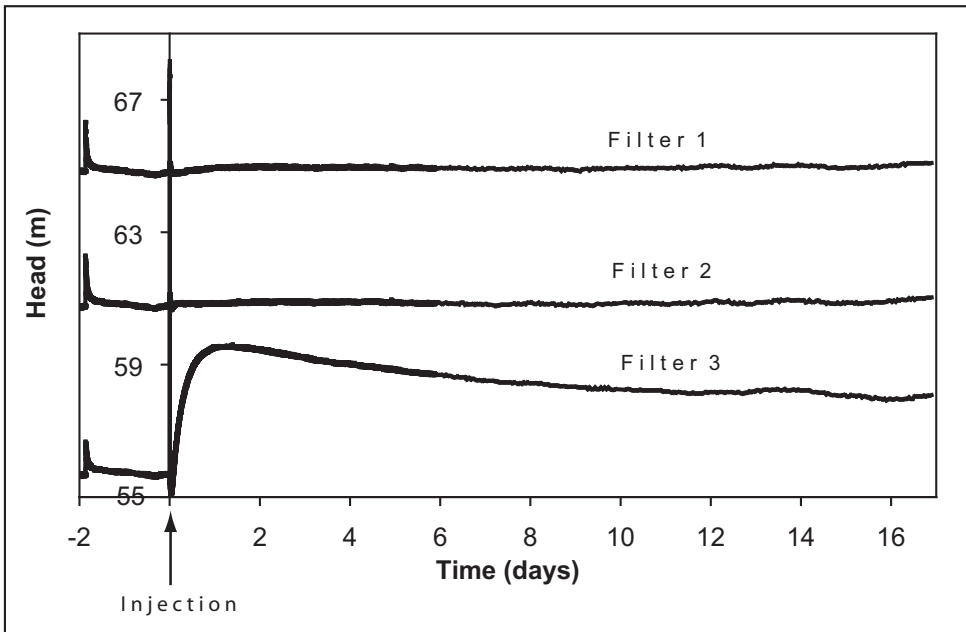

Figure 5.6: Pressure evolution in the piezometer for the third osmosis test: filters located at 3 m (filter 3), 3.5 m (filter 2) and 4 m (filter 1) from the gallery. The osmosis test was performed in the filter located at 3 m from the gallery.

test (TII), the initial hydraulic equilibrium is fully achieved. An inherent difficulty of *in situ* testing in low permeability sediments is to guarantee hydraulic equilibrium as initial condition. In addition to obtaining measurements of fluid pressure and chemistry simultaneously, quantifying the membrane behavior and properties of clayey sediments usually requires observation of a pore water duplicate test to isolate the osmotic effects. The data acquired from filters 1 and 2 was very useful in this case, they were similar to a "pore water duplicate test" and allowed isolation of the osmotic effect.

The injection filter 03 used is located at 3 m, not far away from the gallery. However, we do not expect a significant effect of the excavation disturbed zone (EDZ) on the *in situ* osmosis experiment because of the self-sealing properties of the plastic Boom Clay (Davies and Bernier, 2004). So, if an excavation-induced fissure should have crossed the filter location, this fissure should be closed now. We do not expect any significant change in hydraulic conductivity around the filter 03 used for the osmosis test. However, the local porosity in a sealed fissure could be a little bit higher that in the intact clay matrix. No important oxidation that could decrease the osmotic efficiency is expected at a depth of 3 m in the clay matrix.

At the moment SCK·CEN is considering further experimenting with solutions of different concentration. Besides, additional testing with $NaNO_3$ solutions should be carried to evaluate the osmotic effect induced by the salts released by intermediate level bituminized waste. A few days before publishing of this thesis the results of additional tests became. Three independent reference experiments with Boom Clay pore water (0.014 M $NaHCO_3$) were carried out. The aim was to assess the magnitude and the effect of the hydraulic perturbation which could be caused by the pump during the 10 minute water recirculation cycle. At a first glance, it was not observed any drastic effect from the pump that could really jeopardize the results of the previous osmosis experiments. However detailed inspection, revealed that small perturbations occurred, caused by handling of the tubing for the injection procedure. These perturbations are being further investigated. Additionally, a third osmosis test with a solution of 0.7 M $NaHCO_3$ corresponding to 50 times the pore water concentration in the Boom clay was performed. Using the inferred parameters from modelling of the second test (see Chapter 6) we have predicted for this third osmosis test a maximum pressure build up of 4.4 m approximately 17 hours after injection. The experimental data is shown in Figure 5.6. The observed pressure peak and the corresponding time of the peak are in good agreement with the preliminary predictions.

References

Bader, S., Kooi, H., 2005. Modelling of solute and water transport in semi-permeable clay membranes: Comparison with experiments. Advances in Water Resources (28), 203–214.

Cey, B., Barbour, S., Hendry, M., 2001. Osmotic flow through a Cretaceous clay in southern Saskatchewan, Canada. Canadian Geotechnical Journal (38), 1025–1033.

Davies, C., Bernier, F., 2004. Impact of the excavation disturbed or damage zone (EDZ) on the performance of radioactive waste geological repositories. In: Proceedings of a European Commission Cluster Conference held in Luxembourg on 3-5 November 2003. Conference jointly organised by the European Commission and EIG Euridice (Belgium). European Commission, Nuclear Science and Technology. EUR series. Luxembourg.

De Cannière, P., Put, M., Neerdael, B., 1994. Hydraulic characterization of the Boom Clay Formation from the HADES underground laboratory in Mol: evolution and assessment of the piezometric techniques. In: Hydraulic and hydrochemical characterisation of argillaceous rocks. Proceedings of an international workshop at Nottingham, United Kingdom, 7-9 June 1994. OECD/NEA documents (disposal of radioactive waste). pp. 159–166.

De Craen, M., Wang, L., Van Geet, M., Moors, H., 2004. Geochemistry of Boom Clay pore water at the Mol site - Status 2004. 179 pp., sck·cen scientific report blg-990 Edition.

Garavito, A., Bader, S., Kooi, H., Richter, K., Keijzer, T., 2002. Numerical modeling of chemical osmosis and ultrafiltration across clay membranes. Development in Water Sciences 1, 647–653.

Hendry, J., Wassenaar, L., Kotzer, T., 2000. Chloride and chlorine isotopes as tracers of solute migration in a thick, clay rich. Water Resources Research (36), 285–296.

Henrion, P., Monsecour, M., Fonteyne, A., Put, M., De Regge, P., 1985. Migration of radionuclides in Boom Clay. Radioactive Waste Management and the Nuclear Fuel Cycle (6(3-4)), 313–359.

Horseman, S., Higgo, J., 1994. Summary report on the workshop on Determination of Hydraulic and Hydrochemical Characterisation of Argillaceous Rocks. In: Workshop on Determination of Hydraulic and Hydrochemical Characterisation of Argillaceous Rocks. OECD Documents Disposal of Radioactive Waste. Nottingham, United Kingdom, pp. 7–14.

Kooi, H., Garavito, A., Bader, S., 2003. Numerical modelling of chemical osmosis and ultrafiltration across clay formations. Journal of Geochemical Exploration (78-79), 333–336.

Marivoet, J., Van Keer, I., Wemaere, I., Hardy, L., Pitsch, H., Beaucaire, C., Michelot, J., Marlin, C., Philippot, A., Hassanizadeh, M., Van Weert, F., 2000. A palaeohydro-geological study of the Mol site (PHYMOL project), 101 pp. Work carried out under a cost-sharing contract with the European Commission, Nuclear Science and Technology, 4th Framework Program (1994-1998) under contract N F14W-CT96-0026., final report: eur 19146 en Edition.

Merceron, T., Mossman, J., 1994. The Archimède-Argile Project: acquisition and regulation of the water chemistry in a clay formation. In: Hydraulic and hydrochemical characterisation of argillaceous rocks. Proceedings of an international workshop at Nottingham, United Kingdom, 7-9 June 1994. OECD/NEA documents (disposal of radioactive waste). pp. 119–131.

Neuzil, C., 2000. Osmotic generation of "anomalous" fluid pressures in geological environments. Nature (403), 182–184.

Noy, D., Horseman, S., Harrington, J., Bossart, P., Fisch, H., 2004. An Experimental and modelling study of chemico-osmotic effects in the Opalinus Clay of Switzerland. In: Heitzmann, P. ed. (2004) Mont Terri Project - Hydrogeological Synthesis, Osmotic Flow. Reports of the Federal Office for Water and Geology (FOWG), Geology Series (6), 95–126.

SAFIR 2 Report, O., 2001. SAFIR 2 Report, Safety Assessment and Feasibility Interim Report 2; coordinated by De Preter P., Lalieux P. and Cool W. (eds.). ONDRAF/NIRAS, Belgian Agency for Radioactive Waste and Enriched Fissile Materials., four volumes, 13 chapters; nirond 2001-06 e. Edition.

Shackelford, C., Malusis, M., Olsen, H., 2001. Clay membrane barriers for waste containment. Geotechnical News (2), 39–43.

Vandenberghe, N., 1978. Sedimentology of the Boom Clay (Rupelian) in Belgium. Verhand. Kon. Acad. Wetenschappen Belgi, XL (147), 137.

Wemaere, I., Hardy, L., Van Keer, I., Marivoet, J., Labat, S., Sillen, X., 2000. A palaeohy-drogeological study of the Mol site (PHYMOL Project). Topical report 4: Climatic effects in the regional hydrogeological model for the performance of the Boom Clay Formation, DOC RTD/0056/2000 - EN. EC, DG for Research. Brussels, 72 pp.

Numerical Modelling of Osmotic Processes

In addition to experimental evidence, a theoretical framework is essential to comprehensively understand the role of osmosis on water and solute transport in low-permeability materials. Appropriate theories and mathematical models of osmosis in groundwater flow may be useful for the interpretation of the hydrogeological evolution of sedimentary basins and may constitute an excellent predictive tool for many practical problems as pollution and waste-containment assessment. In the past, several theories of osmosis have been applied to elucidate the origin of anomalous pressures and salinities in low permeability environments. Recently, the number of theoretical investigations considering osmotic effects has been increasing. Nevertheless, there is a limited number of studies that deal with predictions of the evolution of pressure and salinity *within* a clay formation that behaves as a semi-permeable membrane. In this chapter a chemical osmosis continuum model (Garavito et al., 2002; Kooi et al., 2003; Bader and Kooi, 2005) has been applied to one laboratory study and two *in situ* experiments.

6.1   Coupled Osmotic Flows and Existing Formulations

Coupled flow and transport phenomena are described within the framework of irreversible thermodynamics (Katchalsky and Curran, 1965). As mentioned in Chapter 1 this theory accounts for the different types of flows that are related to different types of driving forces (Table 2.1). The theory was developed under the following assumptions (Mitchell, 1993):

1. Local equilibrium.
2. Linear phenomenological equations $J_i = \sum_j^n L_{ij} X_j$; where J_i is a flux of the type i driven by n different j type potential gradients. L_{ij} terms are the conductivity coefficients for the flow.
3. Validity of Onsager reciprocal relations ($L_{ij} = L_{ji}$).

Thus each type of flow relates to its corresponding driving force ($i = j$) and to the other type of driving forces ($i \neq j$). The latter flows are known as coupled flows.

Darcy's Law and Fick's law are simplified versions of the coupled flow theory (Table 2.1). Fluid flow caused by driving forces other than hydraulic gradients is referred to as os-

mosis. In this study we consider only hydraulic and chemical gradients. Thus, the chemical osmosis continuum model (Garavito et al., 2002; Kooi et al., 2003; Bader and Kooi, 2005) that we applied only contains the coupled flow and transport equations describing chemical osmosis, hydraulic flow and diffusion.

Discontinuous formulations where flows are cast in terms of differential values of pressure and concentration across the membrane (Kedem and Katchalsky, 1965; Katchalsky and Curran, 1965; Yeung, 1990; Yeung and Mitchell, 1993; Olsen et al., 2000) have been used extensively to calculate average membrane efficiencies from laboratory experimental data for steady-state ultrafiltration or osmotic equilibrium conditions (Hanshaw and Coplen, 1973; Keijzer, 2000; Cey et al., 2001). Others, (Greenberg et al., 1973; Mitchell et al., 1973; Malusis and Shackelford, 2002a,b; Manassero and Dominijanni, 2003; Bader and Kooi, 2005; Noy et al., 2004; Oduor, 2004) have derived contimuum transport formulations that, together with conservation equations for solute and water, yield a set of coupled differential equations for continuum models that allow simulation of transient flow and transport conditions *within* membranes. Mitchell et al. (1973) used a one-dimensional model to investigate the pore pressure reduction in a clay layer subjected to saline boundary conditions at top and bottom. In a similar study, Greenberg et al. (1973) simulated settlement due to consolidation of a confining layer in the Oxnard basin, California, following seawater intrusion into a contiguous aquifer. Barbour and Fredlund (1989) also simulated osmotic consolidation of a semi-permeable membrane. Soler (2001) used a one-dimensional model to study the role of coupled transport phenomena, including thermal osmosis, in radionuclide transport from a repository of high level nuclear waste in the Opalinus Clay, Switzerland. The model was reduced, however, to a conventional diffusion-advection equation with a constant advection velocity, thereby negating the feedback of temporal and spatial changes in the concentration gradients on osmotic transport. The equations presented by Greenberg et al. (1973) were modified and used by Noy et al. (2004) to interpret the results obtained in laboratory and *in situ* experiments in the Opalinus Clay. Oduor (2004) developed a transient model that is able to describe ultrafiltration effects. The model was tested against existing experimental laboratory data reproducing them accurately.

Garavito et al. (2002), Malusis and Shackelford (2002a,b), Kooi et al. (2003) , Manassero and Dominijanni (2003), Bader and Kooi (2005) presented all continuum formulations useful for simulation of transient flow and transport across semi-permeable membranes.

The model presented by Garavito et al. (2002), Kooi et al. (2003), Bader and Kooi (2005) incorporates the strong dependence of the efficiency of the membrane on the local and momentary concentration (Bresler, 1973). This model is presented below and used later in this study.

6.2   Continuum Transport Model Used in this Study

Bader and Kooi (2005) have deduced the equations of chemically and hydraulically coupled flows of solution, J_v (m^3/m^{2}s) and solute mass, J_s^m (kg/m^{2}s) to have the following forms:

$$J_v = -\frac{k}{\mu}(\rho_0 g \nabla h - \sigma \nabla \pi) \tag{6.1}$$

$$J_s^m = -D^* \nabla (\rho w) + (1 - \sigma) \rho w J_v \tag{6.2}$$

where h represents the (fresh water) hydraulic head (m), k is the intrinsic permeability (m^2), μ is the fluid viscosity (Pa·s), π is osmotic pressure (Pa), ρ is the fluid density (kg/m^3), w is the solute mass fraction (-), D^* is the diffusion coefficient (m^2/s) in the presence of a porous medium, including membrane effects, and σ is the reflection coefficient, or efficiency, of the membrane. In the absence of membrane effects, D^* includes a correction for both tortuosity and porosity relative to the free water diffusion coefficient; the membrane effect describes the restriction of molecular diffusion by the membrane. D^* does not include solute sieving associated with either hydraulically-driven or osmotically-driven fluid flow. This is dealt with in the second term in equation (6.2). Note that the use of head in the flow equation implies that density-driven fluid flow is neglected. The gradient of osmotic pressure is computed as:

$$\nabla \pi = (\frac{RTf\rho}{m_i})\nabla w \tag{6.3}$$

where R is the universal gas constant (J/mol ^oK), T is the temperature (^oK), f is the number of moles of ions into which 1 mole of the electrolyte dissociates (-) and m_i is the molecular weight (kg/mol). The model accounts for transient flow and transport conditions due to storage associated with the compressibility of both the fluid and the solid matrix in the following way. The transport constitutive laws (equations (6.1) and (6.2)) are substituted in mass conservation equations for the solution and solute in a deformable porous medium:

$$\nabla \cdot (\rho J_v) = -n \frac{\partial \rho}{\partial t} - \frac{\rho}{1-n} \frac{\partial n}{\partial t} \tag{6.4}$$

$$\nabla \cdot (J_s^m) = -n \frac{\partial(\rho w)}{\partial t} - \frac{\rho w}{1-n} \frac{\partial n}{\partial t} \tag{6.5}$$

where n is porosity and t is time. Equation (6.4) was derived by Palciauskas and Domenico (1980) by combining mass conservation for both the fluid phase and the solids and considering the fact that equation (6.1) describes flow relative to the solids. Material derivatives are replaced here by partial derivatives. This is allowed if the deformation (strain) of the porous medium is small. Equation (6.5) is the equivalent form for conservation of solute. An equation of state relates the solution density to both mass fraction and fluid pressure:

$$\rho = \rho_0 \exp(\beta \rho_0 g h + \gamma w) \tag{6.6}$$

where β is solution compressibility (Pa^{-1}), γ is an empirical coefficient of value 0.69 (-) and ρ_0 is the reference solvent (water) density Leijnse (1992). For incompressible grains, porosity changes are governed by:

$$\frac{1}{(1-n)}\frac{\partial n}{\partial t} = \rho_0 g \beta_p \frac{\partial h}{\partial t} \tag{6.7}$$

where β_p denotes pore compressibility (Pa^{-1}). Substitution of (6.6) and (6.7) in (6.4) and (6.5) yields:

$$-\frac{1}{\rho}\nabla \cdot (\rho J_v) = S_s \frac{\partial h}{\partial t} + \gamma \frac{\partial w}{\partial t} \tag{6.8}$$

$$-\frac{1}{\rho}\nabla \cdot (J_s^m) = w S_s \frac{\partial h}{\partial t} + n(1+\gamma w)\frac{\partial w}{\partial t} \tag{6.9}$$

where S_s denotes specific storage (m^{-1}).

In the absence of membrane effects and if density variations associated with solute transport are neglected - that is , if $\gamma = 0$ - equation (6.8) yields the conventional diffusion equation of groundwater flow. Additionally, if changes in solute mass due to storage changes of the solution are neglected (first term right-hand side of equation (6.9)), equation (6.9) yields the conventional advection-diffusion equation for solute transport.

To account for the strong dependency of σ on w and b we used the relationship described by Bresler (1973) shown in Figure 6.1. Also shown in Figure 6.1 are the marker points for a spline function that Neuzil (2000) used to fit the relationship of Bresler (1973) for his analysis. For modelling we approximated the relationship of Bresler (1973) with linear segments between the same marker points. The relationship of Bresler (1973) was chosen among other models based on the study of Keijzer (2000) that suggested that this model appears to be valid over the entire porosity and concentration range encountered in natural geological environments.

The effective diffusion coefficient for a semi-permeable membrane (D^*) is related to the membrane efficiency Katchalsky and Curran (1967); Manassero and Dominijanni (2003); Bader and Kooi (2005) as:

$$D^* = D(1-\sigma) \tag{6.10}$$

where D is the diffusion coefficient without membrane effects. Malusis and Shackelford (2002b) provide actual measured data that show a close resemblance to this relationship.

The above equations for coupled osmotic transport were implemented in the generic modelling code FlexPDE (PDE, 2001). The code was subsequently used to model different existing experiments: one laboratory osmosis experiment with bentonite reported by Keijzer (2000) and two osmosis *in-situ* experiments: the experiment in the Pierre Shale reported by Neuzil (2000) and the experiment carried out in the Boom Clay as part of this study (Chapter 5). In Chapter 7 the model is applied to the Triassic Dunbarton Basin scenario (Marine and Fritz, 1981) in which anomalous pressures have been regarded as induced osmotic pressures.
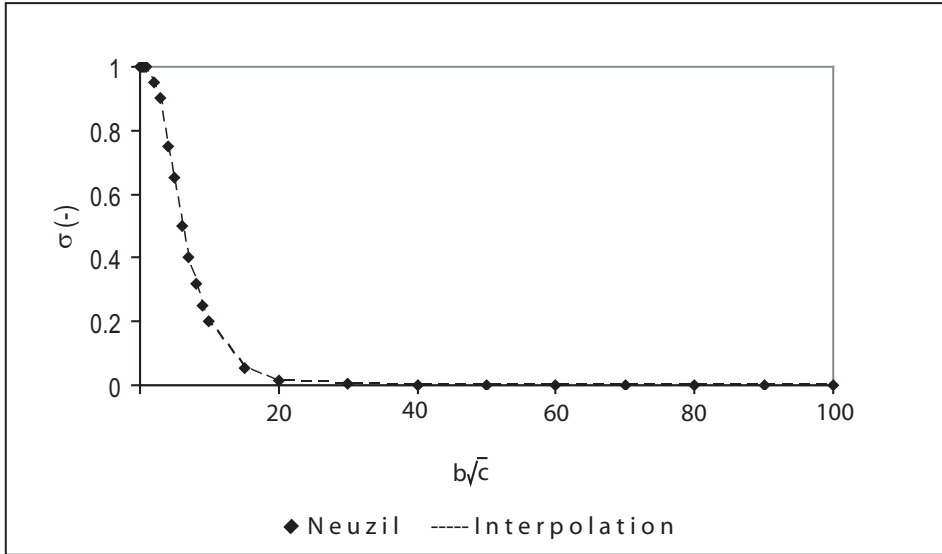
Figure 6.1: Osmotic efficiency σ as a function of concentration ($c = w/m_i$) and b. w corresponds to mass fraction and m_i to molar mass. Symbols represent the data points from Bresler's relationship used in the present study and the study of Neuzil (2000). Straight line segments between the symbols indicate the interpolation scheme used in the present study.

6.3 Numerical Modelling of a Laboratory Osmosis Test with Compacted Bentonite

Keijzer (2000) reported on the results of a series of osmosis experiments using a cylindrical flexible wall permeameter. Experiments were conducted on compacted and non-compacted Ankerpoort Colclay bentonite. The semi-permeable behavior of the bentonite was evaluated by measuring the osmotically-induced fluxes across the bentonite and inferring the corresponding reflection coefficient. A bentonite sample approximately 2 mm thick was placed within the permeameter between two saturated porous stones connected each one to a closed reservoir. One of the reservoirs contained a low concentration NaCl solution (0.01 mol/l) and the other a high concentration solution (0.1 mol/l). In this section the data corresponding to a compacted bentonite (AWyc) were modelled. Model equations previously presented are in terms of head and S_s. However at an earlier stage of this project the older version of the code was in terms of pressure and S_s was accounted for by β. The compressibility β was increased/decreased to simulate the storage capacity within the reservoirs. The pressure evolution across the membrane and the EC changes during the experiment with AWyc are shown as dots in Figure 6.2. Mass fraction (w) was converted to

EC using an empirical relationship for NaCl solutions ($EC = uFw\rho_f M_s$) with u the mobility of NaCl ions, F Faraday's constant, ρ_f the fluid density and M_s the solute molecular weight. In the figure, two phases can be recognized. In the first phase (first 150 hours) the differential pressure increases due to the imposed chemical gradient that induces water movement from the low concentration water reservoir into the more concentrated water reservoir. In the second phase differential pressure decreases as the chemical gradient becomes smaller between the two reservoirs due to diffusion across the membrane.

The model domain (Figure 6.3), was structured based on the experimental set up given by Keijzer (2000). Similarly, initial and boundary conditions (no flow boundary conditions) were assigned based on the experimental conditions for the AWyc experiments. The 2.3 mm thick bentonite membrane with $n = 0.5$ and $k = 1.2 \cdot 10^{-19}$ m^2, is in between two approx. 7 mm thick porous stones. For the numerical experiment, the model domain consisted of three regions. One corresponding to the bentonite membrane (assumed to be saturated with high NaCl concentration water) and two reservoirs representing the two porous stones: one saturated high with NaCl concentration water and the other saturated with low concentration water. Within the reservoirs, porosity and permeability are set to high values ($n = 1$ and $k = 1 \cdot 10^{-14}$ m^2). The diffusion coefficient and σ inferred by Keijzer (2000) were used for the clayey part of the domain. Keijzer (2000) inferred an osmotic reflection coefficient $\sigma = 0.023$ from the maximum differential pressure and the associated differential concentration and a diffusivity of $D = 1 \cdot 10^{-9}$ m^2/s from the decline in differential concentration during the second phase of his experiment. For modelling, the latter value is corrected for porosity relative to the value reported by Keijzer (2000) which accounted for tortuosity only. Efficient mixing in the two reservoirs is simulated by assigning diffusion coefficient three orders of magnitude higher than that in the membrane ($D = 1 \cdot 10^{-9}$ m^2/s). For the entire domain the pressure initial condition is set to zero. Initial mass fraction for the left reservoir and the bentonite is $w = 5.6 \cdot 10^{-3}$ (high NaCl water concentration), and for the right reservoir $w = 5.6 \cdot 10^{-4}$ (low NaCl water concentration). It is assumed that hydraulic storage capacity within the reservoirs is controlled only by the water compressibility ($\beta = 4.6 \cdot 10^{-10}$) Pa^{-1}. The numerical experiment was run using these parameters and conditions. Figure 6.2 displays the differential pressure evolution and EC evolution within the right reservoir resulting from this simulation (S1).

Comparison with the experimental data shows that the magnitude of the maximum differential pressure is quite well reproduced. However the maximum occurs too early and the decay in pressure during subsequent times is too fast. Additionally the EC in the low salinity reservoir increases much more slowly than observed. In other simulation (S2) the fluid compressibility for the two reservoirs is increased to $\beta = 2 \cdot 10^{-6}$ Pa^{-1} an effective value meant to simulate the potentially much larger storage capacity of the reservoirs due to their expansion contraction upon pressure increase/decrease Neuzil (1982). For this simulation the first phase of differential pressure buildup is better reproduced. In order to improve the correspondence with the EC data in simulation 3 (S3) the diffusivity is increased by a factor of ten ($D = 1.06 \cdot 10^{-11}$ m^2/s). In this way the first phase of differential pressure buildup is better reproduced and the misfit in the decline in differential pressure is larger than that for S1.
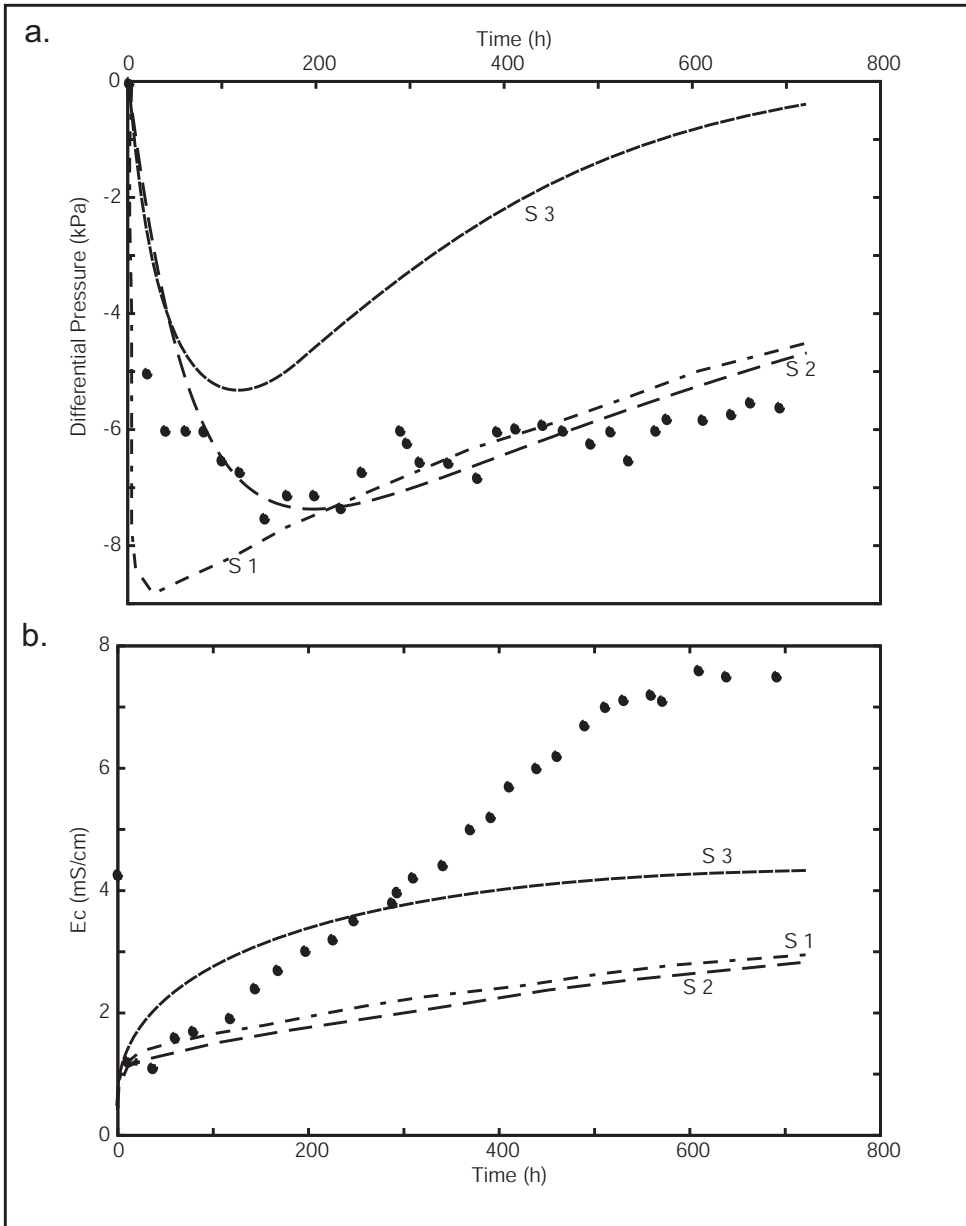
Figure 6.2: Experimental data and model predictions of the differential pressure (a) and electrical conductivity (EC) evolution (b) of the low salinity reservoir for the laboratory osmosis experiment by Keijzer (2000)
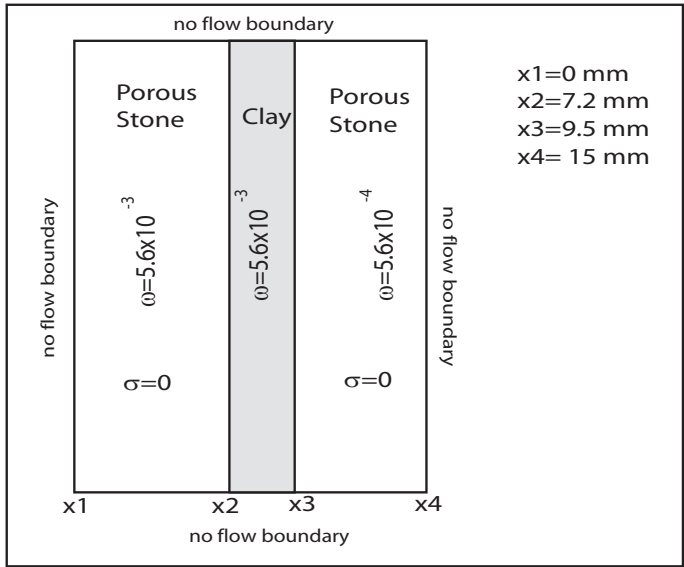
Figure 6.3: Model configuration used for simulations of the laboratory osmosis experiment by Keijzer (2000)

With the present model equations, the development of the differential pressure agrees quite well with observations; however the pressure and salinity data cannot be simultane-ously reproduced. Keijzer (2000) suggested a rapid decrease in semi-permeability after about 240 hours due to the shrinkage of the double layer of the clay platelets, enhancing flocculation and making the clay more permeable. To what extent such changes would in-deed account for the observed trends has not been ascertained. However, it is not expected that the slow decrease in differential pressure can be better accounted for.

6.4 Numerical Modeling of a Long-term In-Situ Chemical Osmosis Experiment in the Pierre Shale, South Dakota

First direct evidence that osmosis can be significant in geological environments came from a field experiment in the Cretaceous-age Pierre Shale in South Dakota described by Neuzil (2000). To conduct the experiment, waters of different salinity were added to four boreholes and the water levels and TDS were monitored. By analyzing the pressure and TDS changes over nine years, at which time osmotic equilibrium was thought to have been reached, Neuzil (2000) calculated membrane properties of the Pierre Shale, notably the thickness of the water film between the clay platelets b and the corresponding reflection coefficient σ. His results imply that, when sufficiently compacted, shale membranes are capable of generating osmotic pressures up to about 20 MPa, a pressure equivalent to 2 km

of head.

The analysis of Neuzil (2000) considered only the final water levels and TDS values to calculate the shale's osmotic efficiency; the evolution of the system from the initiation of the experiment to that time was not analyzed. Because the implications of the experiment are far-reaching, a more complete analysis of it was warranted. Together with Chris Neuzil and Henk Kooi we have simulated the experiment in its entirety, including all the changes in borehole water-levels and TDS from initiation to the end of the experiment (Garavito et al., 2005). Our specific aims were to: (a) model the evolution of the system and test to what extent our approach allows us to explain its behavior, and (b) compare the inferred model parameters with those obtained by Neuzil (2000) for equilibrium conditions. We will first describe the experiment of Neuzil (2000) in more detail, followed by the modelling process and results. Finally, the findings from the modelling are discussed.

6.4.1 Neuzil's (2000) Experiment

The host medium for Neuzil's (2000) in situ experiment, the Cretaceous Pierre Shale, is a low permeability claystone found over much of central North America. It and its equivalents extend more than 2000 km from northwestern New Mexico, USA into Alberta and Saskatchewan, Canada. Its thickness exceeds 500 m over much of its extent and reaches nearly 3 km in the Denver Basin. At the experiment site the Pierre Shale is approximately 70 % to 80 % clay of which about 80 % is mixed-layer smectite/illite (Neuzil, 2000).

Hydraulic properties of the shale at various scales have been measured and reported by Bredehoeft and Milly (1983), Corbet and Bethke (1992), Neuzil (1993) and Neuzil (1994). Permeability values in the range of 10^{-17} to 10^{-21} m^2 have been inferred from tests on cores, in situ permeability tests, and large-scale groundwater flow studies. The wide spread in values appears to be due to sparse secondary permeability features, perhaps fractures, that generally are not detected by in situ tests. Specific storage of the shale ranges from 10^{-4} to 10^{-5} m^{-1}. At the site of the osmosis experiment, pore pressures in the shale apparently are very low (close to atmospheric) because of erosional unburdening and resulting mechanical rebound of the Pierre Shale (Neuzil, 1993). Hence, the vertical hydraulic gradient in the shale is approximately unity. Horizontal hydraulic gradients are of the order of 10^{-2}. The native pore water contains about 3.5 g/l NaCl.

In the experiment four 80 m deep, air-drilled boreholes were used. The boreholes are 15 m apart with a diameter of approximately 14 cm. Exchange of water between the borehole and the shale occurs along an 18 m long screen in the bottom part of each hole. From the time of the construction to the beginning of the test, the boreholes remained dry due to the low permeability of the formation and the low pore pressures. Subsequently one hundred liters of water was added to each borehole. Two boreholes (HC1 and HC2) were filled with high salinity water (35 g/l), one (DUP) received an approximate duplicate of the expelled pore water (3.5 g/l) and one (DI) received de-ionized water. Slight differences in the borehole diameter caused initial water levels to vary up to 3 m.

All wells showed water level decline due to the low pore pressure (Figure 6.4a). Osmosis effects were revealed by differences with respect to DUP (Figure 6.4b) because water levels
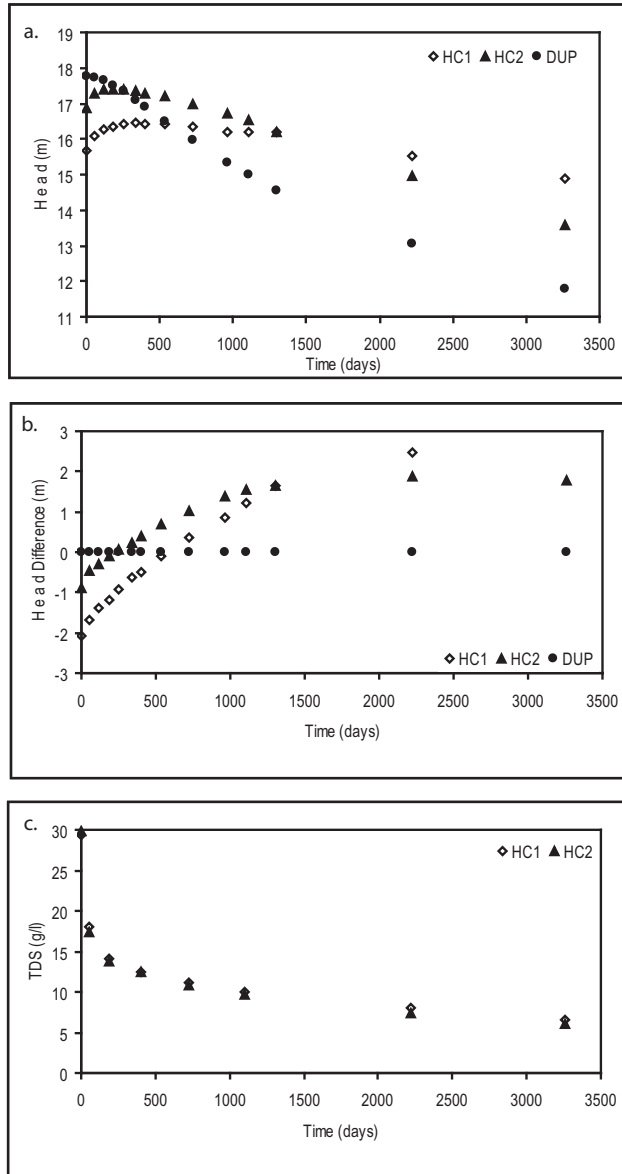
Figure 6.4: Water levels and TDS (total dissolved solids) borehole responses. (a). Observed hydraulic response of the individual boreholes. Head is measured relative to the common base level of the boreholes. HC1, HC2 and DUP refer to boreholes with 35, 35 and 3.5 g/l TDS, respectively. (b). Water levels corrected for the regional hydraulic head gradient and plotted as differences from borehole DUP to isolate osmotic responses. (c).TDS in boreholes HC1 and HC2.

in DUP were assumed to respond solely to hydraulic disequilibrium while the other water levels were affected by both hydraulic and osmotic mechanisms. In particular, the relative increase in water levels in the HC boreholes is interpreted to result from flow from the shale into the relatively saline boreholes caused by osmosis. TDS in the HC boreholes decreased due to this inflow of lower salinity pore water and also because of diffusion of NaCl from the borehole into the formation. The observed TDS in the HC boreholes shows two distinct phases: an initial phase where TDS decreases rapidly followed by a phase of slower decrease. Neuzil (2000) concluded that the rapid decrease during the first phase was due to precipitation of mirabilite, which he substantiated by solubility calculations.

Table 6.1: Changes in head and TDS after 9 years (time at which the pressure peak is reached) and inferred values for σ and *b* in the Pierre Shale (Neuzil, 2000).

Borehole	Final TDS	Δh (m water)	b (Å)	σ (max and min c)	A_s (m²/g)
HC1	6.52	2.16	44.7	0.045 to 0.14	41.3
HC2	6.13	1.46	48.7	0.038 to 0.1	38

Because the increase in water level in HC1 and HC2 relative to DUP had slowed significantly or stopped after nine years, Neuzil (2000) concluded conditions were close to osmotic equilibrium. This permitted analysis of the experiment by solving:

$$\triangle p = \int_{cmax}^{cmin} \sigma(c)\frac{d\pi}{dc}dc \tag{6.11}$$

where *p* is fluid pressure, π is osmotic pressure (a function of water activity), *c* is solute concentration expressed as mass per volume of solution, and *cmax* and *cmin* are the concentrations in the borehole and undisturbed shale, respectively. Solving equation (6.11) allowed the shale's specific surface area (A_s) to be computed which, in turn, made it possible to predict the shale's membrane properties for a range of solute concentrations and compaction states. Table 6.1 lists the values of the reflection coefficient σ that were computed from the final, equilibrium pressures and concentrations using equation (6.11). Table 6.1 also lists the specific surface area and mean thickness of the fluid layer (water film) between clay platelets in the shale *b* that controls the dependency of σ on concentration (Bresler, 1973). An effective ionic diffusivity $D^* = 3 \cdot 10^{-11}$m²/s that includes all porous media and membrane effects was computed by analyzing the TDS increase data in the DI borehole that was initially filled with de-ionized water. As already noted, Neuzil (2000) did not consider the pressure build up, or pre-equilibrium, phase in his analysis.

6.4.2 Model Configuration

Figure 6.5 shows the configuration of the model domain. It consists of a vertical radial section bounded on the left by the axis of borehole, which is a symmetry boundary. The

domain extends 5 m radially, which is sufficient to avoid any influence from the right-side boundary condition. The height of the section initially equals the water level in the borehole, which differs slightly amongst wells. However, as explained below, the model height changes incrementally as water level in the well increases or decreases. The domain is divided into three regions; two of high permeability representing the interior of the screen in the borehole and the sand pack around the screen, and one of low permeability representing the shale. The boundary conditions of head and mass fraction (*h* and *w*) and the initial values for TDS are indicated in Figure 6.5. The equations are solved accounting for the radial geometry. Head is referenced to the bottom of the domain.

   The initial head in the well bore and sand pack part of the model domain was set equal to the initial water level in the well bore (this also equals initial model height). For the initial hydraulic head in the clay part of the domain a constant value of 9 m above datum was adopted, which represents the vertically averaged value along the total filter height if fluid pressures are assumed to initially be close to atmospheric pressure. This implies

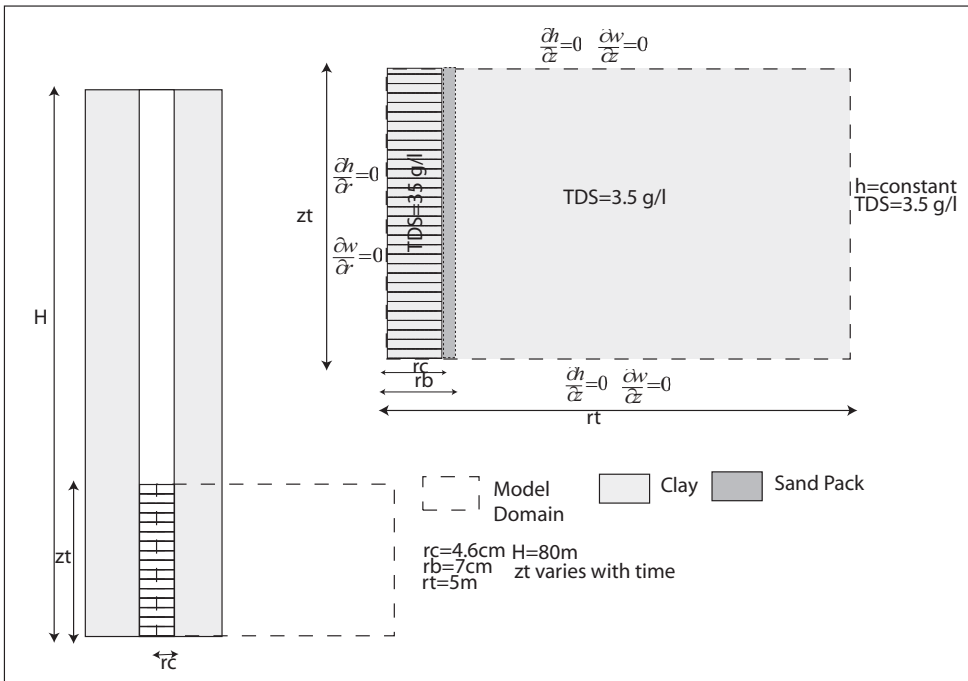**Figure 6.5:** Model configuration and initial and boundary conditions for the osmosis test in the Pierre Shale. From left to right the sub-domains represent the borehole, the surrounding sand pack and the shale. Boundary conditions and initial conditions for concentration are indicated. The height of the model domain z_t decreases in a step-wise fashion in concert with the observed decline in water level in the boreholes.

Table 6.2: Fixed parameters used in all the simulations

	Parameter	Value
TDS(Pore)	Initial TDS pore water(g/l)	3.5
n	Porosity	0.34
$\bar{h}$	Initial Head Shale(m)	9
TDS (Well)	Initial TDS well bore (g/l)	35
$\mathbf{h_0}$ **DUP**	Initial head in well DUP (m)	17.76
$\mathbf{h_0}$ **HC2**	Initial Head in well HC2(m)	16.89

that the vertical variation in fluid flow along the screen that likely exists in the experiment because of the large vertical hydraulic gradient in the shale is ignored or averaged. Thus, flow and transport in the model is essentially treated as one-dimensional radial. This is a rather mild simplification because regions of head higher than and less than in the borehole offset each other. Another complication is the fact that head or water level in the well bore decreases over time. Maintaining the original domain height would overestimate the length of screen over which fluid exchange occurs. We therefore assumed that fluid and solute movement between the borehole and the shale above the water level in the borehole can be neglected. This assumption also was not very restrictive because the shale's small pores prevent air entry, and high humidity in the borehole prevented evaporation of pore water from the borehole walls. In the model, this was incorporated by progressively decreasing the domain height in concert with the decrease in water level in the well bore. To mimic the large storativity for fluid within the well bore, in the corresponding part of the model domain, equation (6.6) was replaced by an effective equation of state:

$$\rho = \rho_0 \frac{h}{z_t} \exp(\gamma w) \qquad (6.12)$$

where ρ should be interpreted as an effective rather than actual density in the well bore part of the domain and z_t is the initial pressure head in the borehole and is reset at the beginning of each stage. The simulation was divided into stages corresponding to the periods of time between observations in the original in situ experiment. A constant value for the diffusion coefficient was used for the shale. Strictly speaking, the diffusion coefficient in a semi-permeable membrane is related to the salt mass fraction according to equation (6.10). In this particular case, however, the negligence of mass fraction dependence is unlikely to affect the modelling results because values of σ only range from 0.04 to 0.21 in the modelling due to this effect (see section 4.3), which corresponds to a variation of D^* of less than 18 percent.

Table 6.3: Parameters used in models

	Parameter	S1	S2	S3	S4
$\mathbf{k}_{DUP}$	Intrinsic Permeability (m^2)	$2 \cdot 10^{-20}$	$1.4 \cdot 10^{-19}$	$1 \cdot 10^{-21}$	$1.4 \cdot 10^{-19}$
$\mathbf{k}_{HC2}$	Intrinsic Permeability (m^2)	$2 \cdot 10^{-20}$	$1.4 \cdot 10^{-19}$	$1 \cdot 10^{-21}$	$1.4 \cdot 10^{-19}$
$\mathbf{D}^*$	Diffusion Coefficient (m^2/s)	$3 \cdot 10^{-11}$	$6 \cdot 10^{-11}$	$6 \cdot 10^{-11}$	$6 \cdot 10^{-11}$
$\mathbf{S}_s$	Specific Storage (m^{-1})	$1.65 \cdot 10^{-5}$	$1.7 \cdot 10^{-5}$	$1.7 \cdot 10^{-5}$	$1.7 \cdot 10^{-5}$
b	Thickness water film (Å)	48.7	40	40	35

6.4.3   Simulation

Here we describe how the evolution of water levels and salinities in boreholes HC1, HC2 and DUP was modelled. First, modelling was carried out to simulate behavior in HC2 and DUP and estimate parameters for the model. We then investigated how well these parameters applied for borehole HC1. Table 6.2 lists the fixed parameter values used in the simulations; these parameter values were predetermined and not varied in the analysis. We first show results for a simulation (S1) using default parameter values (Table 6.3), that correspond to expected hydraulic parameter values for the Pierre Shale as well as b and D^* values that Neuzil (2000) inferred. Then the "best-fit" model (S2) is presented, followed by results of model simulations that illustrate the sensitivity of the fit to key model parameters (S3 and S4 in Table 6.3).

The well bore part of the modelling domain was assigned a permeability many orders of magnitude higher than that for the shale, 100% porosity, and a diffusivity equal to the free water NaCl diffusion coefficient. For the sand pack surrounding the screen, $D^* = 4.25 \cdot 10^{-10}$ m^2/s and $n = 0.25$ were assigned (Neuzil, 2000). To account for the strong dependency of σ on w and b we used the relationship described by Bresler (1973) shown in Figure 6.1.

Figure 6.6 presents the results of model experiment S1 using default parameter values. It is apparent from the figure that large discrepancies occur between model predictions and the observed behavior of both fluid pressure (water level) and concentration. Figure 6.6a and Figure 6.6b show that the predicted head decline for both DUP and HC2 is much too slow. The same applies, therefore, to the differential head (Figure 6.6d). The large misfit in TDS history for HC2 (Figure 6.6c) is thought to be due partly to the apparent precipitation of mirabilite (Na$_2$SO$_4 \cdot 10$(H$_2$O)) in the HC boreholes discussed by Neuzil (2000).

The approach to achieve a better correspondence between model predictions and observational data was roughly as follows. Because the TDS evolution in HC2 is mainly affected by D^* and relatively insensitive to other model parameters, first the value of D^* was adjusted. Subsequently, the value of k was optimized for DUP since the pressure response of that well is insensitive to σ. Then, with the new estimates of D^* and k, b was optimized, fo-
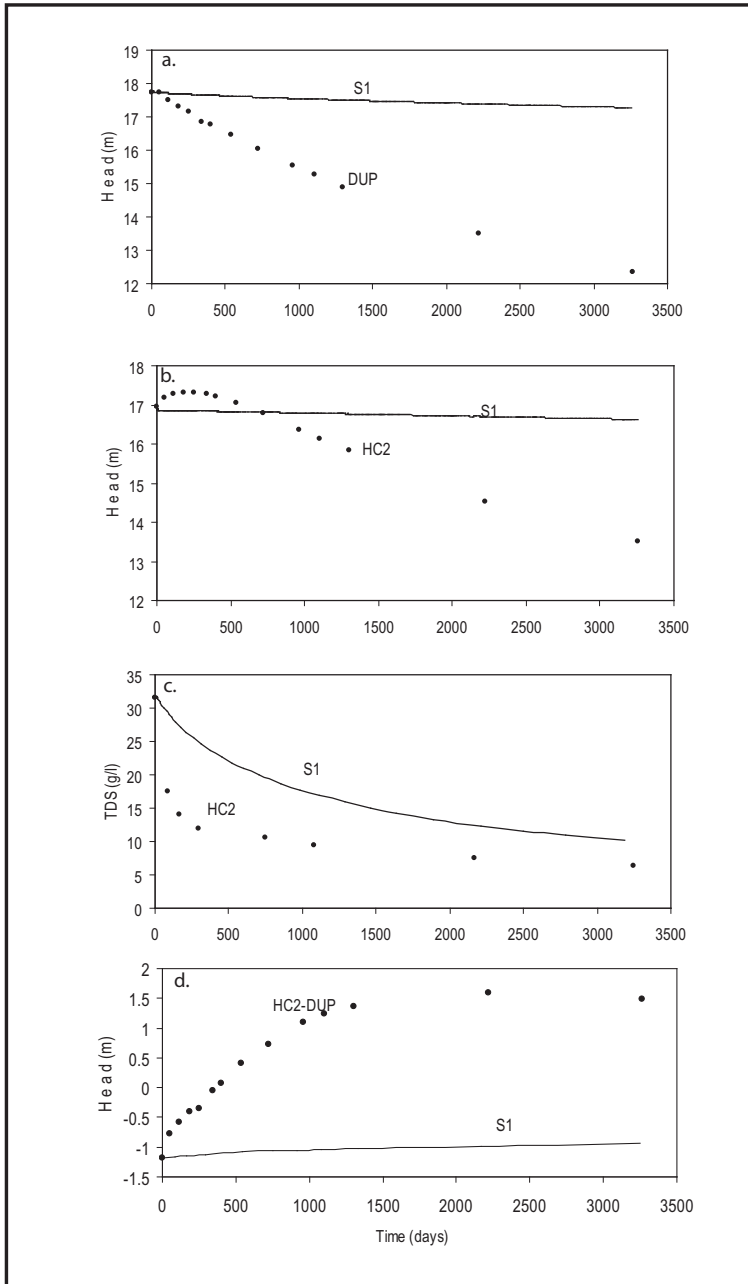
Figure 6.6: Results of model experiment S1 (default parameter values). (a) Head decrease for DUP. (b) Head increase / decrease for HC2. (c) TDS evolution of HC2. (d) Differential head evolution (HC2-DUP).

cusing on the data from HC2. Finally, fine-tuning was accomplished by inspecting all data simultaneously. Figure 6.7 displays the best-fit model (S2). Table 6.3 shows that the permeability for DUP and HC2 had to be increased by about one order of magnitude relative to S1 to account for the observed relatively rapid head decline. We found that it is not possible to accurately reproduce the TDS data at early and late phases simultaneously when a single value of D^* is used (Figure 6.7c). Sensitivity analysis shows that, for the first phase, an unrealistically high diffusion coefficient ($> 3 \cdot 10^{-10}$ m^2/s) is required to account for the rapid decrease in TDS, a finding consistent with modelling results of Neuzil (2000). Furthermore, the change in diffusion coefficient from the early to late stage of the experiment (more than one order of magnitude) is too large to be accounted for by concentration-dependence of the diffusion via the reflection coefficient as discussed in the previous section. In our opinion, these findings corroborate the suggestion of Neuzil (2000) (occurrence of mineral precipitation in the well bore after initiation of the experiment). For the best-fit model we optimized D^* in such a way that a good TDS fit was obtained late in the experiment, at the time when precipitation and redissolution of mirabilite would have ceased.

Our result obtained from modelling (b=40Å) is consistent with the range of values reported in several other studies. Kemper and Maasland (1964) reported values ranging from 35 to 25Å for compacted Na bentonite. We calculated b=160Å for a non-compacted bentonite from experimental data of Keijzer (2000) using the equation

$$b = n/(\rho_b A_s) \tag{6.13}$$

where ρ_b is the dry bulk density (kg/m^3) and A_s the specific surface area (m^2/kg). Although calculated values of b from estimates or measured values of specific surface area are likely associated with considerable uncertainty, the large range of values indicated above suggests that the inferred value of 40Å is reasonably close to the value of 48.7Å obtained by Neuzil (2000). Unfortunately, we are unaware of measured values of specific surface area for the Pierre Shale. The reflection coefficient values at the highest and lowest concentrations are 0.0415 and 0.21, respectively, for S2, which compares to values of 0.038 and 0.1 determined by Neuzil (2000). Figure 6.8 shows the temporal changes in TDS and σ, along a radial section extending 1 m from the axis of the borehole.

We do not know to what extent the inferred model parameters are uniquely constrained by the observational data. From the many experiments we did, we found that k, D^*, S_s and b all control the hydraulic response, but their effects differ. Varying S_s within a reasonable range of 10^{-4} to 10^{-5} m^{-1} (Neuzil, 1993) produced differences in head on the order of cm and changed the time at which the osmotic component of head (osmotic equilibrium) peaked in the differential pressure curve (Figure 6.7d) only by about 10 days. D^* potentially has a much larger influence on the hydraulic response because the concentration in the well bore controls the induced osmotic pressures. However, the required value is quite well constrained by the late TDS history. The relative contributions of k and b to the hydraulic response are more subtle. Both parameters affect both the magnitude of the osmotically-induced pressures and the time to reach osmotic equilibrium conditions. However, k affects both the osmotic and hydraulic fluid exchange between the borehole and the shale to the same degree, while b affects solely the osmotic flow component. The different role of these
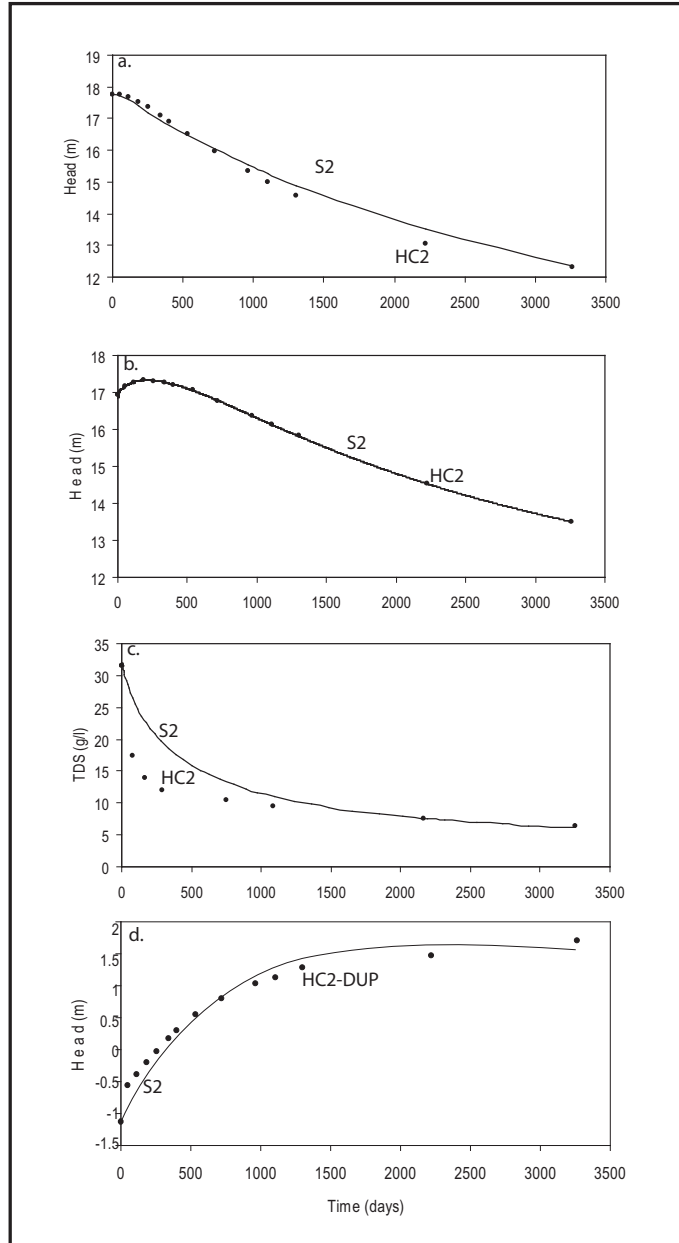
Figure 6.7: Results of model experiment S2 (best-fit model). (a) Head decrease for HC2. (b) Head increase / decrease for HC2. (c) TDS evolution of HC2. (d) Differential head evolution (HC2-DUP).

parameters makes their values appear to be quite well constrained by the modelling. The individual impacts of k and b on the modelling results are illustrated in experiments S3 (Figure 6.9) and S4 (Figure 6.10), respectively. The permeability value used in S3 (10^{-21}) corresponds to the lower limit of typical reported values. Otherwise parameters are the same as in S2. Figure 6.9b shows that for the low permeability, the head in the well keeps on rising and, therefore, that osmotically-driven flow is dominant during the entire nine year period shown. Figure 6.10b and Figure 6.10c show that a decrease of b from 40 to 35$\mathring{A}$ raises the
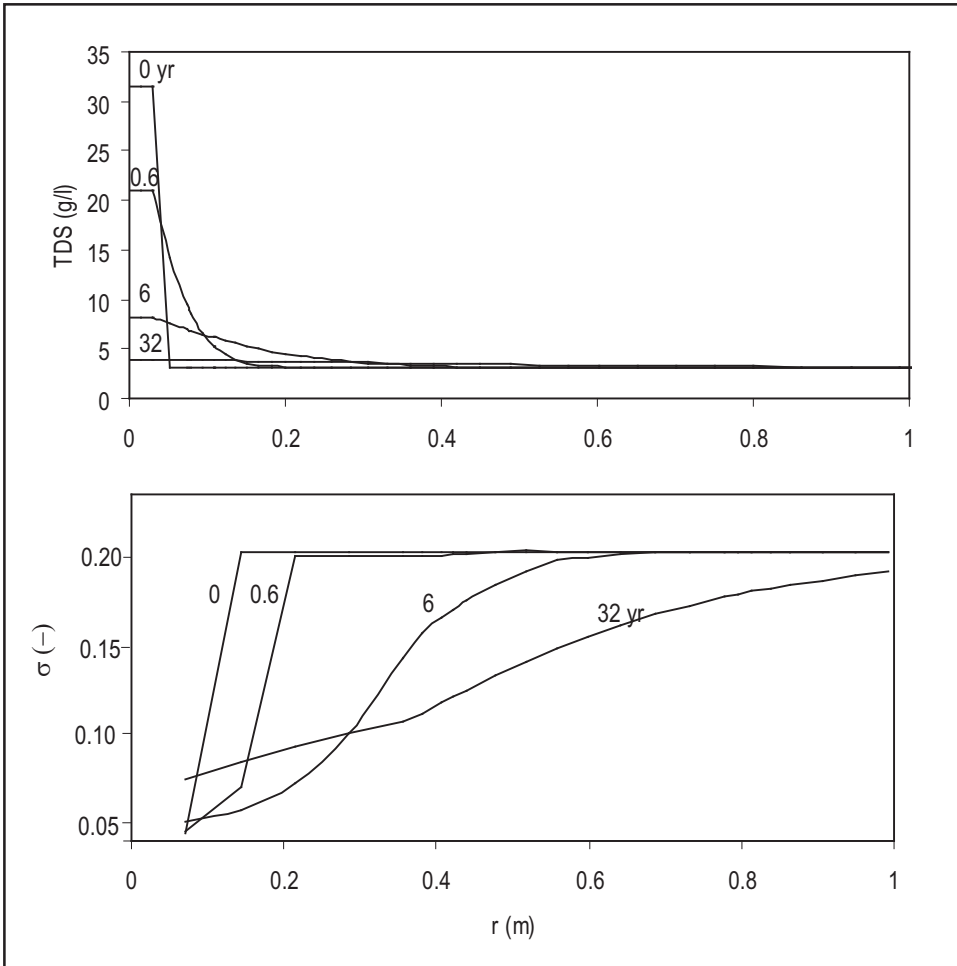
Figure 6.8: Temporal and spatial changes in (a) total dissolve solids (TDS) and (b) osmotic efficiency (σ) shown as functions of radius (r) (distance from the centre of the borehole) for experiment S2. Labels with the curves denote time (t=0 to 32 years).

osmotically-induced head by nearly 1 m.

Similar modelling of well HC1 yielded optimal values of $b = 42Å$ and $k = 9.7 \cdot 10^{-20}$ m^2, while values of S_s and D^* could remain unaltered relative to the modelling of HC2. Values σ=0.045 and 0.146 were inferred for highest and lowest concentration, respectively. The HC1 values for both b and σ are in much better agreement with the values inferred by Neuzil (2000) than the HC2 values. They are shown in Table 6.1.

6.4.4   Discussion of Simulation Results

One of the most conspicuous findings of the modelling is the fact that the inferred permeability for the Pierre Shale appears to be at least one order of magnitude higher than typical values reported in previous studies (Neuzil, 1993, 1994). We note, however, that (Neuzil, 1993, his Table 2) lists several in situ permeability determinations for the Pierre Shale that are in agreement with our higher value. The range in values may reflect small-scale heterogeneity within the shale. For instance, closed fractures or shear zones (Neuzil and Wolff, 1984) may have opened near the borehole forming micro cracks. However, the possibility should be considered that certain differences in the analysis or the assumptions employed in the modelling may have contributed to the discrepancy. It may, for instance, be argued that the progressive reduction of outflow from the wells due to the gradual decrease in saturated height of the borehole has been overestimated in the modelling because a vertically averaged head has been assumed in the shale. In addition, different initial head values in the shale were not tested in the modelling. The ambient pore fluid pressure in the shale could be lower than assumed, that is, it could be below atmospheric even though the shale is fully saturated (Neuzil and Pollock, 1983). Underestimating the hydraulic drive for outflow in the model may, therefore, have been compensated by an artificially high permeability. The significance of the inferred high permeability should, therefore, be interpreted with caution. Further work would be required to verify and quantify the importance of this complicating effect.

Our inferred value of b for HC2 is about 15 per cent smaller than the value obtained by Neuzil (2000). This is somewhat surprising because the observed final differential head is reproduced quite accurately and the relationship of Bresler (1973) has been used in both studies. Several factors may contribute to this discrepancy. First, differences in water level decline in DUP and HC2, and the resulting interaction with the large vertical hydraulic gradient thought to exist in the shale, were not taken into consideration by Neuzil (2000). These effects therefore became part of the pressure differential attributed to osmosis. In our modelling these effects are accounted for, but Neuzil's (2000) computed value of b may be somewhat biased by this effect. Second, the integral method employed by Neuzil (2000) implicitly assumes that the peak differential head corresponds to osmotic equilibrium and, therefore, no-flow conditions over the entire domain where concentrations are higher than the background concentration in the shale. This would normally be true because transient flow is governed by a hydraulic diffusivity that is much larger than solute diffusivity. However, the large effective storage in the boreholes greatly prolonged transient flow conditions. Although the effect of these transient conditions on the inferred b value are probably very

Figure 6.9: Results of model experiment S3 (influence of *k*). (a) Head decrease for DUP. (b) Head increase/decrease for HC2 (c) Differential head evolution (HC2-DUP).
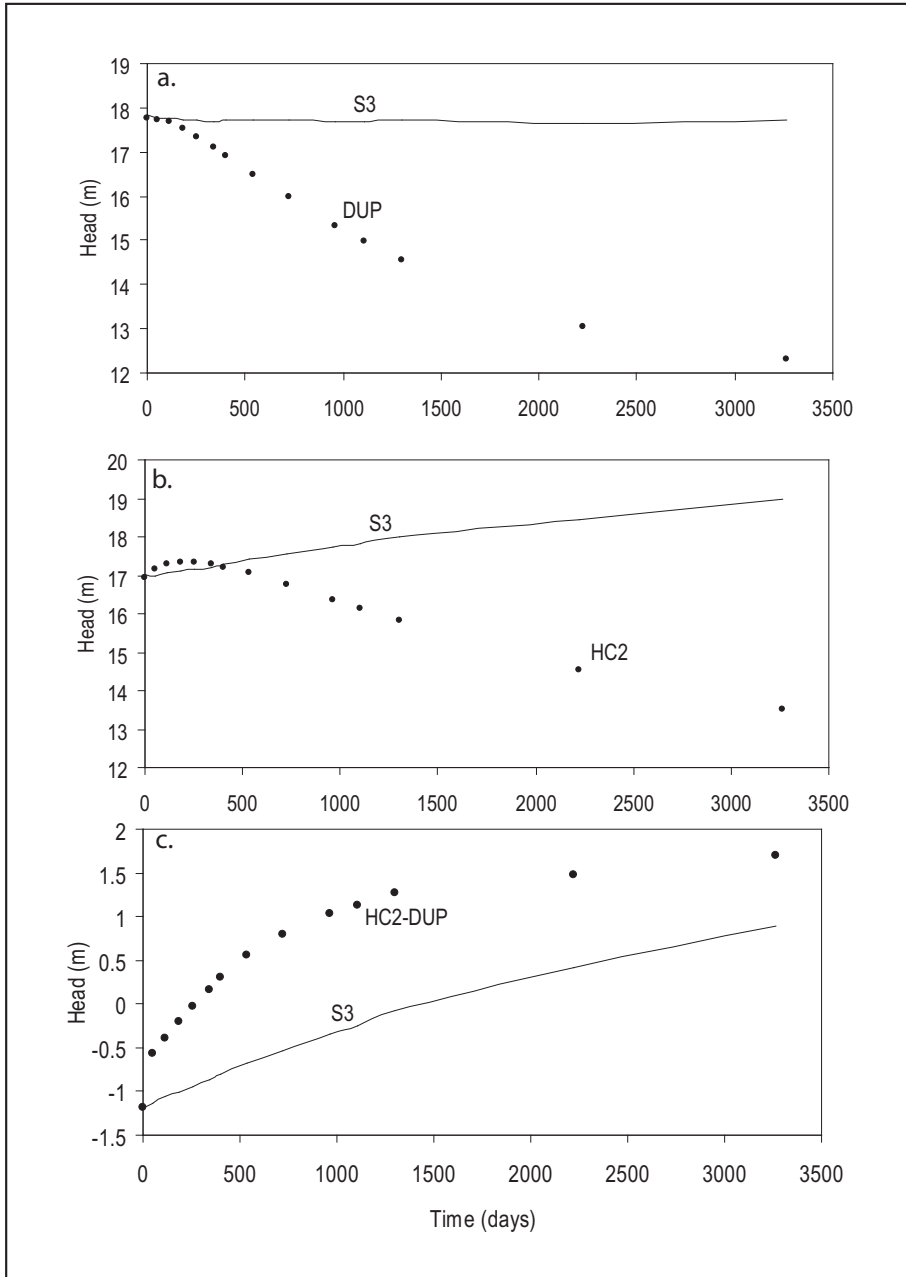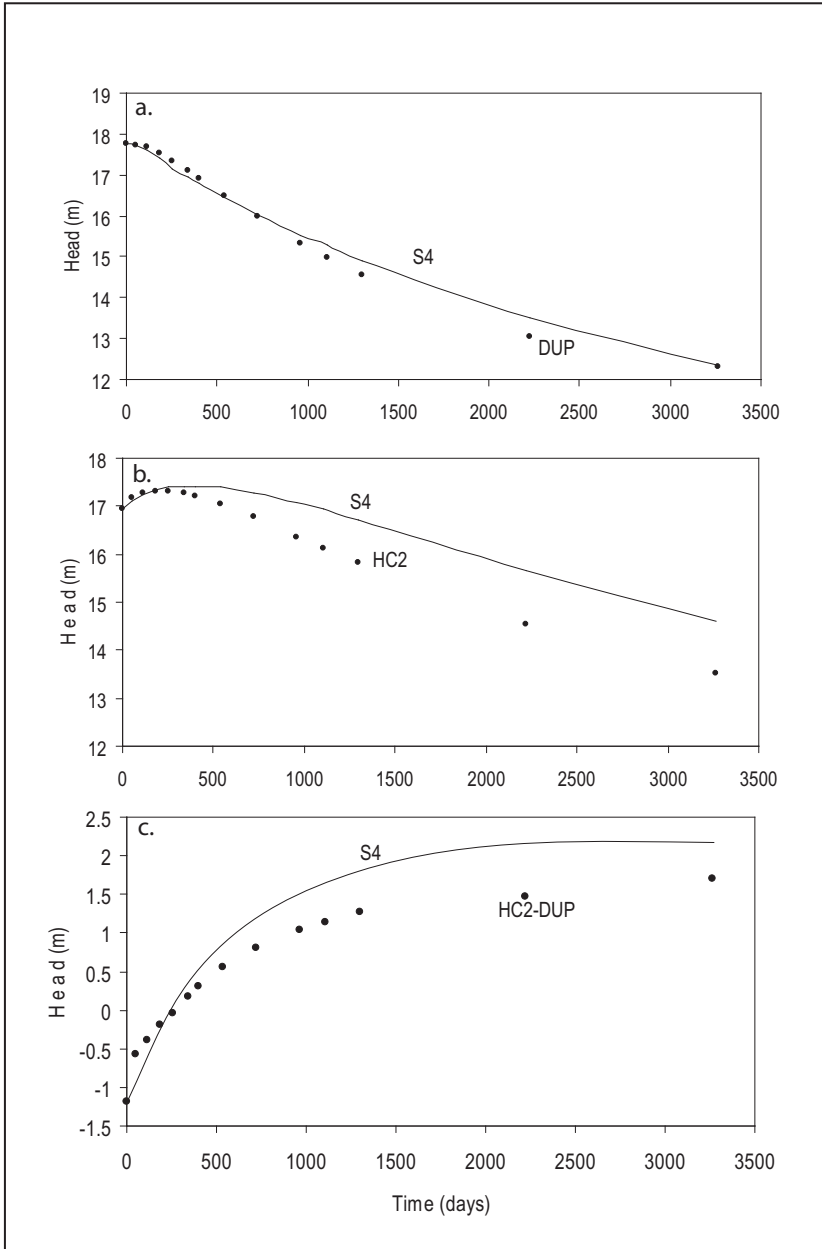
Figure 6.10: Results of model experiment S4 (influence of *b*). (a) Head decrease for DUP. (b) Head increase/decrease for HC2. (c) Differential head evolution (HC2-DUP).

minor, a modelling study would be required to ascertain this. Preliminary tests for a non-radially symmetric problem with constant σ show that relatively minor differences in peak pressure indeed are predicted with the two methods and that this difference is absent when parameter values in the numerical model are chosen that represent quasi-steady flow (zero specific storage). Third, in this study linear interpolation of the markers points used by Neuzil (2000) was used to fit the relationship of Bresler (1973) . Neuzil (2000) fitted a third-order curve to the points so that it was very close to the curve presented by Bresler (1973). Linear interpolation could yield different σ values especially where it is very sensitive to salinity, introducing a source of error that may vary in importance depending on conditions. Fourth, although in our model the final TDS value in the borehole was reproduced quite accurately, at earlier times model TDS values exceed observed values. Our inferred b value may therefore have been underestimated because σ is a function of the product $b\sqrt{c}$. That is, high c corresponds to low b for the same σ.

A further interesting finding from the present modelling was that the response of the DUP borehole is not entirely free of contributions from the membrane behavior of the shale, because the hydraulically forced outflow from the borehole causes accumulation of solute at the filter-clay interface due to ultrafiltration (Figure 6.11). However, the concentration change due to this effect is small (note the expanded vertical scale), and appears to be of negligible importance for the overall assessment of the membrane properties.

Errors in the present analysis may also account for differences in the results. Spatial

Figure 6.11: Comparison of TDS evolution in the DUP borehole for σ > 0 and σ = 0 shows that the DUP response is not completely free of membrane effects. For σ > 0 ultrafiltration of salt occurs and concentration increases slightly.

heterogeneities that affect the transient behavior of the wells and that were not accounted for might exist. For example, if elevated salinities caused volumetric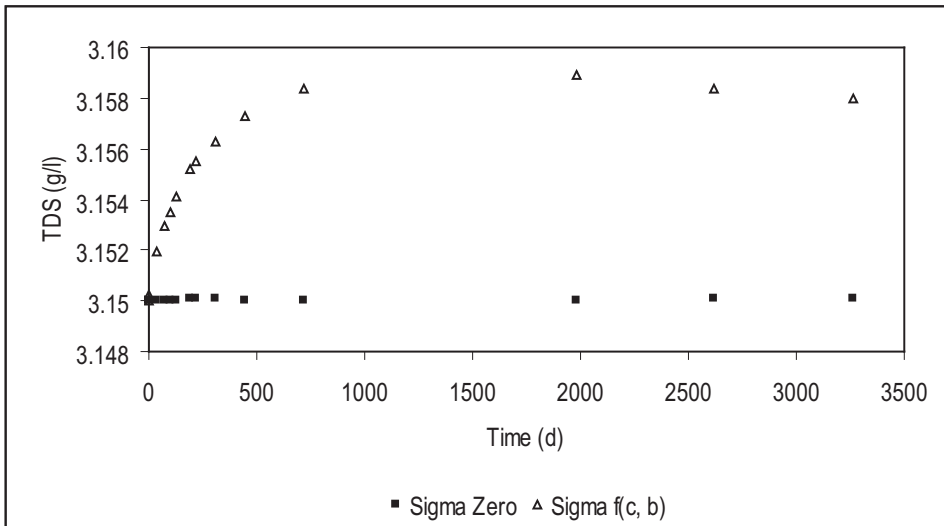 strains in the shale near the HC boreholes (e.g. shrinkage or flocculation of the clay), permeability might have been locally and temporarily affected. We note that the early behavior in borehole HC2 was a strong constraint on the parameter values we arrived at. In particular, the initial rise in water level that can be seen in Figure 6.7b strongly constrained the estimated parameters and may reflect conditions that later changed. Finally, although we have the sense that our results are unique, we cannot be sure of this; non uniqueness of the results must therefore be considered a possibility.

Our findings suggest that the integral method employed by Neuzil (2000) to infer membrane properties from borehole osmosis experiments is an elegant method that can provide reasonably reliable estimates of b and σ from borehole osmosis tests. However, it also appears that complexities that may be encountered in *in-situ* experiments (salt precipitation, large vertical head gradients, disturbance of the formation near the borehole, prolonged transient flow caused by well bore storage, differences in initial water level, and so on) may affect results and, therefore, require careful analysis. The present numerical model appears to provide an excellent tool for performing such assessments in future experiments. Moreover, our model is a useful tool for the design and planning of osmosis experiments because it allows prediction of response times and magnitudes of osmotically-induced pressures for various experimental configurations.

Experimental data and analysis presented by Neuzil (2000) and the predictions of this model both point to chemical osmosis as an important process in long-term groundwater flow and transport in certain settings. Both approaches (Neuzil's integral formulation and the transient model) allow the computation of σ. The full modelling has the advantage that it provides a more complete framework for assessment and allows estimates of hydraulic parameters such as k and S_s.

6.5 Numerical Modelling of the *In-Situ* Chemical Osmosis Experiments in the Boom Clay

In Chapter 5 two chemical osmosis tests performed *in situ* in the Boom Clay and the corresponding results were described. In this section, the modelling and analysis of the data are presented. The pressure evolution within filter 3 (filter in which high concentration solution was injected) was simulated for both tests (TI and TII). Simulations were performed in two steps for the first test (TI). The first step consists in modelling the pressure recovery data prior to the injection, without taking into account any osmotic component. The result of this first simulation is then used as the initial pressure distribution for the second step. The second step corresponds to the simulation (including osmotic effects) of the data after the solution exchange (osmosis test). For the second test (TII) only the second step is followed.
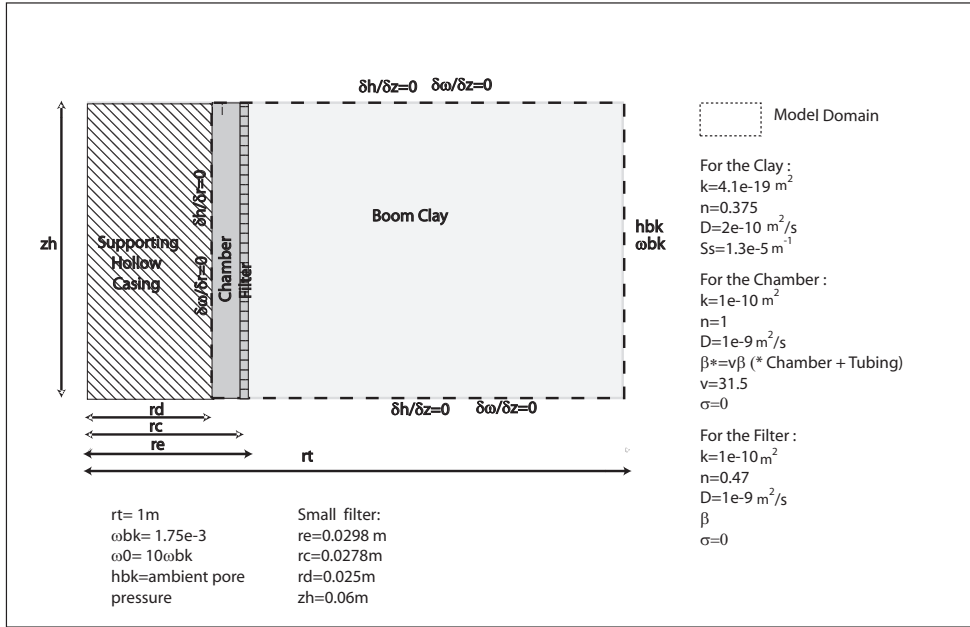
Figure 6.12: Model configuration and initial and boundary conditions for the *in-situ* osmosis test in the Boom Clay.

6.5.1 Model Configuration

Figure 6.12 shows the model configuration. The model domain consists of a vertical section delimited on the left side by the casing support of the piezometer ($r = r_d$). The domain is divided into three regions: one of low permeability corresponding to the clay, and two of high permeability representing the inner part of the piezometer chamber, and the porous filter. The width of the section (obtained by a sensitivity analysis) is 1 m, which is sufficient to avoid influences of the right-side boundary condition. The height of the section is the corresponding length of the *Krebshöge* filter. Anisotropy is not considered and therefore flow and transport in the model is essentially one-dimensional (in the radial direction).

There exists a hydraulic pressure gradient as function of the distance from the gallery. The intrados of the lining of the gallery are at atmospheric pressure while the pore pressure is about 220 m water column at a distance greater than 30 m. The water pressure measured in the filter will thus increase with the distance from the gallery. Since the filter length is only of the order of cm a constant value can be adopted. Previous measurements in this piezometer had shown that the local pore pressure at 3 m from the gallery corresponds to approximately 57.10 m water column.

However, at the moment of onset of the first test (TI) the water pressure had not recov-

Table 6.4: Initial values of head and mass fraction for the different simulations. Here h denotes the head distribution resulting from modelling in the Step 1.

Domain Section	TI				TII	
	Step 1		Step 2		Unique Step	
	h (m water)	w (-)	h (m water)	w (-)	h (m water)	w (-)
Chamber	51.4	-	55.57	w_0	h_{bk}	w_0
Filter	51.4	-	h	w_{bk}	h_{bk}	w_{bk}
Clay	57.1	-	h	w_{bk}	h_{bK}	w_{bk}

ered yet from the disturbance caused by the sensor installation (see Chapter 5 for experiment description). Exchange was conducted at the local pressure at that time (a pressure of 55.57 m water column). This transient pressure situation was modelled from $t = -3$ days up to start of the test or injection time (t=0 days). For this simulation the osmotic effects are not taken into account and sigma is set to zero. Subsequently, the resulting momentary pressure distribution was used as initial condition for the osmosis test simulation. For the second test (TII) the pressure had fully recovered by the moment of initiating the experiment. Therefore the initial pressure condition used is the same for the entire domain (local pore pressure ~ 54.4 m water).

The boundary conditions of pressure/head and mass fraction (h and w) are shown in Figure 6.12. The initial values for mass fraction and head are listed in Table 6.4. The initial concentration w_0 in the filter chamber corresponds to ten times the pore water concentration in the clay (w_{bk}). The porous filter is assumed to be saturated with pore water.

Elastic storage of the tubing is assumed negligible. To account for storativity for solution within the complete system (chamber and tubing), water compressibility is corrected with a volume factor (chamber + tubing volume).

The thickness of the water film (b) between the charged clay platelets is assumed to be 50 Å. This value was calculated using the equation (6.13). Experimental values of porosity, specific surface area, and bulk density for the Boom Clay were used for this calculation.

For the piezometer inner part of the modelling domain, a permeability many orders of magnitude higher than that for the clay, 100 % porosity, and a free water NaCl diffusion coefficient were used.

6.5.2 Simulation

Initially simulations (S1 and S2) using the default parameters were performed. Then several model simulations were performed to evaluate the sensitivity of the model to key parameters. Table 6.5 lists the parameter values used for four simulations (S1, S2, S3 and

Table 6.5: Parameters used for, and inferred from, S1 , S2, S3 and S4 model simulations.

Symbol	Parameter	S1	S2	S3	S4
k	Intrinsic permeability (m^2)	$4 \cdot 10^{-19}$	$4 \cdot 10^{-19}$	$1 \cdot 10^{-19}$	$4 \cdot 10^{-19}$
D	Effective diffusion coeff. (m^2 s^{-1})	$2 \cdot 10^{-10}$	$2 \cdot 10^{-10}$	$1 \cdot 10^{-10}$	$2 \cdot 10^{-10}$
S_s	Specific storage (m^{-1})	$1.3 \cdot 10^{-5}$	$1.3 \cdot 10^{-5}$	$4 \cdot 10^{-6}$	$1.3 \cdot 10^{-5}$
b	Water film thickness (Å)	50	50	61	60
h	Head rise (m)	5.8	5	2.3	2.1
t	Time of peak (h)	4	4.6	35	44
σ	Osmotic efficiency (-) high and low conc.	0.06 - 0.52	0.06 - 0.52	0.07 - 0.41	0.07 - 0.40

S4) and the results obtained. The first two columns (S1 and S2) list the default parameter values that correspond to typical values for the Boom Clay and values representative of the experiment conditions for TI and TII respectively. The third and fourth columns (S3 and S4) show the parameters used to fit the experimental data for each case.

Figures 6.13 and 6.14 display the head evolution within the filter chamber for the two tests and the predicted evolution of S1 and S2. In Figure 6.13, the head evolution for TI corresponds to the observed data and represents not only the osmotically-induced pressure but also the pressure response to the hydraulic disequilibrium condition. The head evolution for TII (Figure 6.14) corresponds to the experimental data corrected with respect to the other two filters. Data were corrected to subtract the background hydraulic pressure and therefore isolate the osmotic effects. Figures 6.13 and 6.14 show large disagreement between model predictions and experimental data. The predicted head increase is larger (higher than 5 m) and occurs earlier than in the experiments (around 4 h).

The sensitivity of the model to different key parameters (k, D , b and S_s) had been previously evaluated in the section 6.4. Based on that analysis some of the responses were verified and used to obtain a good fit to the data. The relative contributions of (k, D, b and S_s) to the hydraulic response are different. For instance, k and b affect both the magnitude of the osmotically-induced pressures and the time to reach osmotic equilibrium. The hydraulic conductivity k affects the osmotic and hydraulic fluid exchange between the piezometer and the clay to the same degree, while b affects only the osmotic flow component. The diffusion coefficient D largely influences the hydraulic response because the concentration controls the induced osmotic pressures. S_s has no effect on the magnitude of the osmotically-induced pressures and slightly affects the time to reach osmotic equilibrium.

Table 6.5 shows that for TI the diffusion coefficient for the clay, permeability, specific storage and the thickness of the water film were modified relative to S1, to obtain a better fit

(Figure 6.13b) : b was increased to reduce the osmotic efficiency (σ) of the membrane and therefore the magnitude of the head peak while k, D and S_s were decreased in such a way that a better fit was obtained for the time of occurrence of the head peak. All values remained within an acceptable range for these parameters, except for the water film thickness b ($\mathring{A}$) (Table 5.1 and Table 6.5). For TII the only parameter varied to fit the experimental data was b (Figure 6.14b).

Figure 6.13: Results of simulations versus experimental observation (TI) as a function of time. (a) Pressure evolution for model simulation S1 (default parameter values). (b) Pressure evolution for model simulation S3 (fit data).

6.5.3 Simulation Results Discussion

The inferred osmotic efficiency (σ) of the undisturbed Boom Clay is high. The predicted values when using default parameters (S1) are $\sigma = 52$ % for the pore water concentration (0.014 M NaHCO$_3$) and $\sigma = 6$ % for the saline solution exchanged (0.14 M NaHCO$_3$).
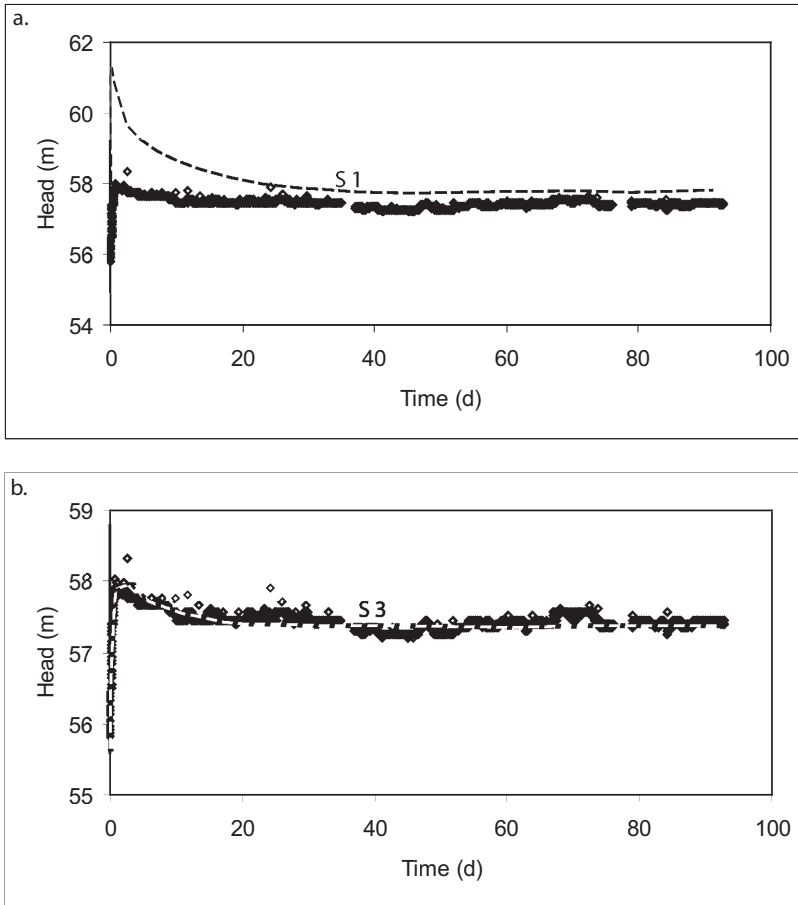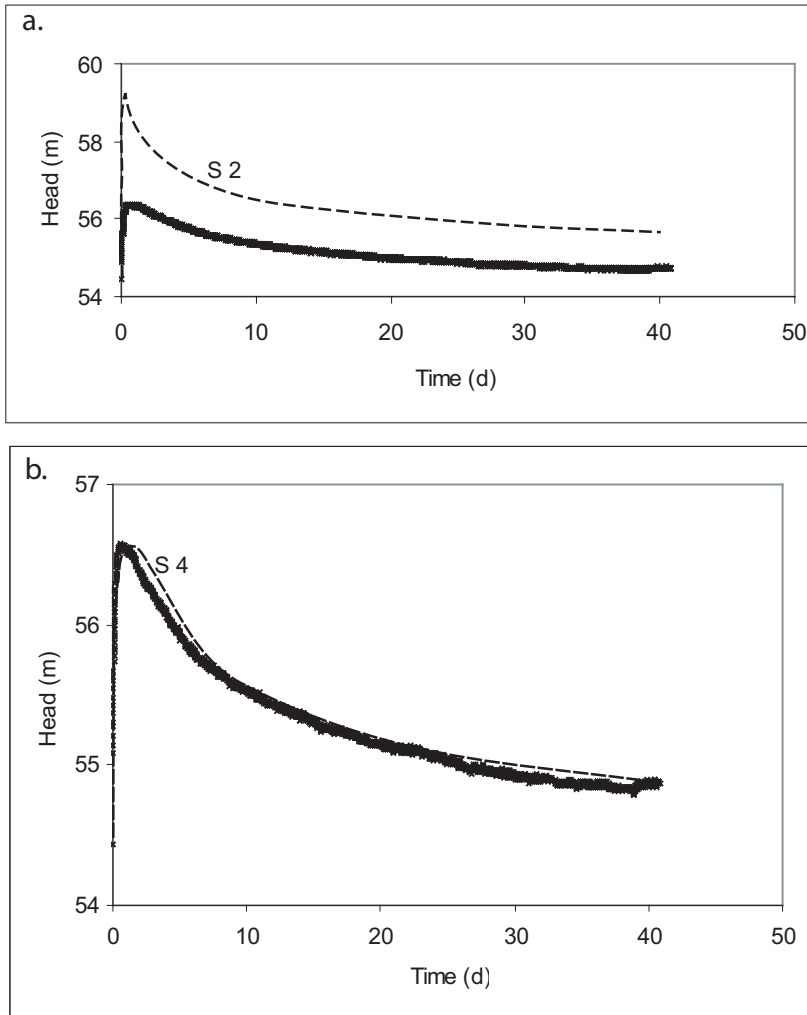

Figure 6.14: Results of simulations versus experimental observation (TII) as a function of time. (a) Pressure evolution for model simulation S2 (default parameter values). (b) Pressure evolution for model simulation S4 (fit data).

However, inferred values from S3 and S4 simulations are slightly different (σ = 41 % - 40 % and 7 % , respectively). This difference may be attributed to the uncertainties regarding the exact inner diameter of the water lines and dimensions of the porous filters of the piezometer. Changes in the volume system influence directly the magnitude and the time to reach osmotic equilibrium. Differences between inferred and measured values of *b* may be also related to the conditions in which experimental value of thickness of water film was determined. This parameter was measured from clay core samples. Furthermore, the inferred value is representative for the entire period of simulation. The prolonged contact of saline water with the clay may induce changes in the structure of the clay and therefore thickness of the water layer.

Figure 6.15 illustrates the temporal and spatial changes in concentration and osmotic efficiency along sections extending 20 cm from the axis of the piezometer for the first experiment (TI). Similar profiles are obtained for TII. The figure shows the rapid decrease of the membrane efficiency at the beginning of the test. However it increases again as the salt diffuses away. It can be observed that after 100 days the concentration within the piezometer and its surrounding is very close to that of the pore water.

Although the interest of SCK·CEN is focused on the effect of high $NaNO_3$ solution concentration (*e.g.*, 5 M and 2.8 M) we adopted a 0.142 M $NaHCO_3$ solution. The use of a $NaHCO_3$ solution facilitated the model calculations. First, the pore water of the Boom Clay is typically $NaHCO_3$ type and NO_3^- is practically absent in the clay pore water. Second, in the model w_{bk} represents the initial clay pore water solute concentration expressed as mass fraction. If a $NaNO_3$ solution is used, the value of w_{bk} should be set to zero in the model. According to Bresler (1973) the efficiency of the membrane greatly depends on the cation concentration. An initial pore water concentration (w_{bk}) set to zero yields a reflection coefficient of 1. Furthermore we also consider that when introducing a solution containing NO_3^-, additional chemical reactions (nitrate reduction, pyrite oxidation, nitrogen production, etc.) between the clay and the $NaNO_3$ solution must be studied and should be included in the simulation. Moreover, microbially-mediated nitrate reduction will likely occur in the free water present in the filter chamber. The concentration of the $NaHCO_3$ solution adopted is only 10 times higher than that of the Boom Clay pore water (w_{bk}). Injection of higher concentration solutions (*e.g.*, 5 M and 2.8 M) imply extremely high cation concentrations, which cause the clay to exhibit very low osmotic efficiencies. Indeed, the σ value is then almost equal to zero because the efficiency of the membrane decreases with the increasing cation concentration.

Results from modelling and the *in situ* experimental data shown in Chapter 5 confirm that the compact Boom Clay behaves as a semi-permeable membrane that is capable to generate osmotically-induced pore pressure variations. A good adequation is observed between the modelling results and the experimental data. The order of magnitude of the osmotically-induced pressure variations observed in Boom Clay is only a few meter of water column (2-4 m H_2O). These observed water pressure variations are small compared to the *in situ* hydraulic pressure (220 m H_2O) and also with respect to the hydraulic disturbances induced by the construction of the underground research laboratory. For the sake of completeness, it remains necessary to extent the modelling to the actual scale of a deep disposal gallery
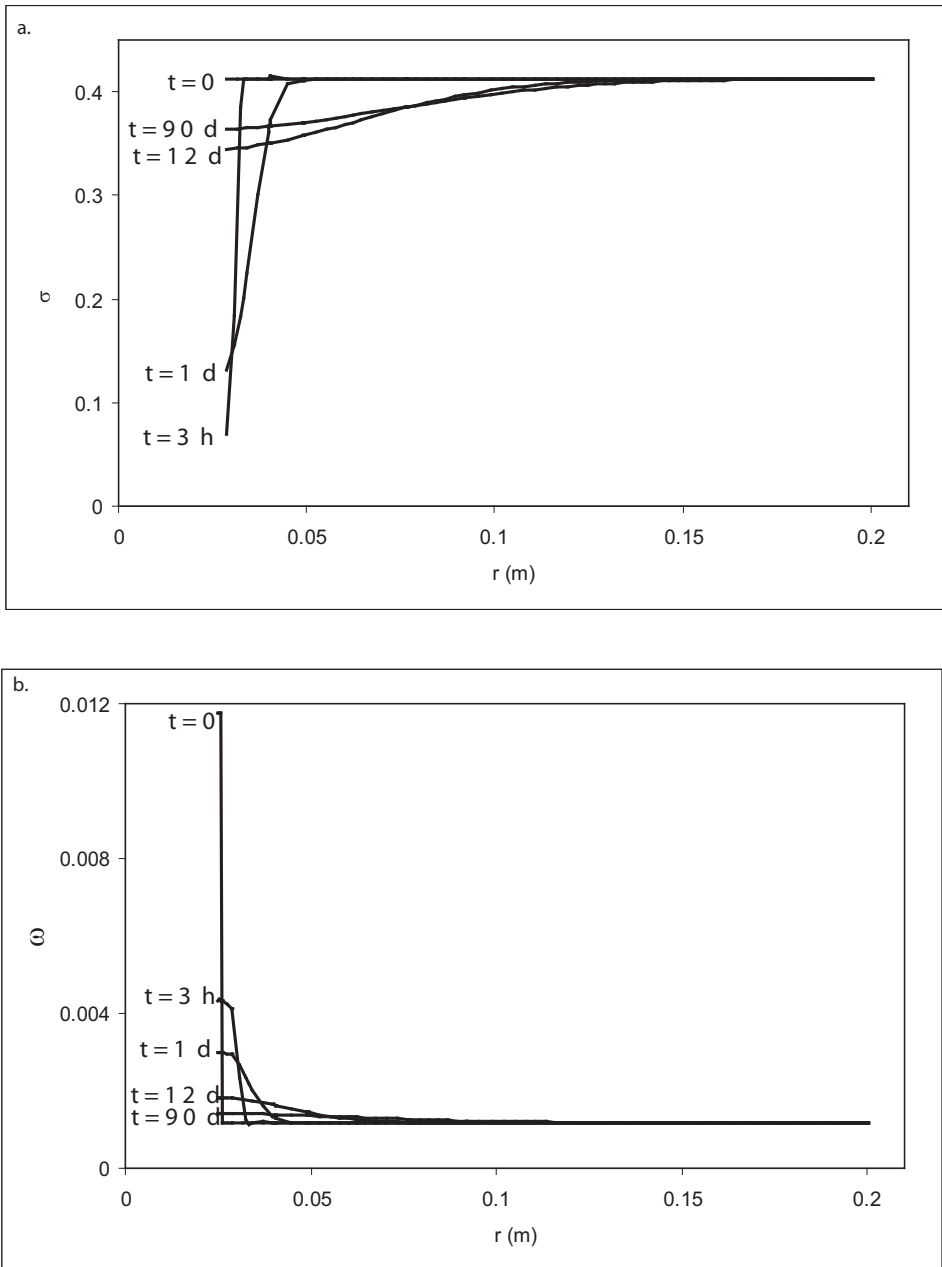
Figure 6.15: Temporal and spatial changes in osmotic efficiency (σ) (a) and solute mass fraction (*w*) (b) along a section extending 20 cm from the center of the piezometer for t = 0 to 90 days.

aimed at hosting nitrate-bearing bituminized intermediate-level waste.

The continuum model constitutes itself a very useful prediction tool for further investigations in this direction. As mentioned in Chapter 5 at this moment SCK·CEN is working on plans to repeat the test in other filters and using high solution concentrations. Additionally, chemical osmosis tests using $NaNO_3$ solutions are being considered.

References

Bader, S., Kooi, H., 2005. Modelling of solute and water transport in semi-permeable clay membranes: Comparison with experiments. Advances in Water Resources (28), 203–214.

Barbour, S., Fredlund, D., 1989. Mechanisms of osmotic flow and volume change in clay soils. Canadian Geotechnical Journal (26), 551–562.

Bredehoeft, J.D., N. C., Milly, P., 1983. Regional flow in the Dakota aquifer: A study of the role of confining layers. U.S. Geological Survey Water Supply Paper 2237, 1–45.

Bresler, E., 1973. Anion exclusion and coupling effects in non-steady transport through unsaturated soils. Soil Sci. Soc. Am. Proc. (37), 663–669.

Cey, B., Barbour, S., Hendry, M., 2001. Osmotic flow through a Cretaceous clay in southern Saskatchewan, Canada. Canadian Geotechnical Journal (38), 1025–1033.

Corbet, T., Bethke, C., 1992. Disequilibrium fluid pressures and groundwater flow in the Western Canada Sedimentary Basin. Journal of Geophysical Research 97 (B5), 7203–7217.

Garavito, A., Bader, S., Kooi, H., Richter, K., Keijzer, T., 2002. Numerical modeling of chemical osmosis and ultrafiltration across clay membranes. Development in Water Sciences 1, 647–653.

Garavito, A., Kooi, H., Neuzil, C., 2005. Numerical Modeling of a Long-term In-Situ Chemical Osmosis Experiment in the Pierre Shale South Dakota. Unpublished .

Greenberg, J., Mitchell, J., Witherspoon, P., 1973. Coupled salt and water flows in a groundwater basin. Journal of Geophysical Research 78 (27), 6341–6353.

Hanshaw, B., Coplen, T., 1973. Ultrafiltration by a compacted clay membrane: II. Sodium ion exclusion at various ionic strengths. Geochimica et Cosmochimica Acta (37), 2311–2327.

Katchalsky, A., Curran, P., 1965. Non equilibrium thermodynamics in bio-physics. Harvard University Press.

Katchalsky, A., Curran, P. F., 1967. Non equilibrium thermodynamics in bio-physics. Harvard University Press.

Kedem, O., Katchalsky, A., 1965. Non-equilibirium Thermodynamics in Biophysics. Press, Harvard University.

Keijzer, T., 2000. Chemical osmosis in natural clayey material. Ph.D. thesis, Universiteit Utrecht, The Netherlands.

Kemper, W., Maasland, D., 1964. Reduction in salt content of solution on passing through thin films adjacent to charged surfaces. Soil Science Society of America Proceedings , 318–323.

Kooi, H., Garavito, A., Bader, S., 2003. Numerical modelling of chemical osmosis and ultrafiltration across clay formations. Journal of Geochemical Exploration (78-79), 333–336.

Leijnse, A., 1992. Three-dimensional modeling of coupled flow and transport in porous media. Ph.D. thesis, Notre Dame Univ., Indiana.

Malusis, M., Shackelford, C., 2002a. Theory for reactive solute transport through clay membrane barriers. Journal of Contaminant Hydrology 59, 291–316.

Malusis, M., Shackelford, C., 2002b. Coupling effects during steady-state solute diffusion through a semi permeable clay membrane. Environmental Science and Technology 36, 1312–1319.

Manassero, M., Dominijanni, A., 2003. Modelling the osmosis effect on solute migration through porous media. Geotechnique (53), 481–492.

Marine, I., Fritz, S., 1981. Osmotic model to explain anomalous hydraulic heads. Water Resources Research 29 (17), 73–82.

Mitchell, J. K., 1993. Fundamentals of soil behavior., 2nd Edition. John Wiley and Sons, New York.

Mitchell, J. K., Greenberg, J., Whiterspoon, P., 1973. Chemico-Osmotic Effects in Fine-Grained Soils. Journal of the Soil Mechanics and Foundations Division, ASCE (SM4), 307–322.

Neuzil, C.E., B. J., Wolff, R., 1984. Leakage and fracture permeability in the Cretaceous Shales confining the Dakota Aquifer in South Dakota. In: First C. V. In: Theis Conference on Geohydrology. Natural Water Well Assoc.Lincoln, Nebraska.

Neuzil, C., 1982. On conducting the modified ”slug” test in tight formations. Water Resources Research 18 (2), 439–441.

Neuzil, C., 1993. Low fluid pressure within the Pierre Shale: a transient response to erosion. Water Resources Research 29 (7), 2007–2020.

Neuzil, C., 1994. Characterization of flow properties, driving forces and pore water chemistry in the ultra-low permeability Pierre Shale, North America. In: Workshop on Determination of Hydraulic and Hydrochemical Characterisation of Argillaceous Rocks. OECD Documents Disposal of Radioactive Waste. Nottingham, UK., pp. 65–74.

Neuzil, C., 2000. Osmotic generation of ”anomalous” fluid pressures in geological environments. Nature (403), 182–184.

Neuzil, C., Pollock, D., 1983. Erosional unloading and fluid pressures in hydraulically "tight" rocks. Journal of Geology 91, 179–193.

Noy, D., Horseman, S., Harrington, J., Bossart, P., Fisch, H., 2004. An Experimental and modelling study of chemico-osmotic effects in the Opalinus Clay of Switzerland. In: Heitzmann, P. ed. (2004) Mont Terri Project - Hydrogeological Synthesis, Osmotic Flow. Reports of the Federal Office for Water and Geology (FOWG), Geology Series (6), 95–126.

Oduor, P., 2004. Transient modeling and experimental verification of hyperfiltration effects. Ph.D. thesis, Department of Geological and Petroleum Engineering, University of Missouri-Rolla.

Olsen, H., Giu, S., Lu, N., 2000. Critical Review of Coupled Flow Theories for Clay Barriers. Transportation Research Record (1714), 57–64.

Palciauskas, V., Domenico, P., 1980. Microfracture development in compacting sediments: Relation to hydrocarbon maturation. American Association of Petroleum Geologists Bulletin. (64), 927–937.

PDE, S., 2001. FlexPDE Version 2.20e1. Scripted finite element model builder and numerical solver.

Soler, J., 2001. The effect of coupled transport phenomena in the Opalinus Clay and implications for radionuclide transport. Journal of Contaminant Hydrology (53), 63–84.

Yeung, A., 1990. Coupled flow equations for water, electricity and ionic contaminants through clayey soils under hydraulic, electrical and chemical gradients. Journal of non-equilibrium Thermodynamics (15), 247–267.

Yeung, A., Mitchell, J., 1993. Coupled fluid, electrical and chemical flows in soil. Geotechnique (43), 121–143.

Case study: Osmosis as Explanation of Anomalous Hydraulic Heads in a Triassic Basin (Savannah River Plant, Aiken, South Carolina)

In the subsurface, anomalous pressures have been commonly observed in deep sedimentary basins in which great differences in salinity exist. Within these environments the degrees of compaction are very high. High degrees of compaction are fundamental to observe high semi-permeable membrane efficiencies. Osmotic processes operating within these deep basins would be able to generate significatively large pressures, and to maintain them over extended geological time scales. Similarly, the semi-permeable membrane behavior of shales could explain observed anomalous salinities and processes like the concentration of brines. In this chapter we present the case of a possible osmotic system. High fluid pressures in the Triassic age Dunbarton Basin have been previously observed and identified as being possibly induced by osmosis. Numerical modelling is applied to this case to confirm if osmotically-induced pressures are generated and maintained over a geologically significant period of time.

7.1 The Dunbarton Basin

The Dunbarton Triassic Basin, located 55 km SE of the Fall Line beneath the Savannah River Site (SRS), S.C., is one of the Triassic-Jurassic rift basins of eastern North America. The Dunbarton Basin is a 50 km long and 10km wide basin filled mainly with Triassic red beds (Figure 7.1).

The basin is bounded on the south-eastern and north-western side by two major faults running semi-parallel to each other. Seismic data shows that the Triassic sediments terminate on the north-western border. In the region further north-west ward, the Coastal Plain deposits are in direct contact with the basement rocks. As a result of vertical movements, steep fault escarpments developed which provided sediments for the basin. Course material was deposited along the escarpments (fanglomerates) while finer material was transported towards and along the axis of the basin through braided river systems.
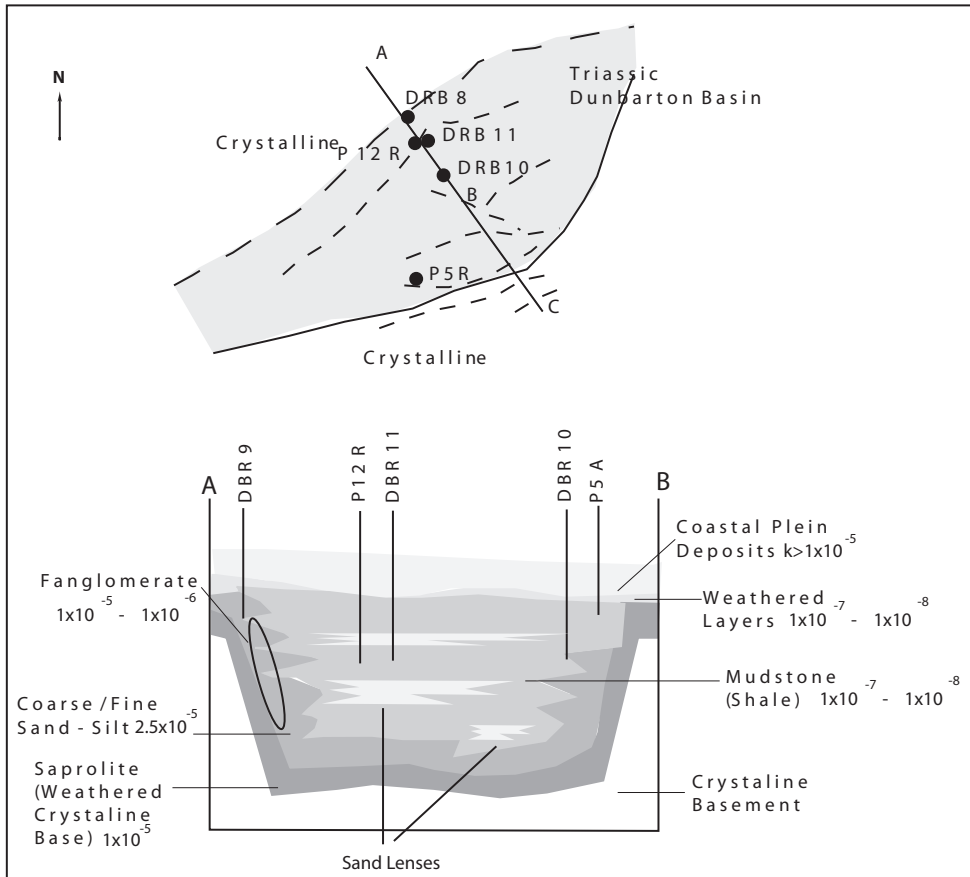
Figure 7.1: a. Outline of the buried Triassic Dunbarton Basin b. Distribution of major geological units. Distribution of hydraulic conductivity (m/day) is based on on values obtained from cores.

7.1.1 Structure of the Dunbarton Basin

Boreholes and later wells D5R, DRB9 and DRB10 constituted the geological database of the Dunbarton Basin for the study of Marine (1974). Several drillings were done in the region to the north-west side of the basin (Figure 7.1).

The geology of the basin consist of 5 major units: 1) the crystalline basement rocks forming the shape of the basin, 2) a layer of intensely weathered basement rock, 3) a sedimentary fill of conglomerate, sand, silt and clay of Triassic-age, 4) a layer of weathered basin fill, and finally 5) a cover of sand, silt and clay of the Coastal Plain deposits. The distribution of the units is presented in Figure 7.1.

The rocks forming the basement of the Dunbarton Basin consist of gneiss, schist and

quartzite (mainly highly metamorphous sedimentary rocks) containing small fractures. An intensely weathered zone overlies the fresh unweathered crystalline rock. The layer is approximately 25 meters thick. In the zone where this layer is in direct contact with the Coastal Plain deposits the minerals have largely been chemically altered to a clay or sandy clay residue. The weathered basin fill zone consists of mostly reddish-brown colored shale, silt- and sandstone, breccia and conglomerate layers. The coarser units are consolidated by a hard claystone matrix. Layers of weathered basin fill are found in and near the top of the Triassic Sedimentary fill (wells: P5R, DRB9). The thickness ranges from 3.7 meter in P5R to between 8.2 and 17.4 meter in DRB9 to possibly 2.7 meter or absent at DRB10. The Coastal Plain deposits cover the Dunbarton Basin sediments discordantly. The deposits consist of clay, silt and sand and are partly consolidated. The base of this unit is formed by a grey sandy clay layer of between 15 to 50 meter thick. Unaltered Triassic sedimentary fill was found at well sites D5R, DRB9 and DRB10. The cored intervals at those wells consisted partly of maroon-colored claystone and siltstone containing grey calcareous nodules, and partly of a grey-brown, fine to very fine-grained sandstone. The entire rock is classified by Marine (1974) as fanglomerate. The approximate thickness of the unaltered sedimentary fill is 1.5 km.

Two additional wells were drilled (DRB 11 and P12R) and cored later. Cores in the upper section showed high clay content (swell and crack when exposed to wetting and drying). The Triassic consisted predominantly of maroon fine-grained mudstone (90 %) and the remaining (10 %) consist of gritty, poorly sorted sandstone.

7.1.2 Hydrogeology

The hydraulic conductivity of the transition of Triassic rock to overlying Coastal Plain deposits (Layers of weathered basin fill) was tested with laboratory techniques and has similar values as the Triassic rock itself. Core samples of Triassic rock obtained from the three wells showed extremely low hydraulic conductivity. Fanglomerates have the highest hydraulic conductivity ($1 \cdot 10^{-6}$ - $1 \cdot 10^{-5}$ m/d), sandstones have a relatively high hydraulic conductivity of $2.5 \cdot 10^{-6}$ m/day, mudstones/shales have a relatively low hydraulic conductivity ($1 \cdot 10^{-7} - 1 \cdot 10^{-8}$ m/day). The low hydraulic conductivity is apparently caused by the completely unsorted character of the Triassic red beds. Although the weathered zone is apparently not tested, it is noted that it has higher hydraulic conductivity than the overlying Triassic rocks and lower than the fractured section of the basement rocks.

A well test in well P5R resulted in an average hydraulic conductivity of $2.4 \cdot 10^{-7}$ m/day for the exposed Triassic red beds, an order of magnitude lower than the values obtained from core samples. Well testing at four levels in the exposed section of well DRB 10 penetrated sediments of extremely low hydraulic conductivity. The apparent hydraulic conductivity of the sediments is about $6 \cdot 10^{-6}$ m/day, a value probably influenced mainly by the higher permeable sandstones in the section.

The specific storage value reported for the mudstones formation is $4 \cdot 10^{-7}$ m^{-1}.

From core analysis is it apparent that the sandstones have an effective porosity of nearly 7 % and a total porosity of 8 % . The mudstones have an effective porosity of 0.5 % and a

total porosity of 3 % .

In the Triassic sediments the hydraulic head in DRB 10 and DRB 11 is higher than the ground surface (artesian). Hydraulic head in DRB 9 shows no over-pressuring (even after packing the well inside the Triassic deposits). Wells DRB 10 and DRB 11 were still recovering from well construction by the time of the manuscripts were written in 1974; but by the time of the study of Marine and Fritz (1981) they had fully recovered showing artesian conditions.

Hydrochemistry shows that dominant ions are sodium, calcium and chloride. Salt originates from evaporites that can be associated with the deposition of the original sediments. Although not found here, evaporites are found in other east-coast Triassic basins.

The chemical compositions of formation water from the DRB wells showed large differences in mineral content within the basin. Water from the overlying Coastal Plain sediments has a total dissolved solids value TDS of 38 mg/l, while TDS for water coming from the surrounding crystalline metamorphic rock is 6000 mg/l. Water from the center from the Triassic Basin is highly mineralized (18,000 mg/l) and water from near the edge of the Dunbarton Basin- Crystalline rock is lower in dissolved solid content (11,900mg/l).

7.2 Osmotic Phenomena Operating Within the Basin

High pressures were observed by Fritz (1986) in two wells drilled in the Triassic-age Dunbarton Basin. The heads found in these two wells (192m and 140m above sea level) are well above the local water table developed in the overlying Cretaceous coastal plain sediments (58m above sea level). Marine and Fritz (1981) have exposed and evaluated several of the possible causes or mechanisms of geopressured reservoirs to explain the high observed heads in the DRB wells. They concluded that most of the commonly used explanations for existence of anomalous pressures were not applicable in this basin; and pointed to osmotic membrane phenomena as possible explanation.

Marine and Fritz (1981) proposed the following conceptual model. The sediments of the Dunbarton Basin consist of lenses of sand and clay. The clayey parts work as the membrane while the sandy parts act as the reservoirs of the saline water. The saline groundwater has been in the Triassic rock as a result of previous dissolution of evaporitic sediments during and after deposition. The overlying coastal plain sediments (deposited during late Cretaceous and Cenozoic) act as the container of the fresh water. Water from the coastal plain sediments moves towards and through the Triassic rock due to osmosis, raising the pressure within the Triassic rock above that in the Coastal Plain sediments. When osmotic equilibrium pressure is reached the net inflow of water into the Triassic basin stops confining fluids within the basin. The fluid confinement only applies to the net fluid flow flux, but fluid continues moving slowly in both directions through the membrane. As the membrane is not completely ideal, diffusion of salt through the membrane occurs. Slow salt diffusion out of the Triassic rock drives salt towards the margin of the basin. However continuous fresh water inflow from the Coastal Plain decreases the concentration of the water at the margins of the Basin isolating an "osmotic cell" in the center of the Triassic rock. Based on the TDS of Triassic Rock water and fresh water in the overlying sediments Marine and Fritz

(1981)calculated the equilibrium osmotic pressure differential to be about 132 m and 177 m of fresh water for DBR10 and DRB11 respectively. Observed anomalous heads are very close to those values and Marine and Fritz (1981) concluded that the clayey membranes of the Triassic Basin have efficiencies of nearly 100 percent. It is not known if the high heads observed in DRB10 and DRB11 exist over the entire basin or only in certain regions. The maintenance of the osmotic equilibrium induced pressure for a long period of time was interpreted by Marine and Fritz (1981) as an indication that there are not large discontinuities in the membrane. Nevertheless these authors concluded that at some point in geologic time the continuous inward movement of fresh water and the slow outward salt leakage will deteriorate the semi-permeable performance of the "osmotic cell".

7.3 Numerical Modelling of Osmotically-Induced Pressures at the Dunbarton Basin

The osmotic flow continuum model (Kooi et al., 2003; Bader and Kooi, 2005) used in Chapter 6 is applied to the Triassic Dunbarton Basin case aiming to : 1) Compare the calculated induced osmotic pressures by Marine and Fritz (1981) for the existing concentration gradients with those resulting from modelling, and 2) To establish if the osmotically-induced pressures can be maintained over a extended geological time scale.

The equations of chemically and hydraulically coupled flows of solution (Kooi et al., 2003; Bader and Kooi, 2005) presented in Chapter 6 were applied. The reflection coefficient is calculated using the (Bresler, 1973) relationship as previously described. The diffusion coefficient is introduced using equation (6.10).

7.3.1 Model Configuration

Figure 7.2 shows the model configuration. Its based on the conceptual cross section across the Dunbarton Triassic Basin presented by Marine and Fritz (1981) and Marine (1974). Two monitoring points (A and B) are placed in the model domain at the approximate location and depth of the wells where anomalous heads were found (DRB10 and DRB11). The model domain consists of a vertical section delimited at the top by the land surface and on the sides and bottom by impervious metamorphic crystalline rock. The domain is divided into two main regions. The Triassic Basin (triassic sediment, weathered layers and fanglomerates) and the coastal plain sediments. It is assumed that the Dunbarton Basin mainly consists of mudstone and claystone due to its low average permeability characteristics. The existence of three smaller regions towards the center of the basin representing sandy lenses is also assumed. Properties assigned to the Triassic basin region are those reported for the mudstone/claystone and properties for the sand lenses are those measured in sandstone. A high permeability value was conferred to the coastal plain sediments. No membrane characteristics ($\sigma = 0$) are assigned to the sandy lenses and coastal plain sediment regions of the domain. The thickness of the water film b adopted for the clayey parts of the basin has been calculated using the equation (6.13) presented by Keijzer (2000).
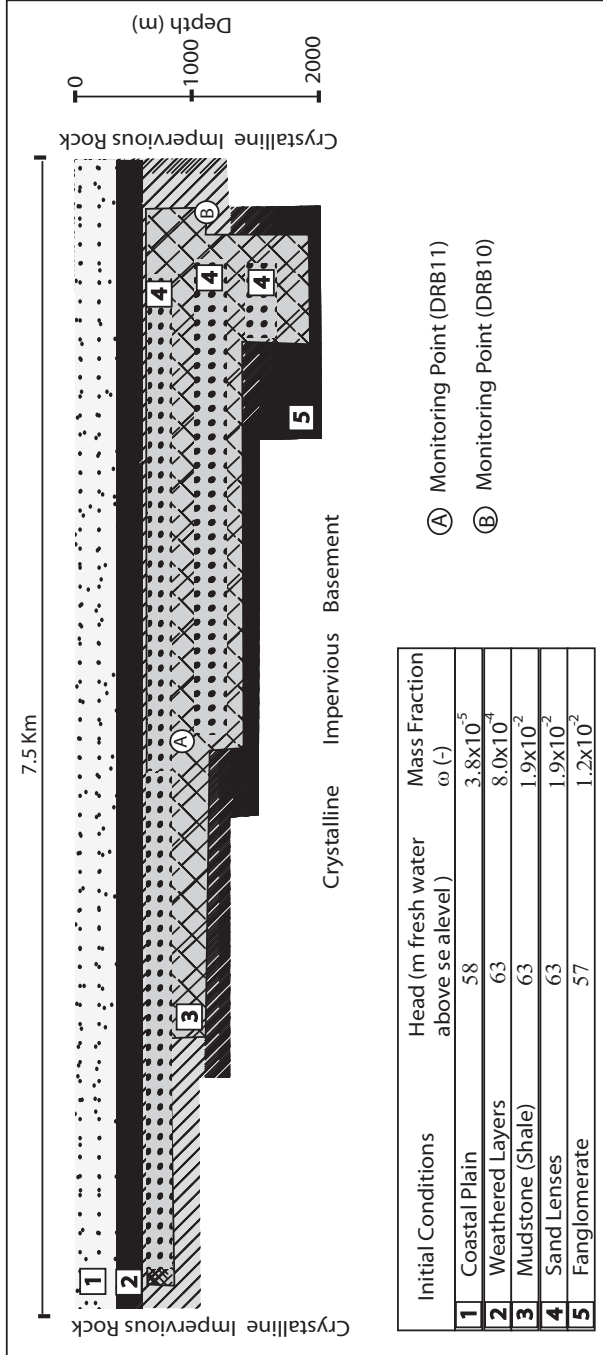
Figure 7.2: Model configuration and initial and boundary conditions for the Triassic Dunbarton Basin modelling.

Initial Conditions	Head (m fresh water above se alevel)	Mass Fraction ω (-)
1 Coastal Plain	58	3.8×10^{-5}
2 Weathered Layers	63	8.0×10^{-4}
3 Mudstone (Shale)	63	1.9×10^{-2}
4 Sand Lenses	63	1.9×10^{-2}
5 Fanglomerate	57	1.2×10^{-2}

Ⓐ Monitoring Point (DRB11)

Ⓑ Monitoring Point (DRB10)

Table 7.1: Head and TDS of wells penetrating the Triassic sediments in the Dunbarton Basin (Marine and Fritz, 1981)

Well	Penetration of Triasic rock (m)	Head (m fresh water a.s.l)	TDS (mg/l)
DRB8 Crystalline rock	0	57	5600
DRB9-Triassic	495	63	5950
Crystalline Rock	21	63	5990
P12R	47	-	800
P5R	31	63	-
54P	0 (Coastal plain only)	58	38
DRB10	925	140	11900
DRB11	673	192	18500

A typical range of values of specific surface for clays is $70 - 120$ m^2/g. Bulk density for clays ranges between 1.4 to 1.9 g/cm^3. Due to the low porosity of the basin, the clayey sediments of the Triassic basin have extremely low values of b (1 to 3 Å) relative to values previously reported for compacted clays (Kemper and Maasland, 1964; Keijzer, 2000).

Initial values of head in the coastal plain sediments, the crystalline impervious rock and the Triassic basin were based on the heads measured in wells (Table 7.1) except for anomalous heads measured in DRB10 and DRB11. The bottom, left-side and right-side boundaries of the domain were assigned no-flow boundaries. For the top of the domain a constant head and constant concentration boundary condition were set (coastal plain measured head and concentration).

The values of permeability, porosity and specific storage used for modelling were mainly based on the core measurements provided by Marine (1974) and are reported in section 7.12 and Figure 7.1.

As for the conceptual model of Marine and Fritz (1981) it is assumed that saline groundwater existed in the Triassic Basin as a result of previous dissolution processes. Initial and boundary conditions for concentration (mass fraction) are also based on measurements taken from wells (including DRB10 and DRB 11). Thus, different initial concentration zones are defined within the domain representing the large differences in mineral content within the basin itself. Figure 7.2 indicates the initial conditions.
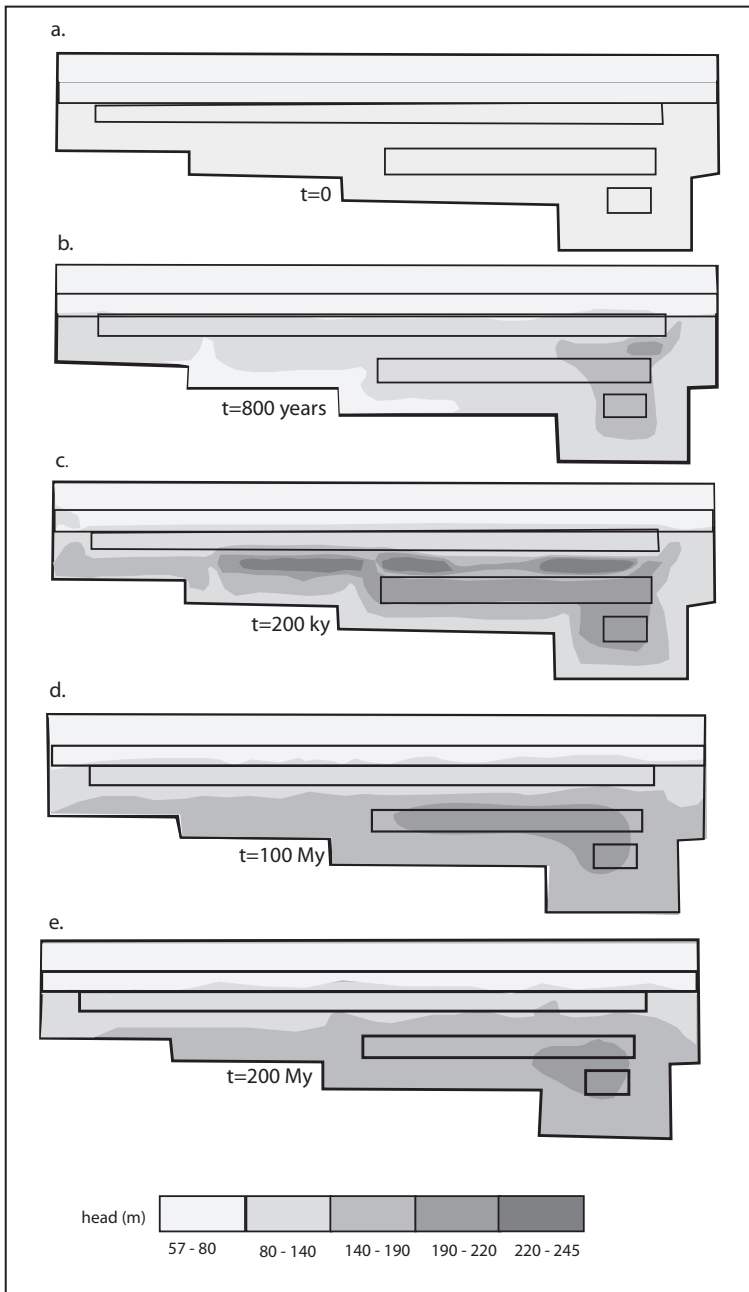
Figure 7.3: Pressure evolution within the entire basin Triassic Basin over a period of 200 million years.

7.3.2   Model Results

From modelling, it is observed that efficiency calculated using the relationship of Bresler (1973) is close to 100 percent for the given concentration differences. Efficiencies for highest and lowest concentrations vary from 0.9897 to 0.9950 respectively. The pressure evolution was monitored for the entire domain and for the points A and B. Figures 7.3 and 7.4 depict the temporal evolution of the fluid pressure in the entire basin and the monitoring points (A and B). Figure 7.3 shows how due to osmosis the low concentration water contained in the coastal plain, weathered layers and the fanglomerate is driven towards the Triassic sediments containing more saline water. In the center of the basin the pressure increases gradually over a long period of time. At monitoring point A for instance, the maximum pressure occurs only after 200 thousand years (Figure 7.4). At point B (DRB10) it occurs much later. The maximum values of pressure are 158 m and 230 m for B and A respectively. After maximum pressure is reached the pressure declines due to the gradual decrease in concentration gradients within the entire basin. The decline however, occurs very slowly and overpressures remain present in the entire basin for longer periods of time (Figure 7.4). The modelling results confirm the observations and predictions of Marine and Fritz (1981). Observed overpressures can be generated and explained by osmotic processes. The magnitude of σ and generated overpressures are very similar to those reported by Marine and Fritz (1981). Modelling was performed over a period of 200 million years that corresponds approximately with the age of the basin.

The values of the parameters used for modelling are mainly based on the core measurements provided by Marine (1974). It is not known to what extent these values are representative of the *in-situ* conditions. Similarly, assumption was made of the unknown value of the thickness of the water film for the Triassic basin sediments. Nevertheless, the agreement of results with those reported by Marine and Fritz (1981) shows that the values used seem to be reasonable as a first approximation. For modelling, it is assumed that the entire basin is constituted by mudstone and claystone and that it behaves as a semi-permeable membrane. This assumption may be not entirely correct. Core data has shown that although the basin consists mainly of clay, it is not uniformly distributed and other type of sediments are present as well. This was the main reason to include the three "arbitrary" sandy lenses in the model configuration.

Keijzer (2000) observed differences when calculating the efficiency of the membrane σ, using the relationship of Bresler (1973) and the Fritz and Marine membrane model (Marine and Fritz, 1981; Fritz, 1986). However in this study when comparing our predictions with those of Marine and Fritz (1981); Fritz (1986) those differences were not observed. The value predicted by Marine and Fritz (1981); Fritz (1986) is similar to our calculated efficiency using Bressler's relationship. In both cases efficiencies are nearly 100 % for the given concentrations. From the model predictions it seems that within the Triassic Dunbarton Basin the potential for osmotic processes to operate exists. Predictions also show that the required conditions exist to maintain the osmotically-induced pressures and to prevent its fast dissipation. Even after 200 million years that is the approximate age of the basin the pressure remains high. The hypothesis of Marine and Fritz (1981) that an "osmotic cell"

may be isolated in the center of the basin is confirmed with our modelling results. Initially, fresh water flows from the margins of the basin towards the center; and it is constantly replenished by infiltrating water from the Coastal Plain sediments. The leaky membrane behavior of the basin causes solute diffusion from the center of the basin towards the margins. Nevertheless membrane efficiencies are so high and close to 100 % that the solute flow towards the margins is very small. In the model of Marine and Fritz (1981) the chemical gradient is said to be maintained for extended periods of time. There will be always a zone of decreased concentration at the margins of the basin and a zone with elevated concentration at the center. This due to the continuous inward movement of fresh water and the slow outward salt leakage. In their opinion, the osmotically-induced pressures can be maintained for a long period of time due to the operation of this isolated "osmotic cell". Unlike their model in our model salt is not leaking out of the basin; and it slowly dilutes in the center of the basin and "quickly" at the margins. Thus, the chemical gradient dissipates and high pressures that were generated likewise.

It is important to keep in mind that the initial conditions (head and concentration) adopted for this modelling exercise were derived from the present situation (well data) and do not correspond to the situation existing right after the Triassic sediments were deposited. Furthermore it has been assumed that the osmotic processes started to operate only after the deposition of the fresh water Coastal Plain Sediments. It may be possible that fresh
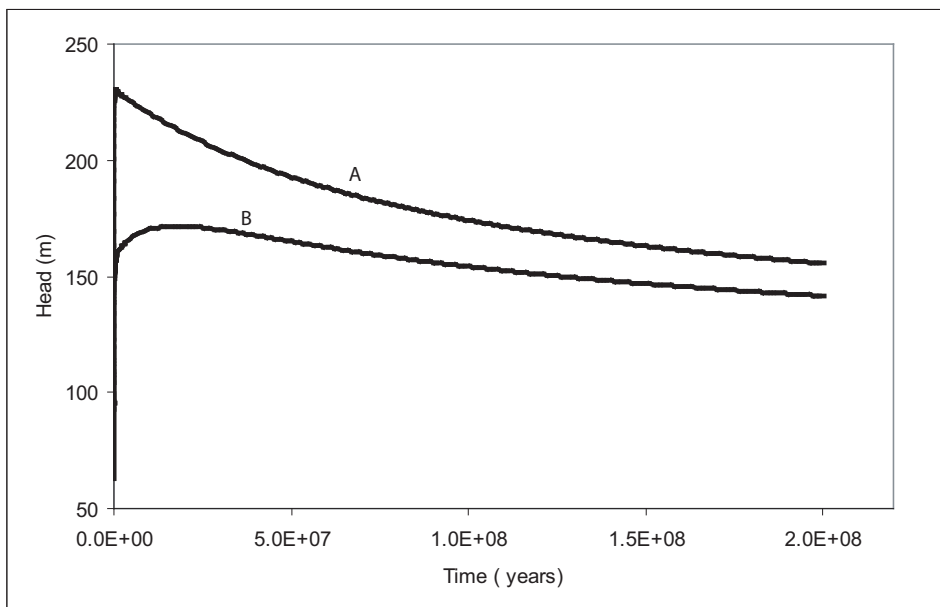
Figure 7.4: Pressure evolution for monitoring points A and B. Pressure rise is observed in both monitoring points due to osmosis. The pressure build-up phase is followed by a slow decline.

water (i.e. water from the crystalline basement) had been also available during deposition of the Triassic fill sediment; and that osmotic effects started to be developed long before the Coastal Plain Sediments were deposited. The modelling presented here is useful to illustrate that the Dunbarton Basin has the potential to behave as semi-permeable membrane and that high osmotically-induced pressures can be maintained. Similarly, to show that osmosis can be an explanation for the anomalous pressures observed. A more comprehensive modelling in which the sequence of depositional events and the total supply of salt within the basin are considered would be the next step.

References

Bader, S., Kooi, H., 2005. Modelling of solute and water transport in semi-permeable clay membranes: Comparison with experiments. Advances in Water Resources (28), 203–214.

Bresler, E., 1973. Anion exclusion and coupling effects in non-steady transport through unsaturated soils. Soil Sci. Soc. Am. Proc. (37), 663–669.

Fritz, S., 1986. Ideality of clay membranes in osmotic processes: a review. Clays and Clay minerals (34), 214–223.

Keijzer, T., 2000. Chemical osmosis in natural clayey material. Ph.D. thesis, Universiteit Utrecht, The Netherlands.

Kemper, W., Maasland, D., 1964. Reduction in salt content of solution on passing through thin films adjacent to charged surfaces. Soil Science Society of America Proceedings , 318–323.

Kooi, H., Garavito, A., Bader, S., 2003. Numerical modelling of chemical osmosis and ultrafiltration across clay formations. Journal of Geochemical Exploration (78-79), 333–336.

Marine, I., 1974. Geohydrogeology of buried Triassic basin at Savannah River plant, South Carolina. American Association of Petroleum Geologists Bulletin (58), 1825–1837.

Marine, I., Fritz, S., 1981. Osmotic model to explain anomalous hydraulic heads. Water Resources Research 29 (17), 73–82.

Chapter 8

General Discussion and Conclusions

The foremost objective of this research was to provide direct evidence demonstrating that clayey sediments behave as semi-permeable membranes in the subsurface. New instrumentation was developed and *in-situ* measurements to determine the semi-permeable properties of a shallow natural clay were performed. Similarly, existing conventional hydraulic-testing instrumentation was used for osmosis testing of both shallow and deep clay formations. Osmotic water and solute flow and transport have been quantified by means of a continuum transport model. The model has been used to simulate different osmosis tests and osmotically-induced anomalous pressure. In this chapter our findings are briefly presented and discussed. Additionally recommendations for further research are given.

8.1   Key Experimental Results

Within this research, *in-situ* tests have been carried out on two very different clay formations; the strongly consolidated, Boom Clay, which exhibits characteristics that are typical for deeper parts of sedimentary basins and the shallow, unconsolidated, plastic Calais Clay, which is more representative for shallow, deltaic environments. Of these formations, evidence for membrane behavior was only clearly found for the Boom Clay and its membrane efficiency could be accurately constrained. By contrast, for the Calais Clay, osmotic behavior could not be ascertained from the field tests. With our specially designed instrumentation (large volume closed reservoir), osmotic effects were not detected for the Calais Clay. Experiments with the BAT probe did reveal distinct differences in response between saline (OT) and reference tests (RT) both for inflow and outflow tests, which appear to be consistent with the presence of osmotic phenomena. However, the response features are not fully understood and it cannot be ruled out that the observed behavior is caused by other processes or conditions. In spite of the latter interesting experimental results, we, therefore, presume that the osmotic behavior of the Calais Clay is either absent or below detection limit of our set of instruments.

For the Boom Clay, the inferred osmotic efficiencies are high (40 %). The high efficiencies are concordant with existing theory and laboratory findings, which suggest that membrane efficiency is favored by low pore water salinity, a high degree of compaction, a high cation exchange capacity and the dominance of Na^+ occupying the exchange complex.

Similarly, the low or negligible membrane efficiency of the Calais Clay is consistent with a low degree of compaction, a relatively high pore water salinity and the low cation exchange capacity mainly dominated by Ca^{+2}. However, numerical modelling of the experimental results for both clays as well as for additional field and laboratory data revealed that the employed theoretical framework (Bresler's relationship) is deficient in accounting for their behavior in detail. This important issue will be discussed in greater detail in section 8.3. First, several practical issues regarding the conducted field experiments will be highlighted.

8.2 Instrumentation and Procedures for Osmosis *In-Situ* Measurements

A major part of the time invested in the research project laid down in this manuscript consisted of trial-and-error experiences that are common to most experimental work. These "negative" and time-consuming experiences are largely "invisible" in the final text of the manuscript. At the same time, however, we feel that the mere process of "doing the work" has yielded us trivial (in hind-sight) and less-trivial insights and ideas that might also be considered products of the present study. Moreover, some of these insights and ideas may prove to be of some use for any future experimental work of this type.

At the initial stage of this research the only study available containing data from osmosis *in-situ* measurements was the one by Neuzil (2000). The experimental set-up used by Neuzil (2000) consisted of conventional open boreholes drilled into the shale. A rather simple and straight forward approach, but involving many complexities. The main limitation of this approach was the extended period of time required for measurements.

Providing direct evidence of osmotic processes at the field scale is time consuming (because of the low permeabilities involved) and complex. For the present research, a shut-in testing method was ultimately adopted and used among various other options. This approach strongly reduced experiment duration (order of days), which allowed experiment replication. However, a few disadvantages and problems of the methods that were used were encountered or came to mind during the research project. These disadvantages may prove valuable for similar future in-situ osmosis studies and will, therefore, be enumerated below.

Lack of mixing within the measurement reservoir. In our experiments, solutions within the reservoirs could not be continuously homogenized. This problem was addressed in our work by explicitly simulating the transport processes and induced chemical gradients within the reservoirs in our numerical modelling. However, some uncertainty/ambiguity in the interpretation cannot be avoided using this approach. This uncertainty does not only apply to the transport parameters and processes within the reservoir, but also to the exact location of the point of concentration measurement within the reservoir. This problem appeared particularly relevant for our specially-designed filter.

Trapped air. It appeared to be a significant problem with the newly designed instrumentation. When the solution is poured in to the reservoir from the top of the instrument a considerable amount of air gets in. Late in the project we surmised that the flat bottom

design of the filter might also have given rise to air entrapment. Several possible solutions were considered but time limitations did not allow their implementation and testing. First the instrument can be modified by building onto it a pointy end as the one built on the conventional push-in probes. Second, the experimenting solution must be de-aired before it is poured inside the reservoir. To avoid aeration while pouring, filling with the de-aired solution can be forced to occur from the bottom of the instrument with the aid of a pipe. Air presence may not only affect the measurements, but also may cause oxidation of the clay (if extended contact periods are allowed) affecting its semipermeable-membrane characteristics.

Initial hydraulic disequilibrium conditions. Independently of the testing method (open borehole or shut-in) a general experimental problem faced is the assurance of an initial hydraulic equilibrium condition ideally required for osmosis testing. Firstly, the natural hydraulic regime within the clay is disturbed by borehole drilling and instrument placement. After instrument placing, the imposition of a chemical concentration gradient is performed by solution pouring or injection. Disequilibrium conditions are generated between the measurement instrument and the clay; unless injection is pressure controlled as it was the case for the second tests carried out in the Boom Clay. As a consequence the system response due to osmosis is superposed to the general water pressure recovery.

Reference testing. The observation of a pore water duplicate test (like DUP experiment in Neuzil (2000) or RT tests of this study) simultaneously with the saline water test is very important for isolation of osmotic effects. Nevertheless, this approach holds the inherent danger that well responses are affected by differences in permeability or osmotic properties amongst wells. These differences end up subsumed in the pressure differentials. If undetected, these differentials may introduce error in the inferred membrane properties. Transient modelling of individual well responses as was carried out in this study for the analysis of the data of Neuzil (2000) may help in the detection of such effects. Moreover, additional experiments in which a single well is used first for the duplicate experiment and subsequently for the saline water experiment could be used to further eliminate error due to different properties at different boreholes. This latter approach was followed during the testing phase of the new instrumentation in the Calais Clay without major complications. However, for more compacted clays the time required to complete one experiment can be significantly lengthened (Noy et al., 2004). In spite of the improvements that this approach may represent, it also engages a disadvantage. When conducting a pore water duplicate test it is very important that this test and the saline water test are carried out simultaneously. Experience gained in this study, showed that differences in timing are not convenient when osmotic effects need to be isolated.

Introduction of "anomalous" water in the measurement reservoir. At the URL in Mol (Belgium), usage of an existing piezometer was an excellent instrumentation alternative for osmosis *in-situ* testing of the Boom Clay. A minor deficiency was identified on the method utilized for solution exchange. The pore water initially contained within the piezometer chamber is exchanged by recirculation of the saline solution. Pumping causes a rapid increase in pressure after which pressure decays rapidly. This jump in pressure may have some effect on the pressure response of the system since pore pressures are inevitable disturbed.

The pumping lasts for 10 minutes, implying that the saline solution potentially can be in contact with the clay and osmotic processes could have been generated within this interval of time. Further, we have assumed that the mixing in the filter chamber was perfect. If that was not the case, the exact initial concentration of the solution in the chamber is not known. During recirculation, saline water is mixed with pore water contained initially within the chamber. Although the necessary pumping time (ensuring several chamber-volumes renewal) was calculated, the uncertainty associated to the exact geometry of the system could have led to miscalculations. When experimenting with push-in probes (BAT probe in this particular case) the contact time between the clay sediment and the experimenting solution is very short before an equilibrium condition is reached. This was likely to occur when performing the so-called "inflow tests", in which the filter tip saturated with saline solution is pushed into the ground; and the solution is in contact with the clay only for a few minutes before being displaced by pore water. For the "outflow tests" the contact time is prolonged (saline solution and clay are in contact during the whole experiment) to allow the osmotic effects to fully develop. The major difficulty faced in this aspect with the newly designed instrumentation had to do with the timing. First, if the instrument is placed into the ground and the solution is not introduced immediately, pore water from the clay starts flowing into the filter, getting mixed with the introduced "anomalous" solution. Second, if a reference test is performed, both solutions ("anomalous" and reference) should be introduced into the respective filters simultaneously.

For future work, implementation of the simple suggested solutions to avoid trapped air within the newly developed instrument will enhance results. Similarly, the experimental techniques should be improved in such a way that the effects of heterogeneities (different properties of spatially distributed boreholes) and differences in timing do not lead to erroneous isolation of osmotic effects.

8.3 Insights from modelling: Implications for membrane theory

The efficiency of clay membranes has been quantified with a continuum transport model. The continuum model formulated by Kooi et al. (2003) and Bader and Kooi (2005) has been demonstrated to be able to reproduce reasonably well the data corresponding to one laboratory experiment on bentonite by Keijzer (2000) and the *in-situ* osmosis experiments in the Pierre Shale and the Boom Clay. It has been also used as a prediction tool of response times and magnitudes of osmotically-induced pressures during the scoping calculations aiming to design the experiments that were performed in the Boom Clay. Further, modelling of osmotically-induced pressures generated within the Dunbarton Triassic Basin allow us to confirm the hypothesis of Marine and Fritz (1981) that overpressures observed in wells at this basin are caused by the semi-permeable membrane behavior of the Triassic sediments (efficiencies of nearly 100 %) and that those pressures can be maintained over extended periods of time.

In general, the model predicted higher reflection coefficients than experimentally ob-

served. The reflection coefficient has been introduced into the model through the Bresler (1973) relationship. According to this relationship, efficiency is dependent on local concentration and thickness of the water film b. Fitting of the experimental data obtained from the Pierre Shale and the Boom Clay was only possible by increasing the value of b with respect to the inferred values from other, prior, methods. Keijzer (2000) has suggested that the relationship of Bresler (1973) is the most adequate to calculate the efficiency of natural clayey sediments in comparison with other models (Groenevelt-Bolt, Kemper-Rollins, and Fritz-Marine). According to Neuzil (2000) this relationship yielded good inferred values of b for his field tests. Heister (2005) found that when comparing her laboratory results (membrane potential experiments) with model predictions, all the models (including Bresler's relationship) overestimated the efficiency of the membrane.

The fact that our modelling seems to overestimate σ (and/or b), may either be related to the "continuum" and/or "transient" nature of it (which are novel features compared to previous studies), or may indicate that Bresler's relationship is not applicable to the specific clays we have studied. Laboratory data, which provide the prime support for Bresler's relationship, are based on experimental work in which the concentration-dependence of the reflection coefficient is reduced to average values of these quantities for the membrane as a whole. Additionally, only osmotic-equilibrium conditions are considered in such osmosis studies, which disregards possible complications associated with transient flows. Neuzil (2000) did take into account spatial variability of the reflection coefficient related to concentration gradients within the membrane in his analysis, but his approach equally ignored potential transient effects. Further complications and uncertainties that may bear on this modelling problem relate to the way b is estimated. The value of b is assumed to be a constant calculated from equation (6.13). According to Bresler (1973), this simplified equation yields good estimates of b. However, this author suggested that "an average hydraulically effective film thickness" can be better estimated using a relationship introduced by Kemper (1961) in which b is dependent on the hydraulic conductivity of the soil and a "soil-water interaction parameter". Ideally, the values of b and concentration estimated at each point in time and space should be used to calculate the temporal and spatial evolution of σ. However Bresler (1973) introduced the reduced variable $b\sqrt{c}$ for computation time saving. Thickness of the water film may be susceptible to changes in solution concentration. According to the Gouy-Chapman theory the double layer thickness increases with decreasing ionic strength. Changes on the double layers may induce swelling or flocculation of the clay, leading to changes in the permeability (Appelo and Postma, 1996). According to van Olphen (1977) the thickness of the water film depends not only on the crystallographic parameters of the clay particle but also on the physico-chemical properties of the pore solution. No studies, including the present one, have considered potential contributions related to temporal variations of b.

Although all of the above features may be relevant to our apparent overestimation of the reflection coefficient σ, we feel that the cause of this discrepancy is more likely a reflection of a more fundamental limitation of Bresler's relationship. That is, laboratory investigations have shown that the efficiency of the membrane is not only dependant on degree of compaction and concentration but also on cation exchange capacity of the clay. This parameter

is not considered within the Bresler's relationship and therefore has not been introduced in our predictions. Heister (2005) concluded that the Bresler's relationship (among other models) is appropriate to calculate the reflection coefficient in natural clayey sediments; but highlighted the importance of incorporating the cation exchange capacity into the models. Heister (2005) attributes the low semi-permeability observed to two main reasons. The first, cation exchange processes occurring within the mixed-ionic clay in contact with a saline solution, that allow salt diffusion within the membrane, therefore reducing its semipermeability. Cation exchange processes are most likely to occur in mixed-ion clays as natural clays. The second explanation that this author provides is a decrease in the semipermeability attributed to the formation of tactoids. According to Heister (2005), in dilute suspensions (at lower concentrations than flocculation values) Ca-montmorillonite exists as tactoids or quasicrystals.

With regard to the continuum model used in these study we have identified few differences and similarities between the recently published continuum formulations (Malusis and Shackelford, 2002a; Manassero and Dominijanni, 2003) and the continuum model of Bader and Kooi (2005). The latter accounts for transient flow and transport conditions due to storage associated with the compressibility of both the fluid and the solid matrix. Transport equations deduced by Bader and Kooi (2005) are identical to those derived by Manassero and Dominijanni (2003). Malusis and Shackelford (2002a), by contrast, use a different form of equation (6.2) which does not explicitly represent the sieving of solute associated with osmotically-driven fluid flow (second term on the right-hand side of our equation (6.2)). This is important because it implies that their diffusion coefficient cannot be directly compared to our D^*.

8.4   Practical Implications of Osmotic Phenomena

Together with the studies of Neuzil (2000) and Noy et al. (2004), the experimental work in the Boom Clay and numerical modelling of the Triassic Dunbarton basin have strengthened the evidence of osmotic phenomena operating within the subsurface. It is clearly shown that osmosis plays an important role in water and solute transport within highly consolidated and compacted clay layers. These findings have direct implications for problems dealing with basic hydrogeological evaluation, paleohydrogeological research and longterm radioactive waste repository design. Highly consolidated clay layers within deep sedimentary basins may still reflect former environmental conditions from periods of thousands of years, due to the slow flow and transport processes occurring within them. Data obtained from those clay-rich deposits are therefore a very useful tool to understand the hydrogeological evolution of groundwater systems. Often, pressure and salinity anomalies occurring in those environments have not properly been explained. With our findings these observations can find an explanation on the light of osmosis. Furthermore it has been shown through modelling that osmotically-induced pressures can be maintained over geologically significant period of time.

For shallow ($\sim$ 200 m depth) groundwater systems that are important in the context of water resources and environment issues, the relevance of osmotic phenomena is much

less clear. Several authors (Keijzer, 2000; Shackelford et al., 2001; Heister, 2005) have listed many practical hydrogeological problems for which osmotic phenomena may be potentially important. Among the problems mentioned are sea-water intrusion, water balances for polder areas, contaminant emissions from waste storage, groundwater extraction in holocene coastal areas, etc. However, no good assessments of the importance have yet been made. That is, very little, if any, knowledge of membrane properties of relatively unconsolidated clay-rich formations exists, in particular for sediments in their natural environment and on scales larger than those of laboratory measurements. Furthermore, no studies have explored or quantified the impact of low, albeit finite osmotic reflection coefficients of sediments on the above-mentioned practical problems. The prime goal of the present research project was to make a significant contribution towards improved understanding of the role of osmotic phenomena by developing *in-situ* measurement techniques, quantifying membrane properties of clayey sediments with these methods and by conducting sensitivity analyses to explore the impact of osmotic behavior for shallow groundwater systems using numerical modelling.

Within this study considerable effort and time were put into the development of measurement techniques. Although the osmotic behavior of the Calais Clay at Groot Mijdrecht was non-detectable or negligible, the use of this shallow layer was extremely convenient for testing the new instrumentation and experimenting with it and the BAT probe system. During the testing phase many complexities and problems appeared that had to be overcome. That implied continuous repetition of the tests. The Calais Clay at the experimenting location was soft and plastic enough to allow insertion of the instrumentation only by pushing it into the ground. Additionally its permeability characteristics in combination with the shut-in testing approach enhanced the short duration of experiments. In this way time was gained and drilling costs avoided. In spite of the fact that we haven't been able to test equipment for many clays, the instrumentation that has been used in this study is available and we consider that it may be very useful for the evaluation of other shallow clay layers.

The membrane properties of the highly consolidated Boom Clay were quantified by means of in-situ experiments. Unfortunately this was not the case for the Calais Clay. The main difference between these two clays is the degree of compaction. Experiments in the Calais Clay were performed at a very shallow depth (6.8 m below NAP), a depth at which this Clay is not highly compacted. Additionally, relatively low efficiencies were predicted with the Bresler's relationship for the Calais Clay (mainly associated to the brackish pore water concentration) and its low cation exchange capacity (mainly Ca occupation) was not taken into account in our predictions.

The fact that the Calais Clay did not show a significant semi-permeable membrane behavior does not imply that other shallow relatively non compacted clays are not capable to act as semi-permeable membranes. The dependence of the efficiency on concentration may suggest that within clay layers containing fresh pore water, the required degrees of compaction to observe membrane behavior may be smaller than those in deep saline clayey sediments. Furthermore, shallow clays at other locations may exhibit a higher exchange capacity than that measured in the Calais Clay.

Although we did not initiate any comprehensive model assessment of osmotic phenom-

ena for shallow groundwater systems, the modelling capability to predict water and solute transport taking into account osmotic effects has been developed. The present numerical model appears to provide an excellent tool for prediction. The importance of osmotic effects in groundwater systems can be assessed by comparison of modelling scenarios in which osmosis is taken into account and scenarios in which it is neglected. The modelling framework provides a wide range of possibilities for prediction and assessment.

References

Appelo, C., Postma, D., 1996. Geochemistry, groundwater and pollution. A.A., Balkema Rotterdam.

Bader, S., Kooi, H., 2005. Modelling of solute and water transport in semi-permeable clay membranes: Comparison with experiments. Advances in Water Resources (28), 203–214.

Bresler, E., 1973. Anion exclusion and coupling effects in non-steady transport through unsaturated soils. Soil Sci. Soc. Am. Proc. (37), 663–669.

Heister, K., 2005. Coupled transport in clayey materials with emphasis on induced electrokinetic phenomena. Ph.D. thesis, Universiteit Utrecht, The Netherlands.

Keijzer, T., 2000. Chemical osmosis in natural clayey material. Ph.D. thesis, Universiteit Utrecht, The Netherlands.

Kemper, W., 1961. Movement of water as affected by free energy and pressure gradients. I Application of classic equations for viscous and diffuse movements to the liquid phase in finely porous media II. Experimental analysis of porous systems in which free energy and pressure gradients act in opposite directions. Soil Science Society of America Proceedings , 260–265.

Kooi, H., Garavito, A., Bader, S., 2003. Numerical modelling of chemical osmosis and ultrafiltration across clay formations. Journal of Geochemical Exploration (78-79), 333–336.

Malusis, M., Shackelford, C., 2002a. Theory for reactive solute transport through clay membrane barriers. Journal of Contaminant Hydrology 59, 291–316.

Manassero, M., Dominijanni, A., 2003. Modelling the osmosis effect on solute migration through porous media. Geotechnique (53), 481–492.

Marine, I., Fritz, S., 1981. Osmotic model to explain anomalous hydraulic heads. Water Resources Research 29 (17), 73–82.

Neuzil, C., 2000. Osmotic generation of "anomalous" fluid pressures in geological environments. Nature (403), 182–184.

Noy, D., Horseman, S., Harrington, J., Bossart, P., Fisch, H., 2004. An Experimental and modelling study of chemico-osmotic effects in the Opalinus Clay of Switzerland. In: Heitzmann, P. ed. (2004) Mont Terri Project - Hydrogeological Synthesis, Osmotic Flow. Reports of the Federal Office for Water and Geology (FOWG), Geology Series (6), 95–126.

Shackelford, C., Malusis, M., Olsen, H., 2001. Clay membrane barriers for waste containment. Geotechnical News (2), 39–43.

van Olphen, H., 1977. An introduction to clay colloid chemistry. Krieger Publising Comapny, Florida.

Samenvatting

Transport van water en opgeloste stoffen in klei-rijke sedimenten verloopt in de regel lang-zaam. Advectie van opgeloste stoffen is beperkt in kleien; diffusie is daarom vaak het dominante transportproces. De geringe transportsnelheden in laag-permeabele kleilagen maken dat deze sedimenten vaak een schat aan gegevens over paleohydrologische condi-ties bevatten. Voorts worden zij gebruikt als afscheidende laag (Eng.: "liner") of barrière bij vuilstorten en recentelijk worden zij ook in beschouwing genomen als opslagmedium voor ondergrondse berging van radioactief afval. Een goed begrip van de processen die het transport van water en opgeloste stoffen in deze sedimenten veroorzaken is daarom essen-tieel voor de studie van de hydrogeologische ontwikkeling van grondwatersystemen alsook voor het garanderen van het goed functioneren van kleien als barrières en opslagmedia voor contaminanten.

Naast diffusie kunnen ook osmotische processen (chemische osmose en ultrafiltratie) mogelijk een belangrijke bijdrage leveren aan de beweging van water en opgeloste stoffen in klei-rijke sedimenten indien ze blootgesteld zijn aan gradiënten in zoutconcentratie. Chemi-sche osmose is gedefinieerd als vloeistofstroming die wordt gedreven door een chemische concentratiegradiënt. Ultrafiltratie is het uitzeven van opgeloste stoffen tijdens stroming van de vloeistof. Deze verschijnselen doen zich voor in kleien doordat deze zich gedragen als semi-permeabel membraan. Dit gedrag ontstaat door de aanwezigheid van electrische dubbellagen (electrische velden) tussen de kleideeltjes in het sediment. Het membraange-drag is met name sterk wanneer de electrische dubbellagen in de poriën elkaar overlappen. Door dit overlappen wordt het transport van ionen gehinderd ten opzichte van het trans-port van water. De mate van overlapping van dubbellagen is gerelateerd aan de mate van compactie van de klei. De mate van compactie heeft daarom een belangrijke invloed op de mate waarin de klei membraangedrag vertoont. Een ideaal membraan is volledig impermea-bel voor opgeloste stoffen. Niet ideale, of lekkende membranen laten beperkt transport van opgeloste stoffen toe. Laboratorium studies hebben herhaaldelijk aangetoond dat natuurlijke en industriële kleien zich kunnen gedragen als semi-permeabel membraan. In hoofdstuk 2 van dit proefschrift wordt een uitgebreidere beschrijving gegeven van de basisconcepten van osmotische verschijnselen en de theoretische concepten van chemische osmose en van het semi-permeabel membraangedrag van kleien. Verder geeft het hoofdstuk een kort overzicht van bestaande laboratoriumstudies en veldstudies naar deze verschijnselen.

Het doel van het werk dat wordt gepresenteerd in dit proefschrift was om meer duidelijkheid en inzicht te verkrijgen in het vóórkomen en de relevantie van osmotisch gedrag van klei-rijke sedimenten onder *in-situ* omstandigheden in het veld. Daartoe zijn veldexperimenten uitgevoerd om membraaneigenschappen te kwantificeren en is procesmodellering gebruikt om bestaande en nieuwe metingen te interpreteren en om voorspellingen te doen. Het onderzoek maakte deel uit van een groter door TRIAS gefinancierd onderzoeksprogramma waarin twee collega promovendi - Katja Heister aan de Universiteit Utrecht en Sam Bader aan de Technische Universiteit Delft, later ook Universiteit Utrecht - zich respectievelijk richtten op laboratoriumonderzoek naar osmotische- en electro-osmotische processen en de ontwikkeling van mathematische modellen voor de beschrijving van osmotische processen.

Hoofdstuk 3 rapporteert over het ontwerpen en testen van veldinstrumentarium voor de huidige studie en bespreekt de voor- en nadelen van verschillende alternatieve procedures voor het verrichten van veldmetingen om membraangedrag te bestuderen. Op basis van deze evaluatie is voor het huidige onderzoek gekozen voor een zogenaamde ”shut-in” testmethode waarbij opbouw van osmotische druk wordt gemeten in een van de atmosfeer afgesloten reservoir.

Veldmetingen zijn uitgevoerd aan ”Calais klei” in centraal Nederland en aan Boomse klei in noord België. De Calais klei is een Holocene, estuariene, ongeconsolideerde, plastische klei die zich op geringe diepte onder maaiveld bevindt, terwijl de Boomse klei een sterk geconsolideerde, mariene, doch zoete klei is waarbij metingen tevens zijn verricht op grote diepte onder maaiveld. In hoofdstuk 4 wordt het onderzoek aan de Calais klei gepresenteerd en bediscussieerd. Experimenten zijn zowel uitgevoerd met het speciaal ontwikkelde instrumentarium als met bestaande instrumenten (BAT probe). Op basis van de metingen kan helaas geen harde uitspraak worden gedaan over de aan- of afwezigheid van osmotische eigenschappen van de klei. Membraangedrag lijkt echter zeer gering of afwezig. De oorzaak hiervan zou verband kunnen houden met de hoge cation-uitwisselingscapaciteit van deze klei. De resultaten zijn consistent met laboratoriummetingen aan deze klei die aan de Universiteit Utrecht (Katja Heister) zijn uitgevoerd.

In hoofdstuk 5 worden twee in-situ experimenten aan Boomse klei besproken die werden uitgevoerd in het Ondergrondse Onderzoekslaboratorium (URL) van het Studiecentrum voor Kernenergie (SCK-CEN), te Mol, België. De experimenten zijn verricht in het kader van een groter onderzoeksprogramma naar de geschiktheid van de Boomse klei voor ondergrondse opslag van radioactief afval. Interesse van SCK-CEN heeft vooral betrekking op de vraag of osmotisch-gedreven stroming, veroorzaakt door potentiële toekomstige lekkage van grote hoeveelheden nitraat-rijke bitumineus radioactief afval, vloeistofdrukken zou kunnen genereren die de afsluitende eigenschappen van de klei sterk zou kunnen aantasten. Voor de experimenten is gebruik gemaakt van bestaande piëzometers. Analyse en modellering van de experimentele gegevens (beschreven in hoofdstuk 6), tonen aan dat de membraaneigenschappen (uitgedrukt in de osmotische efficiëntie σ) van de Boomse klei sterk aanwezig zijn onder onverstoorde chemische condities (σ =0.41 bij 0.014 M $NaHCO_3$), maar sterk afneemt bij toenemende concentraties (σ =0.07 bij 0.14 M $NaHCO_3$). De membraaneigenschappen van de klei zijn relevant voor de veilige berging van radioactief af-

val. Echter, de geobserveerde osmotisch-geïnduceerde druk in de experimenten is vrij klein (0.2 bar = 2 m waterkolom) in vergelijking met de *in-situ* hydrostatische druk (220 m waterkolom) en met de hydraulische verstoringen die zijn ontstaan door de constructie van het ondergrondse laboratorium. Voor een volledige evaluatie blijft het daarom noodzakelijk om modellering uit te voeren op de schaal van de ondergrondse opslag gallerijen als geheel.

In hoofdstuk 6 wordt een drietal procesmodelleringsstudies besproken. Voor de modellering is gebruik gemaakt van een numeriek eindige-elementen model voor het oplossen van gekoppelde partiële differentiaalvergelijkingen. De set van vergelijkingen is ontwikkeld in samenwerking met collega promovendus Sam Bader. De vergelijkingen beschrijven niet-stationair transport. Tevens is in de simulaties de sterke concentratieafhankelijkheid van de osmotische efficiëntie meegenomen die wordt beschreven door de Bressler relatie. De eerste studie betreft modellering van data van een bestaand laboratorium osmose experiment (T. Keijzer) met bentoniet. In het experiment werden vloeistofdruk- en zoutgehalteveranderingen geregistreerd in twee reservoirs aan weerszijde van het kleimembraan die bij aanvang verschillende zoutgehalten bevatten. Het model blijkt wel algemene karakteristieken goed te simuleren zoals die in het algemeen worden waargenomen in dit type osmose experimenten: een differentiële drukopbouw door osmotisch gedreven water transport gevolgd door een geleidelijke afname van het drukverschil die wordt veroorzaakt door de geleidelijke afname van de concentratiegradiënt in het membraan door moleculaire diffusie; echter voor het gekozen laboratorium experiment bleek het niet mogelijk de experimentele druk- en zoutgehalteverandering gelijktijdig goed te reproduceren. Dit duidt mogelijk op structuurveranderingen in de klei die zijn ontstaan tijdens het experiment en die niet in beschouwing zijn genomen in de numerieke simulaties. De tweede toepassing betreft modellering van een in-situ osmose experiment in de Pierre shale in South Dakota in de Verenigde Staten. De gegevens van dit veldexperiment dat negen jaar duurde zijn eerder op een vereenvoudigde manier genterpreteerd waarbij alleen gebruik werd gemaakt van de vloeistofdruk en concentratie registraties die behoren bij osmotisch evenwicht. In hoofdstuk 6 wordt modellering van de gehele dataset gepresenteerd. Die modellering geeft een waarde van de osmotische efficiëntie σ van 0.21 voor het totale zoutgehalte van 3.5 g/l dat lokaal aanwezig is in de Pierre shale. Deze waarden zijn in goede overeenstemming met wat eerder werd gevonden. De nieuwe modellering geeft tegelijkertijd waarden voor de intrinsieke doorlatendheid, specifieke berging en de diffusie coefficiënt die realistisch zijn voor de Pierre shale. De resultaten van de derde toepassing - van modellering van de experimenten aan de Boomse klei - zijn boven reeds besproken.

In hoofdstuk 7 is het model gebruikt om de bijdrage van osmose aan gemeten hoge poriewaterdrukken in het Dunbarton bekken in de Verenigde Staten te onderzoeken. In de literatuur worden voor klei-rijke formaties van Trias ouderdom waarin zich water met een hoog zoutgehalte bevindt, stijghoogten gerapporteerd voor twee putten (192 en 140 m boven zeeniveau) die veel hoger zijn dan de daarbovengelegen lokale grondwaterspiegel (58 m boven zeeniveau) in de kustvlakte. Eerder is op basis van een eenvoudige berekening van osmotische drukken voor de betreffende zoutgehalten voorgesteld dat osmose verantwoordelijk is voor de hoge vloeistofdrukken in het bekken en dat de kleien zich gedragen als een ideaal membraan ($\sigma = 1$). Toepassing van het eindige-elementen model geeft aan dat

de efficiënties voor de hoogste en laagste gemeten concentraties respectievelijk 0.9897 en 0.9950 bedragen en dat de grootte van de gemeten stijghoogten goed kan worden gereproduceerd. De modellering laat verder zien dat de overdrukken grotendeels bewaard kunnen blijven in het bekken over een periode van 200 miljoen jaar, wat ongeveer overeenkomt met de ouderdom van het bekken.

Hoofdstuk 8 sluit af met een algemene discussie en een samenvatting van de conclusies van de studie. Daarin worden onder andere ideeën gepresenteerd voor verdere verbetering van de veldexperimentele methoden. Tevens wordt beargumenteerd dat de invloed van reactief transport op osmotische efficiëntie van kleirijke sedimenten verder moet worden onderzocht en dat dit aspect meegenomen zou moeten worden in procesmodellering.